

Special Observing Period (SOP) Data for the Year of Polar Prediction site Model Intercomparison Project (YOPPsiteMIP)

Zen Mariani¹, Sara M. Morris^{2,11}, Taneil Uttal², Elena Akish^{3,2}, Robert Crawford¹, Laura Huang¹, Jonathan Day⁴, Johanna Tjernström¹², Øystein Godøy¹², Lara Ferrighi¹², Leslie M. Hartten^{3,2}, Jareth Holt⁶, Christopher J. Cox², Ewan O'Connor⁹, Roberta Pirazzini⁹, Marion Maturilli¹³, Giri Prakash¹⁰, James Mather⁸, Kimberly Strong⁵, Pierre Fogal⁵, Vasily Kustov^{7,14}, Gunilla Svensson⁶, Michael Gallagher^{3,2}, Brian Vasel¹¹

¹Meteorological Research Division, Environment and Climate Change Canada, Toronto, Canada

²NOAA Physical Sciences Laboratory, Boulder, CO, USA

³Cooperative Institute for Research in Environmental Science, University of Colorado, Boulder, Colorado, USA

⁴European Centre for Medium-Range Weather Forecasts, Reading, UK

⁵Department of Physics, University of Toronto, Toronto, Canada

⁶Department of Meteorology, Stockholm University, Sweden

⁷Arctic and Antarctic Research Institute, Air-sea interaction department, St. Petersburg, Russia

⁸Pacific Northwest National Laboratory, Richland, WA, USA

⁹Finnish Meteorological Institute, Finland

¹⁰Environmental Sciences Division, Oak Ridge National Laboratory, Oak Ridge, TN, USA

¹¹NOAA Global Monitoring Laboratory, Boulder, CO, USA

¹²Norwegian Meteorological Institute, Norway

¹³Alfred Wegener Institute, Helmholtz Centre for Polar and Marine Research, Potsdam, Germany

¹⁴Freelance entrepreneur, Belgrade, Serbia

Correspondence to: Zen Mariani (zen.mariani@ec.gc.ca) and Sara Morris (Sara.Morris@noaa.gov)

Abstract. The rapid changes occurring in the polar regions require an improved understanding of the processes that are driving these changes. At the same time, increased human activities such as marine navigation, resource exploitation, aviation, commercial fishing, and tourism require reliable and relevant weather information. One of the primary goals of the World Meteorological Organization's Year of Polar Prediction (YOPP) Project is to improve the accuracy of numerical weather prediction (NWP) at high latitudes. During YOPP, two Canadian supersites were commissioned and equipped with new ground-based instruments for enhanced meteorological and system process observations. Additional pre-existing supersites in Canada, the United States, Norway, Finland, and Russia also provided data from ongoing long-term observing programs. These supersites collected a wealth of observations that are well-suited to address YOPP objectives. In order to increase data useability and station interoperability, novel Merged Observatory Data Files (MODFs) were created for the seven supersites over two Special Observing Periods (February to March 2018 and July to September 2018). All observations collected at the supersites were compiled into this standardized NetCDF MODF format, simplifying the process of conducting pan-Arctic NWP verification and process evaluation studies. This paper describes the seven Arctic YOPP supersites, their instrumentation, data collection and processing methods, the novel MODF format, and examples of the

39 observations contained therein. MODFs comprise the observational contribution to the model intercomparison effort, termed
40 YOPP supersite Model Intercomparison Project (YOPPsiteMIP). All YOPPsiteMIP MODFs are publicly accessible via the
41 YOPP Data Portal (Whitehorse: <https://doi.org/10.21343/a33e-j150>, Iqaluit: <https://doi.org/10.21343/yrnf-ck57>, Sodankylä:
42 <https://doi.org/10.21343/m16p-pq17>, Utqiagvik: <https://doi.org/10.21343/a2dx-nq55>, Tiksi: [https://doi.org/10.21343/5bwn-
w881](https://doi.org/10.21343/5bwn-
43 w881), Ny-Ålesund: <https://doi.org/10.21343/y89m-6393>, Eureka: <https://doi.org/10.21343/r85j-tc61>), hosted by MET
44 Norway, with corresponding output from NWP models.

45 **1 Introduction**

46 In the Arctic there is a recognized lack of process-level information supplementing meteorological observations to characterize
47 the atmosphere and the cryosphere for operational forecasting (Cassano et al., 2011; Illingworth et al., 2015; Lawrence et al.,
48 2019). As the climate continues to change, information on weather and climate is becoming more critical in ensuring the health
49 and safety of local communities. Unfortunately, climate models do a poor job of capturing key features of Arctic climate, such
50 as the Arctic amplification factor, likely as a result of inaccurate representation of key physical processes, as shown by
51 Rantanen et al. (2022). Similarly, the accuracy of weather forecasts in the Polar Regions is also lower than in mid-latitudes
52 (Jung et al., 2016) partly due to the scattered and limited availability of observing networks (Lawrence et al., 2019). Advances
53 in Polar weather forecast prediction are expected to improve weather forecasts and climate predictions elsewhere (Jung et al.,
54 2016 and Day et al., 2019), but understanding the causes of poor model performance in the Arctic is limited by the availability
55 of observatory data. Data from observatories, where sometimes hundreds of parameters are measured, are needed for detailed
56 investigations into the cause of model error, such as boundary-layer processes and turbulent exchanges (e.g., Day et al., 2024).

57
58 To address the need to improve Numerical Weather Prediction (NWP) performance in the Polar Regions, the World
59 Meteorological Organization (WMO) launched the international Polar Prediction Project with its flagship activity, the Year of
60 Polar Prediction (YOPP). During YOPP's core phase, from mid-2017 to mid-2019, several intensive observing periods were
61 conducted with close coordination between the international network of polar observatories and weather forecast centers. The
62 aim was to produce highly-concentrated sets of observed and modelled data for supporting forecast evaluation and process
63 studies (Koltzow et al., 2019; Goessling et al., 2016; Jung et al., 2016).

64
65 One of the flagship activities of YOPP was the YOPP supersite Model Intercomparison Project (YOPPsiteMIP), an initiative
66 to assess the performance of NWP systems at the process level by comparing with observatory data (Day et al., 2024). To
67 achieve this, a dataset of weather forecasts was produced by various NWP centers for supersite locations. In the Arctic the
68 dataset covers two Special Observing Periods (SOPs), SOP1 (February 1 – March 31, 2018) and SOP2 (July 1 – September
69 30, 2018). During this period the number of routine observations (e.g. radiosonde launches, buoy deployments, etc.) were

70 enhanced in the Arctic (doubled in the case of radiosondes), field campaigns were conducted, and enhanced observations from
71 the designated YOPP “supersite” observatories were taken. In general, the suite of several additional instruments that enable
72 an enhanced measurement program, including remote sensing, radiation, and other meteorological sensors, is what
73 distinguishes a ‘supersite’ from a typical weather site. This paper documents the efforts to compile the supersite (hereafter
74 referred to as “sites”) data collected during this period as part of the YOPPsiteMIP. These sites (Figure 1) are distributed over
75 a diverse range of geographical locations capturing some of the diversity in the terrestrial high-latitude climate zones.

76
77 Prior to YOPP, data collection, processing, geophysical variable reporting cadences, and file output type and format were not
78 standardized across the sites, which are operated by different international agencies and consortiums. This lack of
79 interoperability made performing multi-site comparisons, evaluations, and process studies difficult and time consuming,
80 deterring potential users of the data (Wohner et al., 2022). In order to address this problem, the concept of standardized Merged
81 Observatory Data Files (MODFs) was developed as part of the YOPPsiteMIP (Uttal et al., 2024). This concept is based on
82 combining measurements from multiple international research observatories’ instruments into a single NetCDF file that
83 complies with established data management standards. Prior to MODFs, there generally existed no standardized procedures
84 for coordinated data management at these research sites such as those that have been developed for operational datasets. Thus,
85 the data from these sites’ separate instruments were scattered between separate files with different authors, formats, metadata,
86 post-processing techniques, physical archive locations, and requirements for usage. As such, they could not be amalgamated
87 to provide a pan-Arctic observational dataset.

88
89 MODF files bring together observations from different earth system components in a standardized NetCDF file format to
90 enable utilization of research-grade, process-level observations for model evaluation and parameterization development. At
91 the same time, MODFs are compatible with and mirror Merged Model Data Files (MMDFs) that are produced by each NWP
92 centre participating in YOPP (Day et al., 2024). Each geophysical variable observed at a site is matched to its corresponding
93 NWP model geophysical variable using a standardized data format, cadence, and file structure. Uttal et al. (2024) provides a
94 generalized overview for the content and data structure of MODFs, i.e., a single NetCDF data file containing measurements
95 from multiple sources, and a series of tools to facilitate their creation. Table 1 provides information regarding the on-site
96 facility location where measurements were collected and their coordinates for reference. For some sites (e.g., Sodankylä),
97 certain geophysical variables are measured at multiple locations; these are all reported in the MODF with their corresponding
98 measurement coordinates embedded within the file so as to distinguish each measurement. Final DOIs for the MODF_{yms} are
99 listed in Table 2.

100
101 The MODF’s standardized file structure directly aligns with the NWP’s MMDFs. Thus, MODFs easily facilitate observation-
102 model comparisons at any/all of the seven sites (Gallagher and Tjernström, 2024). The purpose of the present work is to

103 describe the construction and contents of MODFs for seven of the YOPP-designated Arctic sites during SOPs 1 and 2
104 (hereafter, “MODF_{ysm}”): Whitehorse, Canada (60.71 °N, 135.07 °W, 682 m a.s.l.); Iqaluit, Canada (63.74 °N, 68.51 °W, 11 m
105 a.s.l.); Sodankylä, Finland (67.367 °N, 26.629 °E, 179 m a.s.l.); Utqiagvik (Barrow), Alaska (71.325 °N, 156.625 °W, 8 m
106 a.s.l.); Tiksi, Russia (71.596 °N, 128.889 °E, 30 m a.s.l.); Ny-Ålesund, Norway (78.923 °N, 11.926 °E, 15 m a.s.l.); and Eureka,
107 Canada (80.083 °N, 86.417 °W, 89 m a.s.l.). Methods used to organize a site’s dataset and develop MODFs are provided. Each
108 sites’ instrumentation and data processing are also described in this work to provide users with additional context and
109 information about the source of the geophysical variables contained in the MODF. The MODFs’ counterpart, MMDFs, are
110 described in Uttal et al. (2024).

111
112 Creating a standardized dataset such as MODF that contains observations from different meteorological and research agencies’
113 sites is an extremely complex, non-trivial task. For the sake of brevity and to reduce redundancy, this paper references site- or
114 instrument-specific publications in order to fully describe all of the aspects of the MODF dataset, including instrumentation,
115 quality control, and processing techniques. In the case where non-trivial aspects about the MODF data arise, the data’s origin,
116 reference publications (e.g., dataset dois), and site contacts have been provided. Section 2 describes the data processing chain
117 conducted at each site, including information about the site’s local topography, climate, and instrumentation in order to provide
118 site-specific context to aid the interpretation of model-observation comparisons. Section 3 describes the instrumentation and
119 calculated variables. Section 4 describes the standardized MODF dataset file format, quality control, and post processing,
120 which in some cases differed slightly from site-to-site. Section 5 describes the MODF data structure, attributes, and example
121 Figures that illustrate the available dataset. Data and code availability is provided in Section 6, and concluding remarks are
122 provided in Section 7.

123 **2 Site Descriptions**

124 To properly contextualize and interpret the observations contained within the MODF since they come from vastly different
125 sites. A map of the distribution of the sites is shown in Figure 1. While all sites are also designated surface synoptic observation
126 (SYNOP) stations, the meteorological data provided in the MODFs is significantly more detailed and includes additional
127 geophysical variables and thus is not the same as the SYNOP data. Table 3 lists the geophysical variables observed at each
128 site that are stored in the standardized MODF format, their measurement location(s), and other attributes; the MODF
129 featureType corresponds to the type of geophysical variable being observed at each site (they are split up into broad categories).

130 **2.1 Whitehorse, Canada**

131 The Whitehorse site (Figure 2) was commissioned as part of the Canadian Arctic Weather Science (CAWS) project (Mariani
132 et al., 2018; Joe et al., 2020). CAWS was initiated to evaluate upper air observing technologies that can complement and
133 improve Polar forecasts, perform satellite calibration / validation over Arctic terrain, and to provide recommendations to
134 optimize the Canadian Arctic observing network. The site's instruments (Figure 2 and Table 4) are installed on an elevated
135 platform, all within a few meters of each other. The site is located at the Erik Nielsen Whitehorse International Airport, which
136 is situated on a plateau ~50 m above the rest of the city. The city is located in a valley between the Yukon Ranges to its West
137 (~1.6 km a.s.l.) and East (~1.4 km a.s.l.); this complex mountainous terrain strongly influences the weather systems that reach
138 Whitehorse, which mostly originate from the Eastern Pacific or over Alaska.

139
140 Whitehorse experiences cold to temperate average monthly temperatures ranging from -15 to 14 °C (annual mean of -2 °C)
141 and average monthly precipitation ranging from 7 to 38 mm (annual total of ~500 mm). Since the city is in the rain shadow of
142 the Coast Mountains, precipitation totals are relatively low year-round. The primary surface wind direction follows the valley
143 (NNW). The soil type at and around the site is a mixture of grained alluvial and colluvial slopes and, as part of the Boreal
144 Cordillera ecozone, the surface type is primarily Boreal Forest, including complex plateaus, mountains, valleys and Cordilleran
145 vegetation. With a population greater than 26,000 inhabitants, Whitehorse is the primary gateway for air traffic for all of the
146 Yukon Territories, parts of Alaska, and the Western Canadian Arctic. During the YOPP SOPs, radiosondes were launched
147 four times daily.

148 **2.2 Iqaluit, Canada**

149 Like Whitehorse, the Iqaluit site (Figure 3) was commissioned as part of the CAWS project (Mariani et al., 2022). The site is
150 located ~200 m from the airport runway and all instruments (Figure 3 and Table 5) are co-located to within no more than 140
151 m of each other on flat terrain. The city itself is located along the coast in a valley that runs in the NW to SE direction; thus,
152 the primary direction of surface winds, which are frequently severe ($> 15 \text{ ms}^{-1}$), follows this direction. The surrounding region
153 is relatively flat Arctic tundra except for nearby hills (~300 m a.s.l.) approximately two kilometers to the NE of the site.

154
155 Iqaluit experiences an extreme range of average monthly temperatures ranging from -28 to 8 °C (annual mean of -9 °C) and
156 average monthly precipitation ranging from 18 to 70 mm (annual total of ~460 mm). The soil type at and around the site is
157 cryosolic and the surface type is ~70% tundra and ~30% ocean within a 10 km radius of the site. Most storm tracks that reach
158 Iqaluit originate over the Western Canadian Arctic or the Prairies; these storms can produce strong Easterly winds which
159 frequently cause blowing snow that severely reduces visibility during non-summer months. Given the site's proximity to
160 Frobisher Bay (< 600 m), the site is influenced by sea surface conditions during onshore flow (NW). Co-located instrument
161 evaluation studies were conducted for several remote sensing and upper air observations (Mariani et al., 2020, 2021), including

162 preliminary model verification studies during the YOPP SOPs and beyond. Iqaluit has over 8,000 inhabitants and is the primary
163 gateway for air and sea traffic for the central and Eastern Canadian Arctic. During the YOPP SOPs, radiosondes were launched
164 four times daily.

165 **2.3 Sodankylä, Finland**

166 The Sodankylä site (Figure 4) is managed by the Arctic Space Centre of the Finnish Meteorological Institute (FMI-ARC). It
167 is located in the Scandinavian taiga, which consists of a mix of spruces, pines and birches. The instruments (Figure 4 and Table
168 6) at the Sodankylä site are distributed over seven main observational sites, each of them including several installations (48m,
169 24m, 20m or 16m towers, automatic weather stations (AWS), structures supporting snow and soil measurements) that cover
170 an area of approximately 1.5 km². The environment of the observational sites varies between dense forest, sparse forest, forest
171 openings, and wetland, each of these environments having its own particular surface characteristics.

172
173 Sodankylä experiences monthly temperatures ranging from -11 to 15 °C (annual mean of 1 °C) and average monthly
174 precipitation ranging from 35 to 85 mm (annual total of ~660 mm). The site is a calibration/validation site for numerous
175 satellite products (such as snow water equivalent and snow extent (Luoju et al., 2021), and soil freeze-thaw (Cohen et al.,
176 2021 and Rautiainen et al., 2016). The spatial distribution of the observational sites reflects the need of measuring the spatial
177 variability of observed parameters over different spatial scales and satellite footprints (Hannula et al., 2016). During the YOPP
178 SOPs, radiosondes were launched four times daily.

179 **2.4 Utqiagvik (formerly Barrow), USA**

180 The Utqiagvik site (Figure 5) consists of observatories located ~3 km southeast from the coastline where the Beaufort and
181 Chukchi Seas meet. The site is situated over tundra interspersed with thermokarst lakes having a coverage of up to 40% area
182 (Sellmann et al., 1975). There are two primary observatories located outside of Utqiagvik (formerly Barrow), Alaska: The
183 Atmospheric Radiation Measurement (ARM) North Slope of Alaska (NSA) observatory operated by the Department of Energy
184 (DOE), and the Barrow Atmospheric Baseline Observatory facility operated by the National Oceanic and Atmospheric
185 Administration (NOAA) Global Monitoring Laboratory (GML). These observatories are equipped with a suite of
186 meteorological instruments (Figure 5 and Table 7) located 8 km east of the town of Utqiagvik. This is likely beyond the
187 influence of a local heat island in town (Hinkel et al., 2007) and disturbance to snow cover by human activity (Stone et al.,
188 2002). The site includes several towers and space for guest instruments.

189

190 Utqiagvik experiences monthly temperatures ranging from -26 to 9 °C (annual mean of -10 °C) and average monthly
191 precipitation ranging from 35 to 85 mm (annual total of ~770 mm). The climate in Utqiagvik, and much of the Alaskan North
192 Slope, is regulated by seasonal sea ice cover and the dominance of easterlies that circulate around the Beaufort High. This
193 atmospheric pattern is punctuated by episodes of southerly advection of air masses from the north Pacific, which frequently
194 arrive from the direction of the Bering Strait and are influential the timing of seasonal transitions of terrestrial snow cover and
195 sea ice coverage in both autumn and spring (Cox et al., 2017). The GML Barrow Atmospheric Baseline Observatory recently
196 built a newly furnished on-site laboratory that was completed in 2020. The site's previous facility was constructed in 1972
197 (<https://gml.noaa.gov/obop/brw/history/index.html>), and was deconstructed in 2021. The ARM NSA observatory was
198 established in 1997 (Verlinde et al., 2016). Together, the GML and ARM observatories provide an extensive set of long-term
199 measurements at this coastal location. Measurements include properties of aerosols, clouds, precipitation, trace gases, the
200 atmospheric state and the surface energy balance. Unlike the other YOPP sites, radiosondes were launched three times daily
201 during the SOPs.

202 **2.5 Tiksi, Russia**

203 The Tiksi observatory (Figure 6) is 7 km away from the town of Tiksi, Russia, in the Sakha Republic of northern Siberia and
204 is staffed by personnel that commute from the town. Tiksi hosts a 20-m flux tower, a clean air facility, a weather station, a
205 Climate Reference Network (CRN) platform, and a Baseline Surface Radiation Network (BSRN) platform, among other
206 instruments (Figure 6 and Table 8) (Ohmura et al., 1998; Driemel et al., 2018). It is a coastal site, with facilities built in a high
207 latitude tundra regime, comprising several different types of tundra land classifications including shrub (most predominant),
208 lichen, wet/dry fen, grassy, bog, water, bare and meadow (Mikola et al., 2018). Meteorologically, Tiksi is located in a boundary
209 region between Atlantic and Pacific air masses. The resulting variability in atmospheric conditions with air masses originating
210 from various source regions in Russia, Northern America, Europe and Central Asia require careful attention and interpretation
211 of in-situ measurements. Tiksi is also influenced by its location at the mouth of the Lena River, the second largest river draining
212 into the Arctic Ocean and the only major Russian river underlain by permafrost which has impacts on the processes and
213 evolution of surface fluxes. Tiksi is also situated on the coast of the Laptev Sea, which is historically a region of large sea-ice
214 production.

215
216 Tiksi experiences monthly temperatures ranging from -29 to 11 °C (annual mean of -10 °C) and average monthly precipitation
217 ranging from 15 to 65 mm (annual total of ~510 mm). The original Tiksi science station was established in 1932 and at its
218 height had 60-80 staff and families that lived onsite with a school and grocery store comprising an independent community.
219 In collaboration with the Russian Federal Service for Hydrometeorological and Environmental Monitoring (Roshydromet), a
220 partnership was established with NOAA and the FMI in 2005 to collect climate grade meteorological, surface energy budget,

221 greenhouse gases and aerosol data (Uttal et al., 2013). Radiosonde data were incorporated into the Integrated Global
222 Radiosonde Archive (IGRA) and are available through NOAA's National Centers for Environmental Information (NCEI)
223 portal (Durre et al., 2018). Unlike the other YOPP sites, radiosondes had twice daily launches during the SOPs.

224 **2.6 Ny-Ålesund, Norway**

225 At Ny-Ålesund Research Station (Figure 7) in Svalbard, Norway, multi-disciplinary observations are operated by several
226 institutions of different nationalities. The Norwegian Meteorological Institute (aka MET Norway; www.met.no) is operating
227 the standard meteorological surface and synoptic observations (Figure 7 and Table 9) reported to the WMO (Maturilli et al.,
228 2013). The settlement at 78.9°N, 11.9°E, is situated on the south coast of the Kongsfjord, which opens at the west coast of
229 Svalbard towards the Fram Strait. The fjord stretches in southeast-northwest direction from the large glacier plateau to the
230 open ocean, and is surrounded by glaciated mountains with altitudes up to 1 km. This geographical setting impacts the local
231 wind field in the lowermost kilometer, resulting in a mainly southeastern wind direction at Ny-Ålesund, which is temporarily
232 replaced by a north-westerly wind direction when large-scale synoptic wind is also coming from the according direction. Only
233 in calm conditions with wind speed $< 2 \text{ ms}^{-1}$ do katabatic winds from the glaciers south of Ny-Ålesund prevail.

234
235 Ny-Ålesund experiences monthly temperatures ranging from -8 to 9 °C (annual mean of -6 °C) and average monthly
236 precipitation ranging from 17 to 46 mm (annual total of ~590 mm). Ny-Ålesund may be located in the high Arctic, but due to
237 its location in a coastal environment affected by the West Spitsbergen Current, the local climate is quite maritime and relatively
238 warm. During the summer months, air temperatures above freezing and the otherwise snow-covered landscape exhibits tundra
239 ground and the active layer soil surface of permafrost. An overview of the climate conditions and changes in Svalbard is given
240 by the Norwegian Centre for Climate Services (NCCS, 2018), while the specific atmospheric and radiation conditions in Ny-
241 Ålesund are described by Maturilli et al. (2019). For the YOPP SOPs, the radiosonde launch frequency was increased from
242 daily to 6-hourly. Radiosonde launches, four times daily, are contributed by the Alfred Wegener Institute (AWI), and carried
243 out by the German-French AWIPEV research base that AWI jointly operates with the French Polar Institute Paul-Émile Victor
244 (IPEV). The radiosondes and weekly ozone sondes are launched from a balloon platform about 200m west of the MET Norway
245 weather mast. Atmospheric trace gases and cloud condensation nuclei are observed at the Zeppelin Observatory at about 474
246 m a.s.l. on Zeppelin Mountain south of Ny-Ålesund, operated by the Norwegian Polar Institute (NPI), the Norwegian Institute
247 for Air Research (NILU), Stockholm University, the Japanese National Institute of Polar Research (NIPR), and others. The
248 full complement of atmospheric measurements at Ny-Ålesund highlights the interwoven research community that contributes
249 to making Ny-Ålesund an observational site. More information on the Ny-Ålesund Research Station is available at
250 <https://nyalesundresearch.no>.

251 2.7 Eureka, Canada

252 The Canadian Network for the Detection of Atmospheric Change (CANDAC) runs the Polar Environment Atmospheric
253 Research Laboratory (PEARL) (Figure 8) near the Environment and Climate Change Canada (ECCC) Eureka Weather Station
254 (EWS) in Nunavut, Canada. PEARL has three facilities: the Ridge Laboratory (RL), the Zero Altitude PEARL Auxiliary
255 Laboratory (OPAL), and the Surface and Atmospheric Flux Irradiance Extension (SAFIRE). PEARL collects a wide variety of
256 measurements across all three facilities (Figure 8 and Table 10). The observations used from the Eureka station for the
257 MODF_{ysm} (Akish and Morris, 2023a) were primarily measured at the OPAL and SAFIRE on-site facilities. The OPAL lab is
258 situated at approximately 10 m a.s.l. elevation to capture measurements in the lowermost atmosphere. The SAFIRE facility is
259 located about 5 km from the EWS, and it is located away from any structures. At SAFIRE, there is a former BSRN station, a
260 flux tower, and additional remote sensing instrumentation. Additional details about the site including its instrumentation,
261 dataset validation and uncertainties, etc., can be found in Fogal et al. (2013) and at [https://www.pearl-](https://www.pearl-candac.ca/website/index.php/facilities)
262 [candac.ca/website/index.php/facilities](https://www.pearl-candac.ca/website/index.php/facilities). Only a subset of the available measurements collected have been included in the
263 MODF_{ysm} (Akish and Morris, 2023a) due to time constraints and processing resources. Ellesmere Island, where Eureka is
264 situated, is characterized by complex topography that generates mesoscale atmospheric circulations, such as downsloping
265 winds (e.g., Persson and Stone, 2007). The local summertime atmosphere is likely regulated also by nearby ice conditions
266 (Persson and Stone, 2007; Tremblay et al., 2019), which vary between the northern side of the island where multiyear pack ice
267 persists (e.g., Alert) and other coastal areas, which are generally adjacent to seasonal ice cover (e.g., Eureka). However, the
268 general dryness of the atmosphere over Ellesmere is likely a regional anomaly related to location relative to dominant pressure
269 patterns over the Beaufort Sea and near the pole rather than being local (Cox et al., 2012).

270

271

272 Eureka has a minimum monthly average temperature of -37.4 °C in February, a maximum of 6.1 °C in July, and a yearly
273 average of -19 °C. Average monthly precipitation ranges from 9 to 53 mm (annual total of ~285 mm). Details of Eureka's
274 climatology are described in Lesins et al. (2010) and water vapor climatology in Weaver et al. (2017). For the period from
275 1954–2007, the monthly average dry bulb air temperature minimum occurs in February at approximately -37 °C, with the
276 maximum in July at approximately 5 °C. ECCC also publishes climate normals for Eureka at
277 https://climate.weather.gc.ca/climate_normals/results_1981_2010_e.html?stnID=1750&autofwd=1. Eureka is generally
278 colder and drier than Utqiagvik (Cox et al., 2012). The soils are mostly marine deposits, and the topography, apart from the
279 stony ridges, is driven mostly by ground ice (Pollard and Bell, 1998; Pollard et al., 2015). Cloud cover over Eureka is
280 anomalous relative to other Arctic observatories, with generally higher cloud bases, a smaller proportion of supercooled liquid,
281 and a seasonal cycle offset from the typical pattern observed elsewhere (Shupe, 2011; Shupe et al., 2011). Eureka increased
282 their twice daily radiosonde launches to four daily launches during the SOPs.

283

284 3 Instrumentation and Derived Variable Calculation

285 Standard surface meteorological observations (winds, temperature, pressure, humidity, precipitation) were conducted by
286 instruments of similar design, operation, and accuracy at the different sites. The MODF files have an attribute "Instrument,"
287 which specifies the exact instrument model used for each variable at each site. For each site, the full list of measured variables,
288 instrument model and manufacturer, temporal resolution, measurement uncertainty, and operating configuration is provided
289 in Tables 4-10 (note that the information in these tables is also documented in the attributes of the MODFs themselves). The
290 uncertainties provided in these tables originate from the manufacturer and often depend on the meteorological conditions (e.g.,
291 relative humidity observations are less accurate during very low temperatures); as such, the largest reported uncertainty was
292 provided for each geophysical variable to provide a conservative error estimate.

293
294 For all sites, Vaisala RS92 or RS41 radiosondes were used to collect vertical profile observations from the surface up to the
295 stratosphere. For Iqaluit and Whitehorse, however, the radiosonde manufacturer changed during SOP2 from Vaisala (RS92)
296 to GRAW on September 12, 2018 (no impact on the data quality is anticipated). The radiation flux, cloud base height, and
297 snowfall flux observations are the only derived variables that were explicitly calculated in the MODF (as opposed to the direct
298 observations described in the paragraphs above). The heat flux observations were processed using the eddy correlation and
299 bulk method (see for instance Baldocchi, 2014). Additional processing and quality control methods for these observations are
300 discussed in Section 4. Cloud-base height observations were output by the Vaisala CL51 ceilometer at most sites (where
301 available) using a proprietary algorithm to determine the lowest cloud base height; the uncertainty of this algorithm isn't
302 reported but the ceilometer has a reported distance accuracy of ± 5 m from the manufacturer. ARM technical reports, instrument
303 validation / evaluation, and quality control measures are linked and available within the Utqiagvik/Barrow MODF_{ysm} (Akish
304 and Morris, 2023c).

305
306 For all observations, instantaneous time is reported at the instruments' raw sampling cadence in UTC. The typical temporal
307 cadence for most observations are around 1 minute or less. No temporal interpolation or averaging was performed on the data.
308 The only exception to this is for turbulent fluxes (the only calculated variable), where some averaging (1 to 30 minutes,
309 depending on the variable) is implicit in the calculation of fluxes. Heights are reported as above ground level (AGL), with the
310 exception of the soil thermistor string, which reports depths below the surface in units of cm. For more information on the
311 instrumentation used or further details on the instrument accuracy, precision, and co-located validation studies for certain
312 instruments, refer to the site-specific references listed in Section 2 and/or the WMO Guide to Instruments and Methods of
313 Observation (WMO, 2021).

314

315 **4 Dataset Preparation, quality control, and post-processing**

316 Guidelines for creating MODFs were published as a table in both human-readable (PDF file) and machine-readable (JSON
317 files) formats by Hartten and Khalsa (2022). This “H-K Table” adopts the standards and conventions commonly used in the
318 earth sciences, including NetCDF encoding with Climate and Forecast (CF) Conventions and following CMIP6 naming, as
319 agreed upon by the YOPP community (Uttal et al., 2024). This H-K standard facilitates the creation of MODFs using current
320 requirements and the creator’s software of choice, with the MODF toolkits providing tools to assist the user in creating MODFs
321 (Section 6). For the present work, we used H-K Table version 1.3 to guide the criteria for the generation and standardization
322 of naming conventions, units, and global/variable attribute metadata. Observational datasets were collated and formatted for
323 each of the seven sites into a set of NetCDF files in accordance with the table’s criteria. The native variable name is saved as
324 an attribute in the MODFs and as previously discussed, no resampling was performed to harmonize different time stepping
325 (the instrument’s instantaneous raw sampling frequency is reported, usually about minutely). Acceptance of data into the
326 MODF_{ysm} was generally determined by the variable list described in the table. The processing script is openly available and
327 described in Section 6.

328
329 Radiosonde (timeSeriesProfileSonde variables) data in the MODF were binned into 5 m intervals (10 m for Iqaluit and
330 Whitehorse) of geopotential height and all measurements within each bin were averaged. In the case of 5-meter intervals, this
331 most often results in 0, 1, or 2 measurements in each bin: 8%, 82%, 9%, respectively, in SOP1 and 6%, 80%, 13% in SOP2.
332 In both SOP1 and SOP2 at least 99.9% of the measurements have two or fewer measurements, but a given bin can have up to
333 14 measurements. The number of measurements per bin has been included in the dataset to filter for these situations, as have
334 the actual time and height of each measurement (though also averaged within each bin). For surface precipitation observations,
335 no corrections for solid precipitation under-catchment were performed (the dataset is raw in the MODF); where appropriate,
336 users are recommended to process under-catchment corrections via Kochendorfer et al. (2020).

337
338 The present phase of the MODF concept is to use standardized data organization, metadata, and interoperability. While data
339 quality assurance and measurement operation procedures remain in the purview of the contributing stations, considerable effort
340 was undertaken to ensure MODF production followed a transparent, consistent, and standardized data processing chain. This
341 includes efforts to standardize post-processing and filtering techniques (e.g., quality control methods) as much as possible for
342 the same geophysical variable across the different sites. This consistent processing chain is another unique feature of the
343 MODF dataset as it enforces a level of consistency across vastly different observation sites that normally follow their agencies’
344 own data production procedures and methods. A summary of the processing and quality control applied for each site’s
345 observations is provided in Tables 4-10. As discussed in more detail in the below subsections, there are some cases where site-
346 specific data processing could not be avoided; data should be used cautiously and with due consideration to each site’s
347 processing techniques and quality control (QC) methods for the MODF_{ysm}.

348 **4. 1 Whitehorse and Iqaluit, Canada**

349 All geophysical variables observed at the Iqaluit and Whitehorse sites were processed in the same manner and included in the
350 MODF_{ysm} (Huang et al., 2023a; 2023b). For most geophysical variables, limited QC was performed on the raw dataset with
351 the intention to remove obvious outliers only. Details regarding the QC performed are provided in Tables 4-5. A very small
352 number (<5%) of observations were flagged by the QC algorithm. The radiation flux observations should be treated with
353 caution since they typically require additional QC processing prior to analysis; no additional QC was performed on these
354 observations to account for potential frost or snow deposition on the sensors, for instance. No additional QC was performed
355 on the cloud base height data, which was processed by the Vaisala software. Vaisala also processed the raw data feed from the
356 radiosonde observations, which was obtained at 2 s resolution; no additional QC was performed. When no data was available
357 (due to the instrument being down, loss of power at the site, or because it was flagged by the QC algorithm), a missing value
358 (-9999.0) was reported in the MODF_{ysm} (Huang et al., 2023a; 2023b) and is notated via the “missing_value” attribute associated
359 with each variable. Mariani et al. (2020, 2021) provides instrument validation studies and more detailed information on the
360 quality control processing routines for the remote sensing and upper air observations.

361 **4. 2 Sodankylä, Finland**

362 The Sodankylä observations included in the MODF_{ysm} (O'Connor, 2023) are automatically uploaded every day to the FMI
363 open access web site <https://litdb.fmi.fi/> where the data are organized on the basis of platforms and stations. Before being
364 uploaded to the web page, the data undergo an automatic quality check to remove outliers, as described in Table 6. In the
365 current MODF_{ysm} version (O'Connor, 2023), no further quality check was applied to the data, implying that errors from several
366 sources are occasionally included. These sources of error may include snow/frost deposition on radiation and temperature
367 sensors or absorption of solar radiation by unsheltered temperature sensors. In a future version of the MODF_{ysm}, a deeper
368 quality check will be applied to some of the variables included in the current MODF_{ysm} (O'Connor, 2023). This quality check
369 is based on the comparison among the same variables measured at different sites, on visual inspection and, in the case of global
370 radiation, on the comparison with radiative transfer model calculations. This processing will enable the identification of the
371 shortwave data affected by the shadows casted by the vegetation, of errors caused by frost formation on the domes of
372 pyranometers, and of the error in unshaded thermometers caused by the absorption of solar radiation. As in the case of the
373 Eureka observatory, the radiosonde data in the MODF was ingested and processed by IGRA and is available through NOAA's
374 NCEI portal (Durre et al., 2018).

375 **4.3 Utqiagvik (formerly barrow), USA, Tiksi, Russia and Eureka, Canada**

376 The Utqiagvik/Barrow data within the MODF_{ysm} (Akish and Morris, 2023c) originated from both DOE/ARM and NOAA
377 GML datasets, with GML providing datasets for ozone, snow thickness, skin temperature, soil temperature profile. Value added
378 products were generated and disseminated to the users using the ARM Data Discovery interface. Both the ARM and GML
379 datasets were ingested into a single MODF_{ysm} with variable attribution detailing how each variable and data set was quality
380 controlled, processed and accessed, as described in Tables 7-8, 10. The surface ozone data was collected in 1-minute intervals
381 and was manually quality controlled and submitted to NCEI. The measurements collected by the ARM facility were processed,
382 QC analyzed, and archived at the ARM Data Center archive. The long-term Eureka and Tiksi datasets (flux tower and radiation)
383 are hosted by the NOAA Physical Sciences Laboratory (PSL), in collaboration with ECCO (Eureka site only), and
384 Roshydromet (Tiksi site only).

385

386 For the three sites, the radiation measurements were QC'd and processed following Long and Shi (2008) and improved
387 correction of the infrared loss in diffuse shortwave measurements was included (Younkin and Long, 2003). Turbulent heat
388 fluxes were processed and QC'd via Eddy correlation corrections including stability correction, Webb-Pearman correction,
389 frequency correction, sensor separation correction, filtering correction, line-averaging correction, and volume-averaging
390 correction (Cook et al. 2008, Fuehrer and Friehe 2002). Bulk corrections were also employed and utilized ARM data from the
391 radiation, ground, met, and tower. Radiosonde data were ingested and processed by NOAA's NCEI and was processed through
392 IGRA, following their standards (Durre et al., 2018) and is available through NOAA's NCEI portal. The IGRA 2 QA system
393 processed the sonde data, which is based largely on the QA procedures in the IGRA 1 system (Durre et al. 2006; Durre et al.
394 2008). Like the IGRA 1 system, it consists of a deliberate sequence of specialized algorithms, each of which makes a binary
395 decision on the quality of a value, level, or sounding; either the data item passes the check and remains available, or it is
396 identified as erroneous and thus set to missing. For all observations, a second level of manual QC was performed whereby data
397 was reviewed by instrument mentors and visually assessed by the site scientist/data quality office. This included removing
398 non-physical values and outliers, after confirming that they were either biased, incorrect, or collected during site maintenance
399 periods. If data was not available for any of the collected measurements across any of the variables, due to the instrument being
400 down, loss of power at the site, or because it was flagged by the QC algorithm, a missing value (-9999) was reported in the
401 MODF_{ysm} (Akish and Morris, 2023b).

402 **4.5 Ny-Ålesund, Norway**

403 The meteorological measurements used for the MODF_{ysm} (Holt, 2023) are taken from the AWIPEV weather mast (Driemel et
404 al., 2018; Maturilli, 2020b). Except for precipitation, all other data used in the MODF_{ysm} for Ny-Ålesund originated from the
405 following data sets: Maturilli (2020a, 2020b, 2020c, 2022). The precipitation data reported in the MODF_{ysm} are the direct

406 instrument output and no quality checks were applied; as such this data should be treated with caution (Holt, 2023). The Ny-
407 Ålesund observations included in the MODF_{ysm} are a subset of those regularly uploaded in the PANGAEA data repository
408 (www.pangaea.de). Before being uploaded, all data undergo an automatic quality check (described in Table 9). Following this,
409 additional manual/visual inspection was performed as for Utqiagvik, Tiksi, and Eureka. Surface radiation data were validated
410 and have undergone all quality checks of BSRN before archiving (Maturilli, 2020a).

411 **5 MODF Data Structure**

412 The data inside a MODF comprises of all the observations listed in Table 3 for a given observation site. The data itself follows
413 the same standardized format and structure for all observations and sites and is stored into a single NetCDF file using CF
414 conventions. NetCDF file formatting was chosen to best accommodate the high-level of metadata detail required for merging
415 such large quantities of individual measurements together, particularly given the need to be as transparent as possible when
416 reporting instrument-specific details for each observation. NWP model output was stored in MMDFs, matching the MODF
417 format to facilitate model-observation comparisons. Local maps showing the synoptic region around each site are provided in
418 Figure 9, with native spatial grids of the forecast models that participated in YOPPsiteMIP overlaid. This provides visual
419 context of where the site and the nearest NWP grid points exist in and around each site.

420
421 All MODF_{ysm} measurements provided in the data files maintained their native time cadence (typically on the order of minutely)
422 with no averaging undertaken, and details of the collection and processing techniques can be found in the variable attributes
423 within the files. Each DOI in Table 2 contains four (e.g., Whitehorse) or six (e.g., Utqiagvik) files, depending on whether the
424 site had timeSeriesProfile observations on a tower/mast. The filename convention for each MODF is as follows: site name +
425 “obs” + MODF_featureType + start_date + end_date.nc.

426
427 Guidelines for creating inventories of variable and attribute information (metadata) necessary for the MODF file attributes
428 were published in spreadsheet format by Morris and Akish (2022). This “A-M Template” uses variable content criteria from
429 the H-K Table to generate a metadata matrix of attribute and variable information for each of the measurements contained
430 within the MODFs. The template has individual tabs for each of the corresponding CF metadata featureTypes (i.e., timeSeries
431 and timeSeriesProfile) of the MODF NetCDF files, as well as one tab for the Global Attributes of the MODFs. The CF
432 Conventions can be found here: <https://cfconventions.org/cf-conventions/cf-conventions.html>. The attributes within the
433 template are mandatory when applicable, and serve as a guideline for MODF creators. The A-M Template is machine-readable
434 and can be ingested into MODF software to create the final output.

435

436 The file content is well-illustrated in Table 3; other details of the MODF_{ysm} format and structure are outlined in Uttal et al.
437 (2024). MODFs can contain featureTypes such as timeSeries and timeSeriesProfile, which refer to time series having one and
438 two data dimensions, respectively. In cases where data subcategories exist, featureType modifications can be depicted in the
439 file name, for example timeSeriesProfileSonde exist for the MODF_{ysm} . Currently, more than one featureType can be used
440 within an individual MODF file, but all subscribe to the same formatting structure and nomenclature. To generate an MODF,
441 creators would first visit the H-K Table to determine the variables that will be included in their MODF, and then they should
442 utilize the A-M Template to fill in the needed attribute and variables information requested by existing MODF software. Once
443 the A-M Template has been completed, then users can ingest the template into their MODF software to create the final MODF
444 outputs. For the MODF_{ysm} , individual toolkits were developed by MODF makers for each YOPP site. Python code was
445 developed for Whitehorse, Iqaluit and Ny-Alesund, and MATLAB code for Utqiagvik, Tiksi, Eureka and Sodankyla (see
446 Section 6). After the generation of the MODF_{ysm} outputs, the files were run through an MODF checker that identifies the
447 various inconsistencies or issues with the files before their upload to the MET Norway data portal. The MODF_{ysm} checker
448 developed for the YOPPsiteMIP files is part of a larger toolkit being designed to continue the creation of MODFs.

449
450 As an example of the uniformity of the observations (in terms of data format, post-processing, temporal cadence, etc.)
451 contained within each site's MODF_{ysm} and their data coverage during the two YOPP SOPs, Figures 10 and 11 provide the
452 surface downwelling longwave radiation and near-surface temperature observations from each site's MODF_{ysm} during SOP1,
453 respectively and Figures 12 and 13 show the same except for SOP2. The MET Norway data portal and MODF maker toolkit
454 (Sect. 6) also provides plotting tools that work with any MODF or MMDF and can produce similar figures automatically.
455 Periods of interest can be quickly identified by users and analyzed for further investigation and/or comparison with their
456 corresponding MMDFs. MODFs significantly simplify the process of analyzing observations from multiple sites and multiple
457 instruments, as analyses and Figures can be produced for each site using a single code that works for any observed geophysical
458 variable and (if desired) their corresponding NWP model output in the MMDF. In contrast, without MODFs a user would have
459 to contact each meteorological agency individually, find each sites' data repository, obtain data access privileges, find the files
460 they need from multiple instruments, reprocess and reformat multiple uniquely-formatted datasets and file types, then develop
461 several different codes (e.g., readers) specific to each instruments' dataset to ingest the multi-variate datasets and plot them.

462
463 The MODF_{ysm} at Sodankylä are unique in that their measurements are collected across a series of sub-sites in the area;
464 therefore, it is important to describe here the possible methods for extracting the data for specific locations, or for co-located
465 measurements. The Sodankylä station comprises at least 25 distinct locations, the precise number of which is given by the
466 dimension 'site_id' inside the MODF data file. Each distinct location is given a unique index key in the variable 'subsite_name',
467 with these indices also identifying the 'lat', 'lon' and 'soil_type' for each location. The corresponding FMI names for each
468 location are identified in the attribute 'flag_meanings' for the variable 'subsite_name' via their indices; for example, the index

469 value of 16 pointing to IOA003_spot_8, which is one of the automatic weather stations located in the Intensive Observations
470 Area (IOA). There may be multiple locations providing the same measurement. However, not all locations provide the same
471 set of measurements, and to keep the MODF compact, each measurement variable has the location dimension truncated to
472 include only locations which measure that variable; i.e., the location dimension for the measurement variables is 'nsubsites_X',
473 where X is the number of locations making the particular measurement. This set of locations is accessed through the indices
474 given in the attribute 'subsite_name' for the measurement variable, which corresponds to the key given in the 'subsite_name'
475 variable; i.e., a subsite_name attribute of "1, 3, 10" means that these measurements were made at the locations identified by
476 their indices, from which their locations (latitudes and longitudes) and soil_type can also be determined.

477
478 This method permits diverse options of collecting measurements for particular uses. All measurements, for example, at one
479 location can be obtained by identifying the appropriate 'subsite_name' index inside the MODF data file, iterating through the
480 'subsite_name' attribute of each variable to see if it contains the selected index, and, if so, selecting the column or slice of data
481 for the data that matches the location of the index (i.e. if subsite_name = 10 and the subsite_name attribute for a timeSeries
482 variable is "1, 3, 10", the measurement timeSeries for the requested location is in the third column, the next variable may have
483 a subsite_name attribute of "1, 3, 5, 6, 10" and the measurement timeSeries for the requested location is in the fifth column).
484 The user could also select a specific area of interest and identify all measurements made within this region as follows: select
485 the indices for the locations within a specified latitude and longitude range, then iterate through the 'subsite_name' attribute of
486 each variable to see if it contains the selected indices and return the columns or slices that match them.

487
488 Note that each site conducts additional observations not listed in table 3 that will be included in upcoming updates to the
489 MODF_{ysm} with the intent to eventually incorporate all observations into the MODF_{ysm} for each site. This process of developing
490 and appending to MODFs can be extended to other sites and/or research programs that wish to create MODFs of their
491 observations. Given the standardized nature of the MODFs, reading and analyzing datasets from any of the YOPP sites is
492 simplified. Quick-look plotting tools have been developed via the MET Norway YOPP data portal and the MODF maker
493 toolkit (Sect. 6), which enable near-instantaneous plotting of the observations contained within the MODF_{ysm}.

494

495 **6 Data and Code Availability**

496 The MODF_{ysm} for each site are available via the MET Norway YOPP Data Portal (<https://yopp.met.no/>) where they are
497 indexed through FAIR compliant discovery metadata and can be directly accessed at:

498 https://thredds.met.no/thredds/catalog/alertness/YOPP_supersite/obs/catalog.html (Whitehorse:

499 <https://doi.org/10.21343/a33e-j150>, Iqaluit: <https://doi.org/10.21343/yrnf-ck57>, Sodankylä: <https://doi.org/10.21343/m16p->

500 [pq17](https://doi.org/10.21343/a2dx-nq55), Utqiagvik: <https://doi.org/10.21343/a2dx-nq55>, Tiksi: <https://doi.org/10.21343/5bwn-w881>, Ny-Ålesund:
501 <https://doi.org/10.21343/y89m-6393>, Eureka: <https://doi.org/10.21343/r85j-tc61>).

502

503 Proper data citation ensures appropriate credits to authors of both input data sources and merged MODF_{ysm} datasets. Data from
504 each station has been assigned a DOI. The variable attributes of the merged data products contain information about the source
505 datastreams and their DOIs, to more clearly establish data provenance in a traceable manner. When using data from the
506 MODF_{yms}, it is expected that the user references the MODF_{ysm} DOI, and any subsidiary variable DOIs when available.
507 Assigning citations for merged data streams such as the MODF_{ysm} is a challenging and still evolving concept. For example,
508 the US DOE ARM Program uses a combination of DOI and citation structure for continuous data streams, as outlined in
509 Prakash et al. (2016). They recommend when registering DOIs for derived and higher-order data, source DOIs in the metadata
510 of the newly created DOI should be added and linked when possible.

511

512 The source code used to produce the MODF_{ysm} for each site (and MODFs in general) are available via gitlab:
513 <https://gitlab.com/mdf-makers/mdf-toolkit>. This MODF toolkit is openly available for anyone interested in developing their
514 own MODF file or generating quick-look plots of the data contents inside the MODFs. The toolkit is regularly updated as the
515 MODF community grows and new geophysical variables and/or functions are added. Additional site-specific python and
516 MATLAB codes that were used to prepare the observation data files for MODF ingestion are available upon request (e.g.,
517 contact the site principle investigator).

518

519 **7 Concluding Remarks**

520 The enhanced ground-based observations conducted at both Poles during the YOPP fill significant and identified gaps in our
521 current meteorological observation capabilities for the Polar Regions. YOPPSiteMIP MODFs (MODF_{ysm}) have been published
522 for seven of the YOPP Arctic sites, whereby all geophysical variables are stored in an identical, standardized format in a single
523 NetCDF file following CF conventions. This fulfills a key objective of the program to perform single- or multi-variate model-
524 observation comparisons. These MODFs archive data in a manner as similar as possible to corresponding MMDF (see Uttal
525 et al., 2024) that contain high-resolution forecast variables from a single NWP model at and around a site (Figure 9). Thus,
526 combined, MODFs and MMDFs greatly simplify integration of these complex datasets, enabling further scientific study as
527 demonstrated in the recent publications using the latest MODF_{ysm} and MMDF_{ysm} (Day et al., 2024).

528

529 Standardized geophysical variable nomenclature, cadences, metadata, basic QC, and file structure were employed to create
530 these files. MODFs provide the first standardized files for archiving all the different ground-based observation site

531 observations, containing a multitude of geophysical variables observed by (at times) different instruments. This amalgamation
532 of different sites' observations into a standardized, user-friendly MODF format enables easier analysis of the MODF dataset,
533 inter-site comparisons, and detailed NWP model validation, evaluation, intercomparisons, and process-based diagnostic
534 studies that are currently underway (e.g., Figures 10 to 13). The further adoption, creation, and use of MODFs outside of YOPP
535 is encouraged; a suite of tools and documentation is openly available via Gitlab (Sect. 6) for other site managers, researchers,
536 and users to develop and create their own site-specific MODFs outside of YOPP or to analyze an observation sites' dataset.

537

538 The YOPP MODF_{ysm} discussed here provide novel access to datasets of enhanced meteorological observations collected at
539 several sites across the Arctic. The MODF concept is not limited for use in polar regions and could be exported elsewhere.
540 Seven YOPP-designated sites in the Arctic developed and published MODF_{ysm} covering both SOP periods (February – March
541 2018 and July – September 2018), including Iqaluit, Whitehorse, and Eureka in Canada, Utqiagvik in the United States, Tiksi
542 in Russia, Sodankylä in Finland, and Ny-Ålesund in Norway. Additional geophysical variables observed at each of these seven
543 sites will be included in a future update of their MODF_{ysm}, with the goal of having almost all of a site's observations available.
544 Observations at most of these sites continue today beyond YOPP and are available for subsequent analyses, in some cases
545 using updated MODFs generated in near-real time. MODF_{ysm} for the other YOPP sites, including ship-based platforms and
546 sites in the Antarctic, will be made available in the future to complete the YOPP dataset. The MODF_{ysm} described here directly
547 ties to process-oriented verification studies aiming to improve NWP predictions at the Poles by contributing and enabling
548 NWP inter-comparisons.

549

550 **Author contributions**

551 SM, ZM, and TU wrote the first draft of the manuscript. SM and ZM conducted scientific analyses and created tables and
552 figures with JD and JT. All authors managed data archiving, creation of the MODF_{ysm}, and publication to the MET Norway
553 YOPP Data Portal. All authors contributed to the writing and the editing of the manuscript.

554

555 **Competing interests**

556 The authors declare that they have no conflict of interest.

557

558 **Disclaimer**

559 Use of specific instrument manufacturers/models and suppliers mentioned in the manuscript and/or used at the sites is not a
560 commercial endorsement of their products.

561

562 **Acknowledgements**

563 This is a contribution to the Year of Polar Prediction (YOPP), a flagship activity of the Polar Prediction Project (PPP), initiated
564 by the World Weather Research Programme (WWRP) of the World Meteorological Organisation (WMO). We acknowledge
565 the WMO WWRP for its role in coordinating this international research activity. This study was supported by NOAA's Global
566 Ocean Monitoring and Observing Program through the Arctic Research Program (FundRef:
567 <https://doi.org/10.13039/100018302>). Special thanks to the station technicians and operators at the sites for deploying
568 instruments, maintenance, and technical services. In particular, thank you to the radiosonde operators for providing extra daily
569 sonde launches during the two SOP periods. Thank you to Jenn Glaser for her contract work in creating the station graphic in
570 Figure 1, and to Kyrie Newby and Calvin Jesse for creating the Google Earth images in Figure 9. JD was supported by the
571 European Union funded INTERACTIII project (Grant Agreement: 871120). AK and LMH were supported in part by NOAA
572 cooperative agreements NA17OAR4320101 and NA22OAR4320151. Portions of the MODF_{ysm} data were obtained from the
573 Atmospheric Radiation Measurement (ARM) user facility, a U.S. Department of Energy (DOE) office of science user facility
574 managed by the biological and environmental research program. Thank you to MET Norway for hosting the YOPP data portal.
575 All data products are produced by their respective institutions and are available via the YOPP data portal (<https://yopp.met.no>)
576 and directly at: https://thredds.met.no/thredds/catalog/alertness/YOPP_supersite/obs/catalog.html.

577

578

579 **References**

- 580 Akish, E., and Morris, S.: MODF for Eureka, Canada, during YOPP SOP1 and SOP2, Norwegian Meteorological Institute,
581 dataset, <https://doi.org/10.21343/R85J-TC61>, 2023a.
- 582
- 583 Akish, E., and Morris, S.: MODF for Tiksi, Russia, during YOPP SOP1 and SOP2, Norwegian Meteorological Institute,
584 dataset, <https://doi.org/10.21343/5BWN-W881>, 2023b.
- 585
- 586 Akish, E., and Morris, S.: MODF for Utqiagvik, Alaska, during YOPP SOP1 and SOP2, Norwegian Meteorological
587 Institute, dataset, <https://doi.org/10.21343/A2DX-NQ55>, 2023c.
- 588
- 589 Baldocchi, D.: Measuring fluxes of trace gases and energy between ecosystems and the atmosphere – the state and future of
590 the eddy covariance method. *Global Change Biology* (2014)20, 3600–3609, <https://doi.org/10.1111/gcb.12649>, 2014.
- 591
- 592 Becherini, F., Vitale, V., Lupi, A. et al. Surface albedo and spring snow melt variations at Ny-Ålesund, Svalbard. *Bull. of*
593 *Atmos. Sci. & Technol.* 2, 14 (2021). <https://doi.org/10.1007/s42865-021-00043-8>.
- 594
- 595 Cassano, J. J., Higgins, M. E., and Seefeldt, M. W.: Performance of the Weather Research and Forecasting Model for
596 Month-Long Pan-Arctic Simulations, *Monthly Weather Review*, 139, 3469-3488, doi: 10.1175/mwr-d-10-05065.1, 2011.
- 597
- 598 Cohen, J., Rautiainen, K., Lemmetyinen, J., Smolander, T., Vehvilainen, J., and Pulliainen, J.: Sentinel-1 based soil
599 freeze/thaw estimation in boreal forest environments, *Remote Sens Environ*, 254, <https://doi.org/10.1016/j.rse.2020.112267>,
600 2021.
- 601
- 602 Cook, B.I., Bonan, G.B., Levis, S. et al. The thermoinsulation effect of snow cover within a climate model. *Clim Dyn* 31,
603 107–124. <https://doi.org/10.1007/s00382-007-0341-y>, 2008.
- 604
- 605 Cox, C.J., Stone, R.S., Douglas, D.C., Stanitski, D.M., Divoky, G.J., Dutton, E.S., Sweeney, C., George, J.C., and
606 Longenecker, D.U.: Drivers and Environmental Responses to the Changing Annual Snow Cycle of Northern Alaska, *B Am*
607 *Meteorol Soc*, 98, 2559-2577, <https://doi.org/10.1175/BAMS-D-16-0201.1>, 2017.
- 608
- 609 Cox, C.J., Walden, V.P., and Rowe, P.M.: A Comparison of the atmospheric conditions at Eureka, Canada, and Barrow,
610 Alaska (2006-2008), *J Geophys Research*, 117, <https://doi.org/10.1029/2011JD017164>, 2012.
- 611
- 612 Day, J.J., Sandu, I., Magnusson, L., Rodwell, M.J., Lawrence, H., Bormann, N., and Jung, T.: Increased Arctic influence on
613 the midlatitude flow during Scandinavian Blocking episodes, *Q.J.R. Meteorol. Soc.*, 725, 3846-3862,
614 <https://doi.org/10.1002/qj.3673>, 2019.
- 615
- 616 Day, J., Svensson, G., Casati, B., Uttal, T., Khalsa, S.J., Bazile, E., Akish, E., Azouz, N., Ferrighi, L., Frank, H., Gallagher,
617 M., Godoy, Ø., Hartten, L., Huang, L., Holt, J., Di Stefano, M., Mariani, Z., Morris, S., O'Connor, E., Pirazzini, R., Remes,
618 T., Fadeev, R., Solomon, A., Tjerström, J., and Tolstykh, M.: The YOPP site Model Intercomparison Project (YOPPsiteMIP)
619 phase 1: project overview and Arctic winter forecast evaluation, 2024, *submitted to Geoscientific Model Development*
620 *(GMD) August 25, 2023 submitted - under review 2024*.
- 621

622 Driemel A, Augustine JA, Behrens K, Colle S, Cox C, Cuevas-Agulló E, Denn FM, Duprat T, Fukuda M, Grobe H,
623 Haeffelin M, Hyett N, Ijima O, Kallis A, Knap W, Kustov V, Long CN, Longenecker D, Lupi A, Maturilli M, Mimouni M,
624 Ntsangwane L, Ogihara H, Olano X, Olefs M, Omori M, Passamani L, Pereira EB, Schmithüsen H, Schumacher S, Sieger R,
625 Tamlyn J, Vogt R, Vuilleumier L, Xia X, O A, König-Langlo G. Baseline Surface Radiation Network (BSRN): structure and
626 data description (1992–2017) *Earth Syst Sci Data*, 10, 1491–1501, 2018.

627

628 Durre, I., Menne, M. J., and Vose, R. S.: Strategies for evaluating quality assurance procedures, *J Appl Meteorol Clim*, 47,
629 1785-1791, doi: 10.1175/2007jamc1706.1, 2008.

630

631 Durre, I., Vose, R. S., and Wuertz, D. B.: Overview of the Integrated Global Radiosonde Archive, *J Climate*, 19, 53-68, doi
632 10.1175/Jcli3594.1, 2006.

633

634 Durre, I., Yin, X., Vose, R. S., Applequist, S., and Arnfield, J.: Enhancing the Data Coverage in the Integrated Global
635 Radiosonde Archive. *J. Atmos. Oceanic Technol.*, 35, 1753–1770, <https://doi.org/10.1175/JTECH-D-17-0223.1>, 2018.

636

637 Fogal, P. F., LeBlanc, L. M., and Drummond, J. R.: The Polar Environment Atmospheric Research Laboratory (PEARL):
638 Sounding the Atmosphere at 80 degrees North, Arctic, 66, 377-386, 2013.

639

640 Fuehrer, P.L., Friehe, C.A. Flux Corrections Revisited. *Boundary-Layer Meteorology* 102, 415–458.
641 <https://doi.org/10.1023/A:1013826900579>, 2002.

642

643 Gallagher and Tjernström: Accelerating research in weather prediction and model improvement with new free community
644 open source software tools. To be submitted, 2024.

645

646 Goessling, H. F., Jung, T., Klebe, S., Baeseman, J., Bauer, P., Chen, P., Chevallier, M., Dole, R., Gordon, N., Ruti, P.,
647 Bradley, A., Bromwich, D. H., Casati, B., Chechin, D., Day, J. J., Massonnet, F., Mills, B., Renfrew, I., Smith, G., and
648 Tatusko, R.: Paving the Way for the Year of Polar Prediction, *B Am Meteorol Soc*, 97, Es85-Es88, doi: 10.1175/Bams-D-
649 15-00270.1, 2016.

650

651 Hannula, H. R., Lemmetyinen, J., Kontu, A., Derksen, C., and Pulliainen, J.: Spatial and temporal variation of bulk snow
652 properties in northern boreal and tundra environments based on extensive field measurements, *Geosci Instrum Meth*, 5, 347-
653 363, doi: 10.5194/gi-5-347-2016, 2016.

654

655 Hartten, L. M. and Khalsa, S. J. S.: The H-K Variable SchemaTable developed for the YOPPsiteMIP (1.2), Zenodo,
656 <https://doi.org/10.5281/zenodo.6463464>, 2022.

657

658 Hinkel, K.M. and Nelson, F.E.: Anthropogenic heat island at Barrow, Alaska, during winter: 2001-2005, *J Geophys*
659 *Research*, 112, <https://doi.org/10.1029/2006JD007837>, 2007.

660

661 Holt, J.: Merged Observatory Data File (MODF) for Ny Alesund, Norwegian Meteorological Institute, dataset,
662 <https://doi.org/10.21343/Y89M-6393>, 2023.

663

664 Huang, L., Mariani, Z., and Crawford, R.: MODF for Erik Nielsen Airport, Whitehorse, Canada during YOPP SOP1 and
665 SOP2, Norwegian Meteorological Institute, dataset, <https://doi.org/10.21343/A33E-J150>, 2023a.
666

667 Huang, L., Mariani, Z., and Crawford, R.: MODF for Iqaluit Airport, Iqaluit, Nunavut, Canada during YOPP SOP1 and
668 SOP2, Norwegian Meteorological Institute, dataset, <https://doi.org/10.21343/YRNF-CK57>, 2023b.
669

670 Illingworth, A. J., Cimini, D., Gaffard, C., Haeffelin, M., Lehmann, V., Lohnert, U., O'Connor, E. J., and Ruffieux, D.:
671 Exploiting Existing Ground-Based Remote Sensing Networks to Improve High-Resolution Weather Forecasts, *B Am*
672 *Meteorol Soc*, 96, 2107-2125, doi: 10.1175/Bams-D-13-00283.1, 2015.
673

674 Joe, P., Melo, S., Burrows, W. R., Casati, B., Crawford, R. W., Deghan, A., Gascon, G., Mariani, Z., Milbrandt, J., and
675 Strawbridge, K.: The Canadian Arctic Weather Science Project Introduction to the Iqaluit Site, *B Am Meteorol Soc*, 101,
676 E109-E128, doi: 10.1175/Bams-D-18-0291.1, 2020.
677

678 Jung, T., Gordon, N. D., Bauer, P., Bromwich, D. H., Chevallier, M., Day, J. J., Dawson, J., Doblas-Reyes, F., Fairall, C.,
679 Goessling, H. F., Holland, M., Inoue, J., Iversen, T., Klebe, S., Lemke, P., Losch, M., Makshtas, A., Mills, B., Nurmi, P.,
680 Perovich, D., Reid, P., Renfrew, I. A., Smith, G., Svensson, G., Tolstykh, M., and Yang, Q. H.: Advancing Polar Prediction
681 Capabilities on Daily to Seasonal Time Scales, *B Am Meteorol Soc*, 97, 1631-+, doi: 10.1175/Bams-D-14-00246.1, 2016.
682

683 Kochendorfer, J., M. Earle, D. Hodyss, A. Reverdin, Y-A. Roulet, R. Nitu, R. Rasmussen, S. Landolt, S. Buisan, and T.
684 Laine: Undercatch Adjustments for Tipping-Bucket Gauge Measurements of Solid Precipitation. *J. Hydrometeor.*, 21, 1193–
685 1205, <https://doi.org/10.1175/JHM-D-19-0256.1>, 2020.
686

687 Koltzow, M., Casati, B., Bazile, E., Haiden, T., and Valkonen, T.: An NWP Model Intercomparison of Surface Weather
688 Parameters in the European Arctic during the Year of Polar Prediction Special Observing Period Northern Hemisphere 1,
689 *Weather Forecast*, 34, 959-983, doi: 10.1175/Waf-D-19-0003.1, 2019.
690

691 Lawrence, H., Bormann, N., Sandu, I., Day, J., Farnan, J., and Bauer, P.: Use and impact of Arctic observations in the
692 ECMWF Numerical Weather Prediction system, *Q J Roy Meteor Soc*, 145, 3432-3454, doi: 10.1002/qj.3628, 2019.
693

694 Lesins, G., Duck, T. J., and Drummond, J. R.: Climate trends at Eureka in the Canadian high arctic, *Atmos Ocean*, 48, 59-80,
695 doi: 10.3137/AO1103.2010, 2010.
696

697 Long, C. N. and Shi, Y.: An Automated Quality Assessment and Control Algorithm for Surface Radiation Measurements,
698 *Open Atmospheric Science Journal*, 23-37, doi: 10.2174/1874282300802010023, 2008.
699

700 Luoju, K., Pulliainen, J., Takala, M., Lemmetyinen, J., Mortimer, C., Derksen, C., Mudryk, L., Moisander, M., Hiltunen,
701 M., Smolander, T., Ikonen, J., Cohen, J., Salminen, M., Norberg, J., Veijola, K., and Venalainen, P.: GlobSnow v3.0
702 Northern Hemisphere snow water equivalent dataset, *Sci Data*, 8, <https://doi.org/10.1038/s41597-021-00939-2>, 2021.
703

704 Mariani, Z., Crawford, R., Casati, B., and Lemay, F.: A Multi-Year Evaluation of Doppler Lidar Wind-Profile Observations
705 in the Arctic, *Remote Sens-Basel*, 12, <https://doi.org/10.3390/rs12020323>, 2020.
706

707 Mariani, Z.; Hicks-Jalali, S.; Strawbridge, K.; Gwozdecky, J.; Crawford, R.W.; Casati, B.; Lemay, F.; Lehtinen, R.;
708 Tuominen, P.: Evaluation of Arctic Water Vapor Profile Observations from a Differential Absorption Lidar. *Remote Sens.*
709 2021, 13, 551. <https://doi.org/10.3390/rs13040551>, 2021.

710
711 Mariani, Z., Dehghan, A., Gascon, G., Joe, P., Hudak, D., Strawbridge, K., and Corriveau, J.: Multi-Instrument Observations
712 of Prolonged Stratified Wind Layers at Iqaluit, Nunavut, *Geophys Res Lett*, 45, 1654-1660, doi: 10.1002/2017gl076907,
713 2018.

714
715 Mariani, Z., Hicks-Jalali, S., Strawbridge, K., Gwozdecky, J., Crawford, R. W., Casati, B., Lemay, F., Lehtinen, R., and
716 Tuominen, P.: Evaluation of Arctic Water Vapor Profile Observations from a Differential Absorption Lidar, *Remote Sens.*,
717 13(4), 551, <https://doi.org/10.3390/rs13040551>, 2021.

718
719 Mariani, Z., Huang, G., Crawford, R., Blanchet, J. P., Hicks-Jalali, S., Mekis, E., Pelletier, P., Rodriguez, P., and
720 Strawbridge, K.: Enhanced automated meteorological observations at the Canadian Arctic weather science (CAWS)
721 supersites, *Earth System Science Data*, 14, 4995–5017, <https://doi.org/10.5194/essd-14-4995-2022>, 2022.

722
723 Maturilli, M., Herber, A., and König-Langlo, G.: Climatology and time series of surface meteorology in Ny-Ålesund, Svalbard,
724 *Earth Syst. Sci. Data*, 5, 155–163, <https://doi.org/10.5194/essd-5-155-2013>, 2013.

725
726 Maturilli, M.: Basic and other measurements of radiation at station Ny-Ålesund (2006-05 et seq). Alfred Wegener Institute -
727 Research Unit Potsdam, PANGAEA, <https://doi.org/10.1594/PANGAEA.914927>, 2020a.

728
729 Maturilli, M.: Continuous meteorological observations at station Ny-Ålesund (2011-08 et seq). Alfred Wegener Institute -
730 Research Unit Potsdam, PANGAEA, <https://doi.org/10.1594/PANGAEA.914979>, 2020b.

731
732 Maturilli, M.: High resolution radiosonde measurements from station Ny-Ålesund (2017-04 et seq). Alfred Wegener Institute
733 - Research Unit Potsdam, PANGAEA, <https://doi.org/10.1594/PANGAEA.914973>, 2020c.

734
735 Maturilli, M.: Ceilometer cloud base height from station Ny-Ålesund (2017-08 et seq). Alfred Wegener Institute - Research
736 Unit Potsdam, PANGAEA, <https://doi.org/10.1594/PANGAEA.942331>, 2022.

737
738 Maturilli, M., Hanssen-Bauer, I., Neuber, R., Rex, M., and Edvardsen, K.: The Atmosphere above Ny-Ålesund – Climate
739 and global warming, ozone and surface UV radiation / Hop, H. and Wiencke, C. (editors), *Advances in Polar Ecology, The*
740 *Ecosystem of Kongsfjorden, Svalbard*, Springer, ISBN: 978-3-319-46423-7, doi:10.1007/978-3-319-46425-1_2, 2019.

741
742 Mikola, J., Virtanen, T., Linkosalmi, M., Vaha, E., Nyman, J., Postanogova, O., Rasanen, A., Kotze, D. J., Laurila, T.,
743 Juutinen, S., Kondratyev, V., and Aurela, M.: Spatial variation and linkages of soil and vegetation in the Siberian Arctic
744 tundra - coupling field observations with remote sensing data, *Biogeosciences*, 15, 2781-2801, doi: 10.5194/bg-15-2781-
745 2018, 2018.

746
747 Morris, S. M. and Akish, E.: A-M Variable and Attribute Template Table developed for the YOPPSiteMIP (1.2), Zenodo,
748 <https://doi.org/10.5281/zenodo.6974550>, 2022.

749

750 NCCS: Climate in Svalbard 2100 – a knowledge base for climate adaptation, ISSN 2387-3027,
751 <http://dx.doi.org/10.25607/OBP-888>, 2018.

752

753 O'Connor, E.: Merged observation data file for Sodankyla, Norwegian Meteorological Institute, dataset,
754 <https://doi.org/10.21343/M16P-PQ17>, 2023.

755

756 Ohmura, A., Dutton, E.G., Forgan, B., Frohlich, C., Gilgen, H., Hegner, H., Heimo, A., Konig-Langlo, G., McArther, B.,
757 Muller, G., Philipona, R., Pinker, R., Whitlock, C.H., Dehne, K., and Wild, M.: Baseline Surface Radiation Network
758 (BSRN/WCRP): New Precision Radiometry for Climate Research, *B Am Meteorol Soc*, 79, 2115-2136,
759 [https://doi.org/10.1175/1520-0477\(1998\)079<2115:BSRNBW>2.0.CO;2](https://doi.org/10.1175/1520-0477(1998)079<2115:BSRNBW>2.0.CO;2), 1998.

760

761 Persson, O. and Stone, R.: Evidence of forcing of Arctic regional climates by mesoscale processes, AMS Symposium on
762 Connection Between Mesoscale Processes and Climate Variability, San Antonio, Texas, 15-16 January 2007, 2.6,
763 https://ams.confex.com/ams/87ANNUAL/techprogram/paper_119015.htm, 2007.

764

765 Pollard, W. H. and Bell, T.: Massive Ice Formation in the Eureka Sound Lowlands: A Landscape Model, PERMAFROST -
766 Seventh International Conference, Yellowknife, Canada, Collection Nordicana, 1998.

767

768 Pollard, W. H., Ward, M. A., and Becker, M. S.: The Eureka Sound lowlands: an ice-rich permafrost landscape in transition,
769 Dept. of Geography, McGill University, <https://members.cgs.ca/documents/conference2015/GeoQuebec/papers/402.pdf>,
770 2015.

771

772 Prakash, G., Shrestha, B., Younkin, K., Jundt, R., Martin, M., and Elliott, J.: Data Always Getting Bigger—A Scalable DOI
773 Architecture for Big and Expanding Scientific Data, 1, 11, 2016.

774

775 Rantanen, M., Karpechko, A. Y., Lipponen, A., Nordling, K., Hyvarinen, O., Ruosteenoja, K., Vihma, T., and Laaksonen,
776 A.: The Arctic has warmed nearly four times faster than the globe since 1979, *Commun Earth Environ*,
777 <https://doi.org/10.1038/s43247-022-00498-3>, 2022.

778

779 Rautiainen, K., Parkkinen, T., Lemmetyinen, J., Schwank, M., Wiesmann, A., Ikonen, J., Derksen, C., Davydov, S.,
780 Davydova, A., Boike, J., Langer, M., Drusch, M., and Pulliainen, J.: SMOS prototype algorithm for detecting autumn soil
781 freezing, *Remote Sens Environ*, 180, 346-360, doi: 10.1016/j.rse.2016.01.012, 2016.

782

783 Sellmann, P.V., Brown, J., Lewellen, R., McKim, H.L., Merry, C.J.: The classification and geomorphic implications of thaw
784 lakes on the Arctic coastal plain, Alaska. Cold Regions Research and Engineering Laboratory (CRREL); CRREL-No. 344,
785 <https://hdl.handle.net/11681/5852>, 1975.

786

787 Shupe, M.D.: Clouds at Arctic Atmospheric Observatories. Part II: Thermodynamic Phase Characteristics, *J Appl Meteorol*
788 *Clim*, 50, 645-661, <https://doi.org/10.1175/2010JAMC2468.1>, 2011.

789

790 Shupe, M.D., Walden, V.P., Eloranta, E., Uttal, T., Campbell, J.R., Starkweather, S.M., and Shiobara, M.: Clouds at Arctic
791 Atmospheric Observatories. Part I: Occurrence and Macrophysical Properties, *J Appl Meteorol Clim*, 50, 626-644,
792 <https://doi.org/10.1175/2010JAMC2467.1>, 2011.

793
794 Stone, R.S., Dutton, E.G., Harris, J.M., and Longenecker, D.: Earlier spring snowmelt in northern Alaska as an indicator of
795 climate change, *J Geophys Research*, 107, <https://doi.org/10.1029/2000JD000286>, 2002.
796
797 Tremblay, S., Picard, J.-C., Bachelder, J. O., Lutsch, E., Strong, K., Fogal, P., Leaitch, W. R., Sharma, S., Kolonjari, F., Cox,
798 C. J., Chang, R. Y.-W. and Hayes, P. L.: Characterization of aerosol growth events over Ellesmere Island during the
799 summers of 2015 and 2016, *Atmos. Chem. Phys.*, 19, 5589-5604, doi: 10.5194/acp-19-5589-2019.
800
801 Uttal, T., Makshtas, A. and Laurila, T.: The Tiksi International Hydrometeorological Observatory - An Arctic Members
802 Partnership, *WMO Bulletin Vol 62 (1) – 2013*, 2013.
803
804 Uttal, T., Hartten, L.M., Khalsa, S.J., Casati, B., Svensson, G., Day, J., Gallagher, M., Holt, J., Akish, E., Morris, S.,
805 O'Connor, E., Pirazzini, R., Huang, L., Crawford, R., Mariani, Z., Godoy, Ø., Tjernström, J.A.K., Prakesh, G., Hickmon, N.,
806 Maturilli, M., and Cox, C.: Merged Observatory Data Files (MODFs): An Integrated Research Data Product Supporting
807 Process Oriented Investigations and Diagnostics, 2024, *submitted to Model Intercomparison and Improvement Projects*
808 *(MIIPs) for the polar regions and beyond (GMD/ESSD inter-journal SI) submitted October 17, 2023 – under review 2024*.
809
810 Verlinde, J., Zak, B. D., Shupe, M. D., Ivey, M. D., and Stamnes, K.: The ARM North Slope of Alaska (NSA) Sites, *Meteor*
811 *Mon*, 57, doi: 10.1175/Amsmonographs-D-15-0023.1, 2016.
812
813 Weaver, D., Strong, K., Schneider, M., Rowe, P. M., Sioris, C., Walker, K. A., Mariani, Z., Uttal, T., McElroy, C. T.,
814 Vömel, H., Spassiani, A., and Drummond, J. R.: Intercomparison of atmospheric water vapour measurements at a
815 Canadian High Arctic site, *Atmos. Meas. Tech.*, 10, 2851–2880, <https://doi.org/10.5194/amt-10-2851-2017>, 2017.
816
817 Widener, K., Bharadwaj, N., and Johnson, K.: Ka-Band ARM Zenith Radar (KAZR) Instrument Handbook, United States
818 Department of Energy (USDOE), <https://doi.org/10.2172/1035855>, 2012.
819
820 WMO: Guide to Meteorological Instruments and Methods of Observation. WMO-No.8, Geneva, Switzerland, ISBN: 978-
821 92-63-10008-5, <https://library.wmo.int/idurl/4/68662>, 2021.
822
823 Wohner, C., Peterseil, J., and Klug, H.: Designing and implementing a data model for describing environmental monitoring
824 and research sites, *Ecol Inform*, 70, <https://doi.org/10.1016/j.ecoinf.2022.101708>, 2022.
825
826 Younkin, K. and Long, C.: Improved Correction of IR Loss in Diffuse Shortwave Measurements: An ARM Value-Added
827 Product, PNNL; Richland, WA, United States, Medium: ED, doi: 10.2172/1020732, 2003.
828
829
830
831
832
833

834
835
836
837

Table 1. List of facility coordinates for locations where $MODF_{\text{ysm}}$ measurements were collected at each site. The measured variables that are observed at each site are listed (refer to Table 3). In some cases, the same variable is measured at multiple locations for a single site; these observations and their corresponding coordinates are embedded within the MODF. “All” refers to the entire list of the measured variables in Table 3, whereas “All radiation” refers to all radiation-related measured variables.

	Facility Name	Coordinates	Measured Variables (from Table 3)
Whitehorse	Whitehorse	N60.71, W135.07	All
Iqaluit	Iqaluit	N63.74, W68.51	All
Sodankylä	Operative Sounding Station Area; Automatic Weather Station (LUOxxxx)	N67.366618 – N67.367220, E26.628253 - E26.63144	Pressure, Visibility
	CO2 Flux Mast Area (VUOxxxx)	N67.361883, E26.643003 - E26.64323	Total precipitation of water, all wind, vertical velocity, temperature, dew-point temperature, relative humidity, snow thickness, all radiation, cloud base height
	Intensive Observation Area (IOAxxxx)	N67.361654 - N67.361950, E26.633190 - E26.634191	Temperature, relative humidity, snow thickness, snowfall flux, snow water equivalent, all short-wave radiation, soil temperature profile, soil moisture, snow temperature
	Lichen Fence (JAKxxxx)	N67.36710 - N67.36716, E26.634740 - E26.63513	All radiation
	Micrometeorological Mast Area (METxxxx)	N67.361711 - N67.36216, E26.63726 - E26.65117	All wind, temperature, vertical velocity, relative humidity, snow thickness, all radiation, all heat fluxes, friction velocity, soil temperature profile, soil moisture, snow temperature
	Peatland Area (SUOxxxx)	N67.361903 - N67.36707, E26.633802 - E26.654067	Temperature, dew-point temperature, relative humidity, snow thickness, all short-wave radiation, soil temperature profile, soil moisture, snow temperature
Utqiagvik	ARM Facility	N71.19228, W156.3654	All except ozone concentration, snow thickness, and soil temperature profile
	GML Barrow Atmospheric Baseline Observatory	N71.3230, W156.6114	Ozone concentration, snow thickness, and soil temperature profile
Tiksi	Baseline Surface Radiation Network (BSRN)	N71.5862, E128.9188	All radiation observations
	Fluxtower	N71.595, E128.882	All except radiation observations
Ny-Ålesund	Baseline Surface Radiation Network (BSRN)	N78.92278, E11.92725	All radiation observations, pressure, cloud base height
	AWIPEV Met.Tower	N78.92226, E11.92667	All wind, temperature, relative humidity, specific humidity
	Balloon Launch Facility	N78.92301, E11.92271	All timeSeriesProfileSonde observations

Eureka	Baseline Surface Radiation Network (BSRN)	N79.989, W85.9404	All radiation observations
	Fluxtower	N80.083, W86.417	Pressure, all wind, temperature, relative humidity, snow thickness, ground heat flux, soil temperature profile
	Sonde Launch	N79.9833, W85.9333	All timeSeriesProfileSonde observations

838
839

840 **Table 2.** List of final DOIs for each site's MODF_{ysm}.

	DOI	Title	Citation
Whitehorse	https://doi.org/10.21343/a33e-j150	MODF for Erik Nielsen Airport, Whitehorse, Canada during YOPP SOP1 and SOP2	Huang et al., 2023a
Iqaluit	https://doi.org/10.21343/yrnf-ck57	MODF for Iqaluit Airport, Iqaluit, Nunavut, Canada during YOPP SOP1 and SOP2	Huang et al., 2023b
Sodankylä	https://doi.org/10.21343/m16p-pq17	Merged observation data file for Sodankylä	O'Connor, 2023
Utqiagvik	https://doi.org/10.21343/a2dx-nq55	MODF for Utqiagvik, Alaska, during YOPP SOP1 and SOP2	Akish and Morris, 2023c
Tiksi	https://doi.org/10.21343/5bwn-w881	MODF for Tiksi, Russia, during YOPP SOP1 and SOP2	Akish and Morris, 2023b
Ny-Ålesund	https://doi.org/10.21343/y89m-6393	Merged Observatory Data File (MODF) for Ny Ålesund	Holt, 2023
Eureka	https://doi.org/10.21343/r85j-tc61	MODF for Eureka, Canada, during YOPP SOP1 and SOP2	Akish and Morris, 2023a

841

842

843

844
845
846
847
848

Table 3. List of the geophysical variables currently included in each site’s MODF. Note that this table only includes variables currently in the existing MODF_{ysm}, and does not indicate the complete list of variables that are observed at each site. An asterisk (*) denotes a variable not included in the H-K table (Hartten and Khalsa, 2022) and a double asterisk (**) denotes a calculated variable. The level and type(s) of additional processing for the heat fluxes are also provided, where EC = eddy covariance and bulk = bulk method.

MODF featureType	Measured Variables	Whitehorse	Iqaluit	Sodankylä	Utqiaġvik	Tiksi	Ny-Ålesund	Eureka
		lat: 60.71 N lon: 135.07 W	lat: 63.74 N lon: 68.51 W	lat: 67.367 N lon: 26.629 E	lat: 71.325 N lon: 156.625 W	lat: 71.596 N lon: 128.889 E	lat: 78.923 N lon: 11.926 E	lat: 80.083 N lon: 86.417 W
timeSeries Variables	Pressure (Pa)	surface	surface	surface, mean sea-level	surface	surface	surface	surface
	Total precipitation of water in all phases per unit area (kg m ⁻² s ⁻¹)	surface	surface	surface			surface	
	Eastward Wind (m s ⁻¹)	surface	near-surface	near-surface	near-surface (2m)	near-surface (4m)	near-surface (10m)	near-surface (6m)
	Northward Wind (m s ⁻¹)	surface	near-surface	near-surface	near-surface (2m)	near-surface (4m)	near-surface (10m)	near-surface (6m)
	*Wind gust (m s ⁻¹)			near-surface (10m)				
	Vertical velocity (m s ⁻¹)			near surface (2 m)				
	Temperature (K)	near-surface (2m)	near-surface (2m)	skin, near- surface (2m)	skin, near- surface (2m)	skin, near- surface (2m)	near-surface (2m)	skin, near- surface (2m)
	Dew-point Temperature (K)	near-surface (2m)	near-surface (2m)	near-surface (2m)	near-surface (2m)			
	Relative Humidity (1 or %)	near-surface (2m)	near-surface (2m)	near-surface (2m)	near-surface (2m)	near-surface (2m)	near-surface (2m)	near-surface (2m)
	Specific Humidity (1 or kg kg ⁻¹)						near-surface (2m)	
	Ozone Concentration in Air (mole fraction)				surface			
	Snow thickness (m)		surface	surface	surface	surface		surface
	Snowfall Flux (kg m ⁻¹ s ⁻²)				surface	surface		
	Snow water equivalent (kg m ⁻²)				surface			
	Upward Short-wave Radiation (W m ⁻²)		surface	surface	surface	surface	surface	surface
	Downward Short-wave Radiation (W m ⁻²)		surface	surface	surface	surface	surface	surface
	Upward Long-wave Radiation (W m ⁻²)		surface	surface	surface	surface	surface	
	Downward Long-wave Radiation (W m ⁻²)		surface	surface	surface	surface	surface	surface
	Net Short-wave Radiation at the Surface (W m ⁻²)			surface	surface			
	*Horizontal East-facing Long-wave Radiation (W m ⁻²)		surface					
	*Horizontal West-facing Long-wave Radiation (W m ⁻²)		surface					
	*Horizontal South-facing Long-wave Radiation (W m ⁻²)		surface					
	*Horizontal North-facing Long-wave Radiation (W m ⁻²)		surface					
	**Turbulent Latent Heat Flux (W m ⁻²)				surface (EC)	surface (EC, bulk)		
	**Turbulent Sensible Heat Flux (W m ⁻²)				surface (EC)	surface (EC, bulk)		
	**Turbulent time-average eastward stress (Pa)				surface (EC)	surface		
	**Turbulent time-average northward stress (Pa)					surface		
	*Friction Velocity (m s ⁻¹)				surface (EC)			
	Cloud Base Height (m)	ground-based remote sensing	ground-based remote sensing	ground-based remote sensing				ground-based remote sensing
	Ground Heat Flux (W m ⁻²)				near-surface	near-surface	near-surface	
	Visibility (m)				near-surface			

timeSeriesProfile Variables	Atmospheric pressure (Pa)	near-surface (2m, 10m)					
	Total precipitation of water in all phases per unit area (kg m ⁻² s ⁻¹)	near-surface (2m, 10m)					
	Eastward Wind (m s ⁻¹)	near-surface (2m, 10m)	near-surface (18m, 32m, 38m, 48m)	near-surface (2m, 10m, 20m, 40m)	near-surface (2m, 10m)	near-surface (6m, 11m)	
	Northward Wind (m s ⁻¹)	near-surface (2m, 10m)	near-surface (18m, 32m, 38m, 48m)	near-surface (2m, 10m, 20m, 40m)	near-surface (2m, 10m)	near-surface (6m, 11m)	
	Temperature (K)	near-surface (2m, 10m)	near-surface (3m, 8m, 18m, 32m, 48m)	near-surface (2m, 10m, 20m, 40m)	near-surface (2m, 6m, 10m)	near-surface (2m, 10m)	near-surface (2m, 6m, 10m)
	Dew-point Temperature (K)			near-surface (2m, 10m, 20m, 40m)			
	Relative Humidity (1 or %)	near-surface (2m, 10m)	near-surface (3m, 8m, 18m, 32m, 48m)	near-surface (2m, 10m, 20m, 40m)	near-surface (2m, 6m, 10m)	near-surface (2m, 6m, 10m)	
	Soil Temperature Profile (K)	sub-surface (5cm, 30cm)		sub-surface (5cm, 10cm, 15cm, 20cm, 25cm, 30cm, 45cm, 70cm, 95cm, 120cm)	sub-surface (5cm, 10cm, 15cm, 20cm, 25cm, 30cm, 45cm, 70cm, 95cm, 120cm)	sub-surface (5cm, 10cm, 15cm, 20cm, 25cm, 30cm, 45cm, 70cm, 95cm, 120cm)	
	Soil Moisture (kg m ⁻³)	sub-surface (5cm, 30cm)					
	Snow Temperature (K)			near-surface (10cm, 20cm, 30cm, 40cm, 50cm, 60cm, 70cm, 80cm, 90cm, 100cm, 110cm)			
timeSeriesProfileS onde Variables	Atmospheric pressure (Pa)	radiosonde	radiosonde	radiosonde	radiosonde		
	Eastward Wind (m s ⁻¹)	radiosonde	radiosonde	radiosonde	radiosonde		
	Northward Wind (m s ⁻¹)	radiosonde	radiosonde	radiosonde	radiosonde		
	Temperature (K)	radiosonde	radiosonde	radiosonde	radiosonde		
	Dew-point Temperature (K)	radiosonde	radiosonde	radiosonde	radiosonde		
	Specific Humidity (1 or kg kg ⁻¹)				Radiosonde		
	Relative Humidity (1 or %)	radiosonde	radiosonde	radiosonde	radiosonde		

* Denotes a variable NOT included in the H-K Table

** Denotes a calculated variable (not a direct observation)

849

850

851

852

853

854

Table 4. List of the instruments that contributed to the Whitehorse MODF, including details about the instrument manufacturer, measured variables, configuration, temporal resolution, measurement uncertainty, and quality control applied.

<u>MODF featureType</u>	<u>Instrument</u>	<u>Manufacturer</u>	<u>Measured variables</u>	<u>Instrument Configuration</u>	<u>Temporal Resolution</u>	<u>Uncertainty (+/-)</u>	<u>Quality Control</u>
timeSeries Variables	WXT52 0	Vaisala	Atmospheric pressure (Pa)	Solid-state, all-in-one weather instrument in standard aspirated configuration mounted on a pole. No bird spike kit used.	1 min	0.5 hPa	Beyond the standard Vaisala processing, observations were checked against site-based climatology ranges and the rate of change thresholds, which were based on hourly criteria. Observations that fell outside of the 3-sigma normal climatological range were rejected, as were observations that had a rate of change greater than a seasonal-dependant threshold (e.g., >20 hPa/hr change).
timeSeries Variables	WXT52 0	Vaisala	Total precipitation of water in all phases per unit area (kg m ⁻² s ⁻¹)	Solid-state, all-in-one weather instrument in standard aspirated configuration mounted on a pole. No bird spike kit used.	1 min	5%	Beyond the standard Vaisala processing, observations were checked against site-based climatology ranges and the rate of change thresholds, which were based on hourly criteria. Observations that fell outside of the 3-sigma normal climatological range were rejected, as were observations that had a rate of change greater than a seasonal-dependant threshold (e.g., > 10 mm/hr change). No corrections for solid precipitation under-catchment were performed (the dataset is raw in the MODF); where appropriate, users are recommended to process under-catchment corrections via Kochendorfer et al. (2020) (note: undercatchment is less of an issue for the WXT520 observations compared to Pluvio2).
timeSeries Variables	WXT52 0	Vaisala	Eastward Wind (m s ⁻¹)	Solid-state, all-in-one weather instrument in standard aspirated configuration mounted on a pole. No bird spike kit used.	1 min	0.3 ms ⁻¹	Beyond the standard Vaisala processing, observations were checked against site-based climatology ranges and the rate of change thresholds, which were based on hourly criteria. Observations that fell outside of the 3-sigma normal climatological range were rejected, as were observations that had a rate of change greater than a seasonal-dependant threshold (e.g., > 10 m/s/hr change).
timeSeries Variables	WXT52 0	Vaisala	Northward Wind (m s ⁻¹)	Solid-state, all-in-one weather instrument in standard aspirated configuration mounted on a pole. No bird spike kit used.	1 min	0.3 ms ⁻¹	Beyond the standard Vaisala processing, observations were checked against site-based climatology ranges and the rate of change thresholds, which were based on hourly criteria. Observations that fell outside of the 3-sigma normal climatological range were rejected, as were observations that had a rate of change greater than a seasonal-dependant threshold (e.g., > 10 m/s/hr change).

timeSeries Variables	WXT52 0	Vaisala	Temperature (K)	Solid-state, all-in-one weather instrument in standard aspirated configuration mounted on a pole. No bird spike kit used.	1 min	0.3 K	The shelter heating effect is uncorrected beyond the Vaisala standard processing. Beyond the standard Vaisala processing, observations were checked against site-based climatology ranges and the rate of change thresholds, which were based on hourly criteria. Observations that fell outside of the 3-sigma normal climatological range were rejected, as were observations that had a rate of change greater than a seasonal-dependant threshold (e.g., > 5 K/hr change).
timeSeries Variables	WXT52 0	Vaisala	Relative Humidity (1 or %)	Solid-state, all-in-one weather instrument in standard aspirated configuration mounted on a pole. No bird spike kit used.	1 min	3%	The humidity is not corrected in a sub-freezing environment, beyond the standard Vaisala processing. Beyond the standard Vaisala processing, observations were checked against site-based climatology ranges and the rate of change thresholds, which were based on hourly criteria. Observations that fell outside of the 3-sigma normal climatological range were rejected, as were observations that had a rate of change greater than a seasonal-dependant threshold (e.g., > 30 %/hr change).
timeSeries Variables	WXT52 0	Vaisala	Dew-point Temperature (K)	Solid-state, all-in-one weather instrument in standard aspirated configuration mounted on a pole. No bird spike kit used.	1 min	0.5 K	The shelter heating effect is uncorrected and humidity is not corrected in a sub-freezing environment, beyond the standard Vaisala processing. Beyond the standard Vaisala processing, observations were checked against site-based climatology ranges and the rate of change thresholds, which were based on hourly criteria. Observations that fell outside of the 3-sigma normal climatological range were rejected, as were observations that had a rate of change greater than a seasonal-dependant threshold (e.g., > 5 K/hr change).
timeSeries Profile Variables	CL51	Vaisala	Cloud Base Height (m)	Proprietary algorithm determines the lowest cloud base height	1 min	5 m	No QC was performed, beyond the standard Vaisala proprietary algorithm that retrieves cloud base height.
timeSeries ProfileSonde Variables	RS92 / DFM-09	Vaisala / GRAW	Atmospheric pressure (Pa)	Standard radiosonde launch	6 hr	0.5 hPa	Vaisala also processed the raw data feed from the radiosonde observations, which was obtained at 2 s resolution. Data were binned into 10-meter intervals of geopotential height and all measurements within each bin were averaged. No additional QC was performed beyond Vaisala's standard radiosonde processing.
timeSeries ProfileSonde Variables	RS92 / DFM-09	Vaisala / GRAW	Eastward Wind (m s ⁻¹)	Standard radiosonde launch	6 hr	0.15 ms ⁻¹	Vaisala also processed the raw data feed from the radiosonde observations, which was obtained at 2 s resolution. Data were binned into 10-meter intervals of geopotential height and all measurements within each bin were averaged. No additional QC was performed beyond Vaisala's standard radiosonde processing.

timeSeries ProfileSo nde Variables	RS92 / DFM- 09	Vaisala / GRAW	Northward Wind (m s^{-1})	Standard launch	radiosonde	6 hr	0.15 ms^{-1}	Vaisala also processed the raw data feed from the radiosonde observations, which was obtained at 2 s resolution. Data were binned into 10-meter intervals of geopotential height and all measurements within each bin were averaged. No additional QC was performed beyond Vaisala's standard radiosonde processing.
timeSeries ProfileSo nde Variables	RS92 / DFM- 09	Vaisala / GRAW	Temperature (K)	Standard launch	radiosonde	6 hr	0.15 K	Vaisala also processed the raw data feed from the radiosonde observations, which was obtained at 2 s resolution. Data were binned into 10-meter intervals of geopotential height and all measurements within each bin were averaged. No additional QC was performed beyond Vaisala's standard radiosonde processing.
timeSeries ProfileSo nde Variables	RS92 / DFM- 09	Vaisala / GRAW	Dew-point Temperature (K)	Standard launch	radiosonde	6 hr	0.5 K	Vaisala also processed the raw data feed from the radiosonde observations, which was obtained at 2 s resolution. Data were binned into 10-meter intervals of geopotential height and all measurements within each bin were averaged. No additional QC was performed beyond Vaisala's standard radiosonde processing.

857

858

859

Table 5. List of the instruments that contributed to the Iqaluit MODF, including details about the instrument manufacturer, measured variables, configuration, temporal resolution, measurement uncertainty, and quality control applied.

<u>MODF featureType</u>	<u>Instrument</u>	<u>Manufacturer</u>	<u>Measured variables</u>	<u>Instrument Configuration</u>	<u>Temporal Resolution</u>	<u>Uncertainty (+/-)</u>	<u>Quality Control</u>
timeSeries Variables	PTB11 0	Vaisala	Pressure (Pa)	Installed within a naturally vented protective enclosure.	1 min	0.3 hPa	Beyond the standard Vaisala processing, observations were checked against site-based climatology ranges and the rate of change thresholds, which were based on hourly criteria. Observations that fell outside of the 3-sigma normal climatological range were rejected, as were observations that had a rate of change greater than a seasonal-dependant threshold (e.g., >20 hPa/hr change).
timeSeries Variables	Pluvio2	OTT	Total precipitation of water in all phases per unit area (kg m ⁻² s ⁻¹)	Single Alter shield	1 min	5%	Beyond the standard Vaisala processing, observations were checked against site-based climatology ranges and the rate of change thresholds, which were based on hourly criteria. Observations that fell outside of the 3-sigma normal climatological range were rejected, as were observations that had a rate of change greater than a seasonal-dependant threshold (e.g., > 10 mm/hr change). No corrections for solid precipitation under-catchment were performed (the dataset is raw in the MODF); where appropriate, users are recommended to process under-catchment corrections via Kochendorfer et al. (2020).
timeSeries Variables	Wind monitor 5103	RM Young	Eastward Wind (m s ⁻¹)	Four-blade helicoid propeller in standard configuration with a wind vane to measure wind direction	1 min	0.3 ms ⁻¹	Beyond the standard Vaisala processing, observations were checked against site-based climatology ranges and the rate of change thresholds, which were based on hourly criteria. Observations that fell outside of the 3-sigma normal climatological range were rejected, as were observations that had a rate of change greater than a seasonal-dependant threshold (e.g., > 10 m/s/hr change).
timeSeries Variables	Wind monitor 5103	RM Young	Northward Wind (m s ⁻¹)	Four-blade helicoid propeller in standard configuration with a wind vane to measure wind direction	1 min	0.3 ms ⁻¹	Beyond the standard Vaisala processing, observations were checked against site-based climatology ranges and the rate of change thresholds, which were based on hourly criteria. Observations that fell outside of the 3-sigma normal climatological range were rejected, as were observations that had a rate of change greater than a seasonal-dependant threshold (e.g., > 10 m/s/hr change).
timeSeries Variables	HMP35 D	Vaisala	Temperature (K)	Sensor installed in shaded, naturally vented shelter.	1 min	0.1 K	The shelter heating effect is uncorrected beyond the Vaisala standard processing. Beyond the standard Vaisala processing, observations were checked against site-based climatology ranges and the rate of change thresholds, which were based on hourly criteria. Observations that fell outside of the 3-sigma normal climatological range were rejected, as were observations that

had a rate of change greater than a seasonal-dependant threshold (e.g., > 5 K/hr change).

timeSeries Variables	HMP35 D	Vaisala	Dew-point Temperature (K)	Sensor installed in shaded, naturally vented shelter.	1 min	0.2 K	The shelter heating effect is uncorrected and humidity is not corrected in a sub-freezing environment, beyond the standard Vaisala processing. Beyond the standard Vaisala processing, observations were checked against site-based climatology ranges and the rate of change thresholds, which were based on hourly criteria. Observations that fell outside of the 3-sigma normal climatological range were rejected, as were observations that had a rate of change greater than a seasonal-dependant threshold (e.g., > 5 K/hr change).
timeSeries Variables	HMP35 D	Vaisala	Relative Humidity (1 or %)	Sensor installed in shaded, naturally vented shelter.	1 min	0.8%	The humidity is not corrected in a sub-freezing environment, beyond the standard Vaisala processing. Beyond the standard Vaisala processing, observations were checked against site-based climatology ranges and the rate of change thresholds, which were based on hourly criteria. Observations that fell outside of the 3-sigma normal climatological range were rejected, as were observations that had a rate of change greater than a seasonal-dependant threshold (e.g., > 30 %/hr change).
timeSeries Variables	SR50A	Campbell Scientific	Snow thickness (m)	Sonic distance sensor at 50KHz with a perforated flat target base levelled at the surface (0 m a.g.l.)	1 min	1 cm	Observations were checked against site-based climatology ranges and the rate of change thresholds, which were based on hourly criteria. Observations that fell outside of the 3-sigma normal climatological range were rejected, as were observations that had a rate of change greater than a seasonal-dependant threshold (e.g., > 20 cm/hr change).
timeSeries Variables	CMP10 L	Kipp and Zonen	Upward Short-wave Radiation ($W m^{-2}$)	Integrated levelling included, dome, RM Young radiation shield (6 plate), and a CVF4L Ventilation System with Integrated Heater running when temperatures were near zero to prevent frost	1 min	$7 W m^{-2}$	Data is raw and no additional QC was performed, other than the processing performed by Kipp and Zonen. No additional QC was performed on these observations to account for potential frost or snow deposition on the sensors. Data should be treated with caution since they typically require additional QC processing prior to analysis.
timeSeries Variables	CMP10 L	Kipp and Zonen	Downward Short-wave Radiation ($W m^{-2}$)	Integrated levelling included, dome, RM Young radiation shield (6 plate), and a CVF4L Ventilation System with Integrated Heater running when temperatures were	1 min	$7 W m^{-2}$	Data is raw and no additional QC was performed, other than the processing performed by Kipp and Zonen. No additional QC was performed on these observations to account for potential frost or snow deposition on the sensors. Data should be treated with caution

				near zero to prevent frost			since they typically require additional QC processing prior to analysis.
timeSeries Variables	CGR4L	Kipp and Zonen	Upward Long-wave Radiation (W m ⁻²)	Integrated levelling included, dome, RM Young radiation shield (6 plate), and a CVF4L Ventilation System with Integrated Heater running when temperatures where near zero to prevent frost	1 min	7 W m ⁻²	Data is raw and no additional QC was performed, other than the processing performed by Kipp and Zonen. No additional QC was performed on these observations to account for potential frost or snow deposition on the sensors. Data should be treated with caution since they typically require additional QC processing prior to analysis.
timeSeries Variables	CGR4L	Kipp and Zonen	Downward Long-wave Radiation (W m ⁻²)	Integrated levelling included, dome, RM Young radiation shield (6 plate), and a CVF4L Ventilation System with Integrated Heater running when temperatures where near zero to prevent frost	1 min	7 W m ⁻²	Data is raw and no additional QC was performed, other than the processing performed by Kipp and Zonen. No additional QC was performed on these observations to account for potential frost or snow deposition on the sensors. Data should be treated with caution since they typically require additional QC processing prior to analysis.
timeSeries Variables	CGR4L	Kipp and Zonen	*Horizontal East-facing Long-wave Radiation (W m ⁻²)	Integrated levelling included, dome, RM Young radiation shield (6 plate), and a CVF4L Ventilation System with Integrated Heater running when temperatures where near zero to prevent frost	1 min	7 W m ⁻²	Data is raw and no additional QC was performed, other than the processing performed by Kipp and Zonen. No additional QC was performed on these observations to account for potential frost or snow deposition on the sensors. Data should be treated with caution since they typically require additional QC processing prior to analysis.
timeSeries Variables	CGR4L	Kipp and Zonen	*Horizontal West-facing Long-wave Radiation (W m ⁻²)	Integrated levelling included, dome, RM Young radiation shield (6 plate), and a CVF4L Ventilation System with Integrated Heater running when temperatures where near zero to prevent frost	1 min	7 W m ⁻²	Data is raw and no additional QC was performed, other than the processing performed by Kipp and Zonen. No additional QC was performed on these observations to account for potential frost or snow deposition on the sensors. Data should be treated with caution since they typically require additional QC processing prior to analysis.
timeSeries Variables	CGR4L	Kipp and Zonen	*Horizontal South-facing Long-wave Radiation (W m ⁻²)	Integrated levelling included, dome, RM Young radiation shield (6 plate), and a CVF4L Ventilation System with Integrated Heater running when temperatures where near zero to prevent frost	1 min	7 W m ⁻²	Data is raw and no additional QC was performed, other than the processing performed by Kipp and Zonen. No additional QC was performed on these observations to account for potential frost or snow deposition on the sensors. Data should be treated with caution since they typically require additional QC processing prior to analysis.

timeSeries Variables	CGR4L	Kipp and Zonen	*Horizontal North-facing Long-wave Radiation (W m ⁻²)	Integrated levelling included, dome, RM Young radiation shield (6 plate), and a CVF4L Ventilation System with Integrated Heater running when temperatures where near zero to prevent frost	1 min	7 W m ⁻²	Data is raw and no additional QC was performed, other than the processing performed by Kipp and Zonen. No additional QC was performed on these observations to account for potential frost or snow deposition on the sensors. Data should be treated with caution since they typically require additional QC processing prior to analysis.
timeSeries Profile Variables	CL51	Vaisala	Cloud Base Height (m)	Proprietary algorithm determines the lowest cloud base height	1 min	5 m	No QC was performed, beyond the standard Vaisala proprietary algorithm that retrieves cloud base height.
timeSeries Profile Variables	WXT52 0	Vaisala	Atmospheric pressure (Pa)	Solid-state, all-in-one weather instrument in standard aspirated configuration mounted on a pole. No bird spike kit used.	1 min	0.5 hPa	Beyond the standard Vaisala processing, observations were checked against site-based climatology ranges and the rate of change thresholds, which were based on hourly criteria. Observations that fell outside of the 3-sigma normal climatological range were rejected, as were observations that had a rate of change greater than a seasonal-dependant threshold (e.g., >20 hPa/hr change).
timeSeries Profile Variables	WXT52 0	Vaisala	Total precipitation of water in all phases per unit area (kg m ⁻² s ⁻¹)	Solid-state, all-in-one weather instrument in standard aspirated configuration mounted on a pole. No bird spike kit used.	1 min	5%	Beyond the standard Vaisala processing, observations were checked against site-based climatology ranges and the rate of change thresholds, which were based on hourly criteria. Observations that fell outside of the 3-sigma normal climatological range were rejected, as were observations that had a rate of change greater than a seasonal-dependant threshold (e.g., > 10 mm/hr change). No corrections for solid precipitation under-catchment were performed (the dataset is raw in the MODF); where appropriate, users are recommended to process under-catchment corrections via Kochendorfer et al. (2020) (note: undercatchment is less of an issue for the WXT520 observations compared to Pluvio2).
timeSeries Profile Variables	WXT52 0	Vaisala	Eastward Wind (m s ⁻¹)	Solid-state, all-in-one weather instrument in standard aspirated configuration mounted on a pole. No bird spike kit used.	1 min	0.3 ms ⁻¹	Beyond the standard Vaisala processing, observations were checked against site-based climatology ranges and the rate of change thresholds, which were based on hourly criteria. Observations that fell outside of the 3-sigma normal climatological range were rejected, as were observations that had a rate of change greater than a seasonal-dependant threshold (e.g., > 10 m/s/hr change).
timeSeries Profile Variables	WXT52 0	Vaisala	Northward Wind (m s ⁻¹)	Solid-state, all-in-one weather instrument in standard aspirated configuration mounted on a pole. No bird spike kit used.	1 min	0.3 ms ⁻¹	Beyond the standard Vaisala processing, observations were checked against site-based climatology ranges and the rate of change thresholds, which were based on hourly criteria. Observations that fell outside of the 3-sigma normal climatological range were rejected, as were observations that had a rate of change

greater than a seasonal-dependant threshold (e.g., > 10 m/s/hr change).

timeSeries Profile Variables	WXT52 0	Vaisala	Temperature (K)	Solid-state, all-in-one weather instrument in standard aspirated configuration mounted on a pole. No bird spike kit used.		1 min	0.3 K	The shelter heating effect is uncorrected beyond the Vaisala standard processing. Beyond the standard Vaisala processing, observations were checked against site-based climatology ranges and the rate of change thresholds, which were based on hourly criteria. Observations that fell outside of the 3-sigma normal climatological range were rejected, as were observations that had a rate of change greater than a seasonal-dependant threshold (e.g., > 5 K/hr change).
timeSeries Profile Variables	WXT52 0	Vaisala	Relative Humidity (1 or %)	Solid-state, all-in-one weather instrument in standard aspirated configuration mounted on a pole. No bird spike kit used.		1 min	3%	The humidity is not corrected in a sub-freezing environment, beyond the standard Vaisala processing. Beyond the standard Vaisala processing, observations were checked against site-based climatology ranges and the rate of change thresholds, which were based on hourly criteria. Observations that fell outside of the 3-sigma normal climatological range were rejected, as were observations that had a rate of change greater than a seasonal-dependant threshold (e.g., > 30 %/hr change).
timeSeries ProfileSo nde Variables	RS92 / DFM- 09	Vaisala / GRAW	Atmospheric pressure (Pa)	Standard launch	radiosonde	6 hr	0.5 hPa	Vaisala also processed the raw data feed from the radiosonde observations, which was obtained at 2 s resolution. Data were binned into 10-meter intervals of geopotential height and all measurements within each bin were averaged. No additional QC was performed beyond Vaisala's standard radiosonde processing.
timeSeries ProfileSo nde Variables	RS92 / DFM- 09	Vaisala / GRAW	Eastward Wind (m s ⁻¹)	Standard launch	radiosonde	6 hr	0.15 ms ⁻¹	Vaisala also processed the raw data feed from the radiosonde observations, which was obtained at 2 s resolution. Data were binned into 10-meter intervals of geopotential height and all measurements within each bin were averaged. No additional QC was performed beyond Vaisala's standard radiosonde processing.
timeSeries ProfileSo nde Variables	RS92 / DFM- 09	Vaisala / GRAW	Northward Wind (m s ⁻¹)	Standard launch	radiosonde	6 hr	0.15 ms ⁻¹	Vaisala also processed the raw data feed from the radiosonde observations, which was obtained at 2 s resolution. Data were binned into 10-meter intervals of geopotential height and all measurements within each bin were averaged. No additional QC was performed beyond Vaisala's standard radiosonde processing.

timeSeries ProfileSo nde Variables	RS92 / DFM- 09	Vaisala / GRAW	Temperature (K)	Standard launch	radiosonde	6 hr	0.15 K	Vaisala also processed the raw data feed from the radiosonde observations, which was obtained at 2 s resolution. Data were binned into 10-meter intervals of geopotential height and all measurements within each bin were averaged. No additional QC was performed beyond Vaisala's standard radiosonde processing.
timeSeries ProfileSo nde Variables	RS92 / DFM- 09	Vaisala / GRAW	Dew-point Temperature (K)	Standard launch	radiosonde	6 hr	0.5 K	Vaisala also processed the raw data feed from the radiosonde observations, which was obtained at 2 s resolution. Data were binned into 10-meter intervals of geopotential height and all measurements within each bin were averaged. No additional QC was performed beyond Vaisala's standard radiosonde processing.

862

863

864

Table 6. List of the instruments that contributed to the Sodankylä MODF, including details about the instrument manufacturer, measured variables, configuration, temporal resolution, measurement uncertainty, and quality control applied.

<u>MODF featureType</u>	<u>Instrument</u>	<u>Manufacturer</u>	<u>Measured variables</u>	<u>Instrument Configuration</u>	<u>Temporal Resolution</u>	<u>Uncertainty (+/-)</u>	<u>Quality Control</u>
timeSeries Variables	PT100	Vaisala	Temperature (K)	Sensor installed in shaded, naturally vented shelter.	10 min	0.1 K	The shelter heating effect is uncorrected beyond the Vaisala standard processing. Beyond the standard Vaisala processing, observations were checked against site-based climatology ranges and the rate of change thresholds, which were based on hourly criteria. Observations that fell outside of the 3-sigma normal climatological range were rejected, as were observations that had a rate of change greater than a seasonal-dependant threshold (e.g., > 5 K/hr change).
timeSeries Variables	PT100	generic	Temperature (K)	Sensor installed in shaded, naturally vented shelter.	10 min	0.3 K	The shelter heating effect is uncorrected beyond the Vaisala standard processing. Beyond the standard Vaisala processing, observations were checked against site-based climatology ranges and the rate of change thresholds, which were based on hourly criteria. Observations that fell outside of the 3-sigma normal climatological range were rejected, as were observations that had a rate of change greater than a seasonal-dependant threshold (e.g., > 5 K/hr change).
timeSeries Variables	PT100	Pentronic	Temperature (K)	Sensor installed in shaded, naturally vented shelter.	10 min	0.3 K	The shelter heating effect is uncorrected beyond the Vaisala standard processing. Beyond the standard Vaisala processing, observations were checked against site-based climatology ranges and the rate of change thresholds, which were based on hourly criteria. Observations that fell outside of the 3-sigma normal climatological range were rejected, as were observations that had a rate of change greater than a seasonal-dependant threshold (e.g., > 5 K/hr change).
timeSeries Variables	HMP155	Vaisala	Temperature (K)	Sensor installed in shaded, naturally vented shelter.	10 min	0.1 K	The shelter heating effect is uncorrected beyond the Vaisala standard processing. Beyond the standard Vaisala processing, observations were checked against site-based climatology ranges and the rate of change thresholds, which were based on hourly criteria. Observations that fell outside of the 3-sigma normal climatological range were rejected, as were observations that had a rate of change greater than a seasonal-dependant threshold (e.g., > 5 K/hr change).

timeSeries Variables	HMP155	Vaisala	Relative Humidity (1 or %)	Sensor installed in shaded, naturally vented shelter.	10 min	1%	The humidity is not corrected in a sub-freezing environment, beyond the standard Vaisala processing. Beyond the standard Vaisala processing, observations were checked against site-based climatology ranges and the rate of change thresholds, which were based on hourly criteria. Observations that fell outside of the 3-sigma normal climatological range were rejected, as were observations that had a rate of change greater than a seasonal-dependant threshold (e.g., > 30 %/hr change).
timeSeries Variables	HMP35D	Vaisala	Relative Humidity (1 or %)	Sensor installed in shaded, naturally vented shelter.	10 min	0.8%	The humidity is not corrected in a sub-freezing environment, beyond the standard Vaisala processing. Beyond the standard Vaisala processing, observations were checked against site-based climatology ranges and the rate of change thresholds, which were based on hourly criteria. Observations that fell outside of the 3-sigma normal climatological range were rejected, as were observations that had a rate of change greater than a seasonal-dependant threshold (e.g., > 30 %/hr change).
timeSeries Variables	HMP45D	Vaisala	Relative Humidity (1 or %)	Sensor installed in shaded, naturally vented shelter.	10 min	2% (0-90 %RH) 3% (90-100 %RH)	The humidity is not corrected in a sub-freezing environment, beyond the standard Vaisala processing. Beyond the standard Vaisala processing, observations were checked against site-based climatology ranges and the rate of change thresholds, which were based on hourly criteria. Observations that fell outside of the 3-sigma normal climatological range were rejected, as were observations that had a rate of change greater than a seasonal-dependant threshold (e.g., > 30 %/hr change).
timeSeries Variables	SR50	Campbell Scientific	Snow thickness (m)	Sonic distance sensor at 50KHz with a perforated flat target base levelled at the surface (0 m a.g.l.)	10 min	1 cm	Observations were checked against site-based climatology ranges, routine manual observations, and the rate of change thresholds, which were based on hourly criteria. Observations that fell outside of the 3-sigma normal climatological range were rejected, as were observations that had a rate of change greater than a seasonal-dependant threshold (e.g., > 20 cm/hr change).
timeSeries Variables	Distrometer Model: 5.4110.01.200	Thies Clima	Total precipitation of water in all phases per unit area (kg m ⁻² s ⁻¹)	Model with extended heating	1 min	5%	Beyond standard processing, observations were checked against site-based climatology ranges and the rate of change thresholds, which were based on hourly criteria. Observations that fell outside of the 3-sigma normal climatological range were rejected, as were observations that had a rate of change greater than a seasonal-dependant threshold (e.g., > 10 mm/hr change).

timeSeries Variables	Distrometer Model: 5.4110.01.200	Thies Clima	Snowfall flux unit area (kg m ⁻² s ⁻¹)	Model with extended heating	1 min	5%	Beyond standard processing, observations were checked against site-based climatology ranges and the rate of change thresholds, which were based on hourly criteria. Observations that fell outside of the 3-sigma normal climatological range were rejected, as were observations that had a rate of change greater than a seasonal-dependant threshold (e.g., > 10 mm/hr change).
timeSeries Variables	SSG 1000	Sommer Messtechnik	Snow water equivalent (m)	Sensor consists of seven perforated panels having a total measuring surface of 2.8 x 2.4 m with the measurement being made on the centre plate,	1 min	0.3%	Data is raw and no additional QC was performed, other than the processing performed by the sensor.
timeSeries Variables	CMA11	Kipp and Zonen	Downward Short-wave Radiation (W m ⁻²)	Integrated levelling included, dome, RM Young radiation shield (6 plate), and a CVF4L Ventilation System with Integrated Heater running when temperatures where near zero to prevent frost	10 min	7 W m ⁻²	Data is raw and no additional QC was performed, other than the processing performed by Kipp and Zonen. No additional QC was performed on these observations to account for potential frost or snow deposition on the sensors. Data should be treated with caution since they typically require additional QC processing prior to analysis.
timeSeries Variables	CMA11	Kipp and Zonen	Upward Short-wave Radiation (W m ⁻²)	Integrated levelling included, dome, RM Young radiation shield (6 plate), and a CVF4L Ventilation System with Integrated Heater running when temperatures where near zero to prevent frost	10 min	7 W m ⁻²	Data is raw and no additional QC was performed, other than the processing performed by Kipp and Zonen. No additional QC was performed on these observations to account for potential frost or snow deposition on the sensors. Data should be treated with caution since they typically require additional QC processing prior to analysis.
timeSeries Variables	CM11	Kipp and Zonen	Downward Short-wave Radiation (W m ⁻²)	Integrated levelling included, dome, RM Young radiation shield (6 plate), and a CVF4L Ventilation System with Integrated Heater running when temperatures where near zero to prevent frost	1 min	7 W m ⁻²	Data is raw and no additional QC was performed, other than the processing performed by Kipp and Zonen. No additional QC was performed on these observations to account for potential frost or snow deposition on the sensors. Data should be treated with caution since they typically require additional QC processing prior to analysis.
timeSeries Variables	CMP3	Kipp and Zonen	Downward Short-wave Radiation (W m ⁻²)	Installed on a pole	10 min	15 W m ⁻²	Data is raw and no additional QC was performed, other than the processing performed by Kipp and Zonen. No additional QC was performed on these observations to account for potential frost or snow deposition on the sensors. Data should be treated with

								caution since they typically require additional QC processing prior to analysis.
timeSeries Variables	CMP3	Kipp and Zonen	Upward Short-wave Radiation (W m ²)	Installed on a pole		10 min	15 W m ⁻²	Data is raw and no additional QC was performed, other than the processing performed by Kipp and Zonen. No additional QC was performed on these observations to account for potential frost or snow deposition on the sensors. Data should be treated with caution since they typically require additional QC processing prior to analysis.
timeSeries Variables	CMP11	Kipp and Zonen	Upward Short-wave Radiation (W m ²)	Installed on a pole		10 min	7 W m ⁻²	Data is raw and no additional QC was performed, other than the processing performed by Kipp and Zonen. No additional QC was performed on these observations to account for potential frost or snow deposition on the sensors. Data should be treated with caution since they typically require additional QC processing prior to analysis.
timeSeries Variables	CNR4	Kipp and Zonen	Downward Short-wave Radiation (W m ²)	Integrated component with temperature sensor	4-system	10 min	7 W m ⁻²	Data is raw and no additional QC was performed, other than the processing performed by Kipp and Zonen. No additional QC was performed on these observations to account for potential frost or snow deposition on the sensors. Data should be treated with caution since they typically require additional QC processing prior to analysis.
timeSeries Variables	CNR4	Kipp and Zonen	Upward Short-wave Radiation (W m ²)	Integrated component with temperature sensor	4-system	10 min	7 W m ⁻²	Data is raw and no additional QC was performed, other than the processing performed by Kipp and Zonen. No additional QC was performed on these observations to account for potential frost or snow deposition on the sensors. Data should be treated with caution since they typically require additional QC processing prior to analysis.
timeSeries Variables	CNR4	Kipp and Zonen	Downward Long-wave Radiation (W m ²)	Integrated component with temperature sensor	4-system	10 min	7 W m ⁻²	Data is raw and no additional QC was performed, other than the processing performed by Kipp and Zonen. No additional QC was performed on these observations to account for potential frost or snow deposition on the sensors. Data should be treated with caution since they typically require additional QC processing prior to analysis.
timeSeries Variables	CNR4	Kipp and Zonen	Upward Long-wave Radiation (W m ²)	Integrated component with temperature sensor	4-system	10 min	7 W m ⁻²	Data is raw and no additional QC was performed, other than the processing performed by Kipp and Zonen. No additional QC was performed on these observations to account for potential frost or snow deposition on the sensors. Data should be treated with caution since they typically require additional QC processing prior to analysis.

timeSeries Variables	NR-Lite	Kipp and Zonen	Net Short-wave Radiation (W m ⁻²)	Single-component thermopile net radiometer	10 min	25 W m ⁻²	Data is raw and no additional QC was performed, other than the processing performed by Kipp and Zonen. No additional QC was performed on these observations to account for potential frost or snow deposition on the sensors. Data should be treated with caution since they typically require additional QC processing prior to analysis.
timeSeries Variables	NR-Lite2	Kipp and Zonen	Net Short-wave Radiation (W m ⁻²)	Single-component thermopile net radiometer	10 min	15 W m ⁻²	Data is raw and no additional QC was performed, other than the processing performed by Kipp and Zonen. No additional QC was performed on these observations to account for potential frost or snow deposition on the sensors. Data should be treated with caution since they typically require additional QC processing prior to analysis.
timeSeries Variables	PAR Lite	Kipp and Zonen	Photosynthetic Photon Flux density (mol m ⁻² s ⁻¹)	Quantum sensor	10 min	10%	Data is raw and no additional QC was performed, other than the processing performed by Kipp and Zonen. No additional QC was performed on these observations to account for potential frost or snow deposition on the sensors. Data should be treated with caution since they typically require additional QC processing prior to analysis.
timeSeries Variables	PQS1	Kipp and Zonen	Photosynthetic Photon Flux density (mol m ⁻² s ⁻¹)	Quantum sensor	10 min	5%	Data is raw and no additional QC was performed, other than the processing performed by Kipp and Zonen. No additional QC was performed on these observations to account for potential frost or snow deposition on the sensors. Data should be treated with caution since they typically require additional QC processing prior to analysis.
timeSeries Variables	LI190SZ	Licor	Photosynthetic Photon Flux density (mol m ⁻² s ⁻¹)	Quantum sensor	10 min	5%	Data is raw and no additional QC was performed, other than the processing performed by Licor. No additional QC was performed on these observations to account for potential frost or snow deposition on the sensors. Data should be treated with caution since they typically require additional QC processing prior to analysis.
timeSeries Variables	PTB201A	Vaisala	Pressure (Pa)	Installed within a naturally vented protective enclosure.	10 min	0.3 hPa	Beyond the standard Vaisala processing, observations were checked against site-based climatology ranges and the rate of change thresholds, which were based on hourly criteria. Observations that fell outside of the 3-sigma normal climatological range were rejected, as were observations that had a rate of change greater than a seasonal-dependant threshold (e.g., >20 hPa/hr change).
timeSeries Variables	FD12P	Vaisala	Surface horizontal visibility (m)	Optical forward-scatter sensor installed on a pole	10 min	10%	Data is raw and no additional QC was performed, other than the processing performed by the sensor.

timeSeries Variables	WA25 (WAA25 and WAV25)	Vaisala	Eastward Wind ($m s^{-1}$)	Cup anemometer and vane designed for Arctic conditions with integrated heaters to prevent ice buildup		10 min	0.3 $m s^{-1}$	Beyond the standard Vaisala processing, observations were checked against site-based climatology ranges and the rate of change thresholds, which were based on hourly criteria. Observations that fell outside of the 3-sigma normal climatological range were rejected, as were observations that had a rate of change greater than a seasonal-dependant threshold (e.g., > 10 m/s/hr change).
timeSeries Variables	WA25 (WAA25 and WAV25)	Vaisala	Northward Wind ($m s^{-1}$)	Cup anemometer and vane designed for Arctic conditions with integrated heaters to prevent ice buildup		10 min	0.3 $m s^{-1}$	Beyond the standard Vaisala processing, observations were checked against site-based climatology ranges and the rate of change thresholds, which were based on hourly criteria. Observations that fell outside of the 3-sigma normal climatological range were rejected, as were observations that had a rate of change greater than a seasonal-dependant threshold (e.g., > 10 m/s/hr change).
timeSeries Variables	UA2D	Thies Clima	Eastward Wind ($m s^{-1}$)	2-D anemometer	sonic	10 min	2%	Data is raw and no additional QC was performed, other than the processing performed by the sensor.
timeSeries Variables	UA2D	Thies Clima	Northward Wind ($m s^{-1}$)	2-D anemometer	sonic	10 min	2%	Data is raw and no additional QC was performed, other than the processing performed by the sensor.
timeSeries Variables	USA-1	Metek	Eastward Wind ($m s^{-1}$)	3-D anemometer	sonic	10 min	0.1 $m s^{-1}$	Data is raw and no additional QC was performed, other than the processing performed by the sensor.
timeSeries Variables	USA-1	Metek	Northward Wind ($m s^{-1}$)	3-D anemometer	sonic	10 min	0.1 $m s^{-1}$	Data is raw and no additional QC was performed, other than the processing performed by the sensor.
timeSeries Variables	USA-1	Metek	Vertical velocity ($m s^{-1}$)	3-D anemometer	sonic	10 min	0.1 $m s^{-1}$	Data is raw and no additional QC was performed, other than the processing performed by the sensor.
timeSeries Variables	USA-1	Metek	Surface friction velocity (eddy covariance method) ($m s^{-1}$)	3-D anemometer	sonic	10 min	0.1 $m s^{-1}$	Additional filtering of output from eddy covariance processing not performed
timeSeries Variables	USA-1	Metek	Surface turbulent latent heat flux (eddy covariance method) ($W m^{-2}$)	3-D anemometer	sonic	10 min	20%	Additional filtering of output from eddy covariance processing not performed
timeSeries Variables	USA-1	Metek	Surface turbulent sensible heat flux (eddy covariance)	3-D anemometer	sonic	10 min	20%	Additional filtering of output from eddy covariance processing not performed

			method) ($W m^{-2}$)					
timeSeries Variables	USA-1	Metek	Surface momentum flux (eddy covariance method) ($W m^{-2}$)	3-D anemometer	sonic	10 min	25%	Additional filtering of output from eddy covariance processing not performed
timeSeries Variables	HFP01	Hukseflux	Ground heat flux ($W m^{-2}$)	Thermopile buried in soil		10 min	3%	Data is raw and no additional QC was performed, other than the processing performed by the sensor.
timeSeries Profile Variables	QMT103	Vaisala	Bulk soil temperature (K)	Thin steel sheath incorporating sensor, buried in soil		10 min	0.3 K	Data is raw and no additional QC was performed, other than the processing performed by the sensor.
timeSeries Profile Variables	Hydra Probe II	Stevens	Bulk soil temperature (K)	4-needle sensor buried in soil		10 min	0.3 K	Data is raw and no additional QC was performed, other than the processing performed by the sensor.
timeSeries Profile Variables	Hydra Probe II	Stevens	Average layer soil moisture ($kg m^{-2}$)	4-needle sensor buried in soil		10 min	5%	Data is raw and no additional QC was performed, other than the processing performed by the sensor.
timeSeries Profile Variables	GS3	Decagon Devices	Bulk soil temperature (K)	Sensor encapsulated in an epoxy body with stainless steel needles. Buried in soil		10 min	1 K	Data is raw and no additional QC was performed, other than the processing performed by the sensor.
timeSeries Profile Variables	GTE	Decagon Devices	Bulk soil temperature (K)	Sensor encapsulated in an epoxy body with stainless steel needles. Buried in soil		10 min	1 K	Data is raw and no additional QC was performed, other than the processing performed by the sensor.
timeSeries Profile Variables	109-L	Campbell Scientific	Bulk soil temperature (K)	Thermistor encapsulated in an epoxy-filled aluminum housing and buried in soil		10 min	0.3 K	Data is raw and no additional QC was performed, other than the processing performed by the sensor.
timeSeries Profile Variables	CS655	Campbell Scientific	Bulk soil temperature (K)	Two 12-cm-long stainless steel rods connected to a printed circuit board encapsulated in epoxy attached to a shielded cable. Buried in soil		10 min	0.3 K	Data is raw and no additional QC was performed, other than the processing performed by the sensor.
timeSeries Profile Variables	PT100	Pentronic	Bulk soil temperature (K)	Thin steel sheath incorporating sensor, buried in soil		10 min	0.3 K	Data is raw and no additional QC was performed, other than the processing performed by the sensor.
timeSeries Profile Variables	IKES PT100	Nokeval	Bulk soil temperature (K)	Thin steel sheath incorporates a Pt100 sensor with double insulation moulded in		10 min	0.3 K	Data is raw and no additional QC was performed, other than the processing performed by the sensor.

solid rubber with the cable. Buried in soil

timeSeriesProfile Variables	ThetaProbe ML2x	Delta-T Devices	Average layer soil moisture (kg m ⁻²)	4-needle sensor buried in soil	10 min	5.00%	Data is raw and no additional QC was performed, other than the processing performed by the sensor.
timeSeriesProfile Variables	107-L	Campbell Scientific	Snow temperature (K)	Thermistor encapsulated in an epoxy-filled aluminum housing and buried in snow	10 min	0.5 K	Data is raw and no additional QC was performed, other than the processing performed by the sensor.
timeSeriesProfile Variables	PT100	generic	Air temperature (K)	Sensor installed in shaded, naturally vented shelter.	10 min	0.3 K	Data is raw and no additional QC was performed, other than the processing performed by the sensor.
timeSeriesProfile Variables	HMP	Vaisala	Relative Humidity (1 or %)	Sensor installed in shaded, naturally vented shelter.	10 min	0.80%	Data is raw and no additional QC was performed, other than the processing performed by the sensor.
timeSeriesProfile Variables	WAA25	Vaisala	Wind speed (m s ⁻¹)	Cup anemometer with integrated heater to prevent ice buildup	10 min	0.17 m s ⁻¹	Data is raw and no additional QC was performed, other than the processing performed by the sensor.

867

868

869

870
871

Table 7. List of the instruments that contributed to the Utqiagvik MODF, including details about the instrument manufacturer, measured variables, configuration, temporal resolution, measurement uncertainty, and quality control applied.

<u>MODF featureType</u>	<u>Instrument</u>	<u>Manufacturer</u>	<u>Measured variables</u>	<u>Instrument Configuration</u>		<u>Temporal Resolution</u>	<u>Uncertainty (+/-)</u>	<u>Quality Control</u>
timeSeries Variables	PTB-220	Vaisala	Pressure (Pa)	The meteorology station (BMET) uses mainly conventional in situ sensors mounted at four different heights (2m, 10m, 20m and 40m) on a 40 m tower to obtain profiles of wind speed, wind direction, air temperature, dew point and humidity. It also obtains barometric pressure, visibility and precipitation data from sensors at the base of the tower. https://www.arm.gov/capabilities/instruments/twr	Barrow station	1 min	0.15 hPa	Beyond the standard Vaisala processing, observations were checked against other instrumentation on the tower and compared with the surface meteorological instruments and the energy balance bowen ratio. Data was also compared with the SONDE data that was launched some distance away from the tower: https://www.arm.gov/publications/tech_reports/handbooks/twr_handbook.pdf
timeSeries Variables	WS425	Vaisala	Near-surface (2m eastward wind (m s ⁻¹))	The meteorology station (BMET) uses mainly conventional in situ sensors mounted at four different heights (2m, 10m, 20m and 40m) on a 40 m tower to obtain profiles of wind speed, wind direction, air temperature, dew point and humidity. It also obtains barometric pressure, visibility and precipitation data from sensors at the base of the tower. https://www.arm.gov/capabilities/instruments/twr	Barrow station	1 min	0.135 ms ⁻¹	Beyond the standard Vaisala processing, observations were checked against other instrumentation on the tower and compared with the surface meteorological instruments and the energy balance bowen ratio. Data was also compared with the SONDE data that was launched some distance away from the tower: https://www.arm.gov/publications/tech_reports/handbooks/twr_handbook.pdf

timeSeries Variables	WS425	Vaisala	Near-surface (2m) northward wind (m s ⁻¹)	The Barrow meteorology station (BMET) uses mainly conventional in situ sensors mounted at four different heights (2m, 10m, 20m and 40m) on a 40 m tower to obtain profiles of wind speed, wind direction, air temperature, dew point and humidity. It also obtains barometric pressure, visibility and precipitation data from sensors at the base of the tower. https://www.arm.gov/capabilities/instruments/twr	1 min	0.135 ms ⁻¹	Beyond the standard Vaisala processing, observations were checked against other instrumentation on the tower and compared with the surface meteorological instruments and the energy balance bowen ratio. Data was also compared with the SONDE data that was launched some distance away from the tower: https://www.arm.gov/publications/tech_reports/handbooks/twr_handbook.pdf
timeSeries Variables	HMT337 (previously HMP35D/HMP45D)	Vaisala	Near-surface (2m) air temperature (K)	The Barrow meteorology station (BMET) uses mainly conventional in situ sensors mounted at four different heights (2m, 10m, 20m and 40m) on a 40 m tower to obtain profiles of wind speed, wind direction, air temperature, dew point and humidity. It also obtains barometric pressure, visibility and precipitation data from sensors at the base of the tower. https://www.arm.gov/capabilities/instruments/twr	1 min	0.2 K	Beyond the standard Vaisala processing, observations were checked against other instrumentation on the tower and compared with the surface meteorological instruments and the energy balance bowen ratio. Data was also compared with the SONDE data that was launched some distance away from the tower: https://www.arm.gov/publications/tech_reports/handbooks/twr_handbook.pdf
timeSeries Variables	HMT337 (previously HMP35D/HMP45D)	Vaisala	Near-surface (2m) dew point temperature (K)	The Barrow meteorology station (BMET) uses mainly conventional in situ sensors mounted at four different heights (2m, 10m, 20m and 40m) on a 40 m tower to obtain profiles of wind speed, wind direction, air temperature, dew point and humidity. It also obtains barometric pressure, visibility and precipitation data from sensors at the base of the tower. https://www.arm.gov/capabilities/instruments/twr	1 min	0.2 K	Beyond the standard Vaisala processing, observations were checked against other instrumentation on the tower and compared with the surface meteorological instruments and the energy balance bowen ratio. Data was also compared with the SONDE data that was launched some distance away from the tower: https://www.arm.gov/publications/tech_reports/handbooks/twr_handbook.pdf

pabilities/instruments/twr							
timeSeries Variables	HMT337 (previously HMP35D/HMP45 D)	Vaisala	Near-surface relative humidity (%)	The Barrow meteorology station (BMET) uses mainly conventional in situ sensors mounted at four different heights (2m, 10m, 20m and 40m) on a 40 m tower to obtain profiles of wind speed, wind direction, air temperature, dew point and humidity. It also obtains barometric pressure, visibility and precipitation data from sensors at the base of the tower. https://www.arm.gov/capabilities/instruments/twr	1 min	1.7 %	Beyond the standard Vaisala processing, observations were checked against other instrumentation on the tower and compared with the surface meteorological instruments and the energy balance Bowen ratio. Data was also compared with the SONDE data that was launched some distance away from the tower: https://www.arm.gov/publications/tech_reports/handbooks/twr_handbook.pdf
timeSeries Variables	TEI 49i	Thermo Scientific	Ozone concentration in air (mole fraction)	Inlet line samples air from roof of station through filter, while instrument is housed inside station building	1 min	1 ppb	This data set contains continuous UV photometric data of surface level ozone collected at 6m above ground level. Data records consist of UTC time, date, and processed ozone mixing ratio (parts per billion). Data is collected from global locations and is provided in 1 minute and 1 hour averages. Data are archived at the NOAA National Climatic Data Center (NCDC), but are produced and available from NOAA Earth System Research Laboratory (ESRL). https://www.ncei.noaa.gov/access/metadata/landing-page/bin/iso?id=gov.noaa.ncdc:C00894
timeSeries Variables	Toughsonic 30	Senix	Surface snow thickness (m)	Instrument is located on broadband radiation albedo rack	1 min	n/a	Data is compared against meteorological and global radiation data to verify accuracy; pollution/technical events are flagged and/or removed from data set; data values not physically possible are removed
timeSeries Variables	IRT	Apogee	Surface (skin) temperature (K)	Data collected from US Climate Reference Network (CRN)	1 min	0.5 K	Inter-comparison of the 3 temperature sensors: Sensors should be within 0.3° C of one another. An hourly flag message is generated for any departure greater than 0.30° C (i.e., 0.301° C and greater). IR max should exceed the ambient temperature, and IR min should be less than ambient temperature. https://www1.ncdc.noaa.gov/pub/data/uscrn/documentation/program/ManualMonitoringHandbook.pdf

timeSeries Variables	GNDRA D	PSP	Upward surface short-wave radiation (W m ⁻²)	https://www.arm.gov/capabilities/instruments/gndrad	1 min	2.0 W m ⁻²	SIRS Instrument mentors review the Data Quality Office's (DQO) weekly Data Quality Assessment Reports (DQAR). If a problem is detected, a Data Quality Problem Report (DQPR) is issued. The DQPR system is a web-based system by which the mentor, local site operations staff, and the DQO are informed and communicate to resolve a data quality problem (e.g., instrument failure, data collection issue, etc.). A DQPR is typically initiated by the DQO or instrument mentor during data review. Data Quality Reports (DQR) are prepared by instrument mentors as needed to close out corresponding DQPRs. https://www.arm.gov/capabilities/instruments/gndrad
timeSeries Variables	SKYRA D	PSP	Downward short-wave radiation at the surface (W m ⁻²)	https://www.arm.gov/capabilities/instruments/skyrad	1 min	4.0 W m ⁻²	SIRS Instrument mentors review the Data Quality Office's (DQO) weekly Data Quality Assessment Reports (DQAR). If a problem is detected, a Data Quality Problem Report (DQPR) is issued. The DQPR system is a web-based system by which the mentor, local site operations staff, and the DQO are informed and communicate to resolve a data quality problem (e.g., instrument failure, data collection issue, etc.). A DQPR is typically initiated by the DQO or instrument mentor during data review. Data Quality Reports (DQR) are prepared by instrument mentors as needed to close out corresponding DQPRs. https://www.arm.gov/capabilities/instruments/skyrad
timeSeries Variables	GNDRA D	PIR	Upward surface long-wave radiation (W m ⁻²)	https://www.arm.gov/capabilities/instruments/gndrad	1 min	2.0 W m ⁻²	SIRS Instrument mentors review the Data Quality Office's (DQO) weekly Data Quality Assessment Reports (DQAR). If a problem is detected, a Data Quality Problem Report (DQPR) is issued. The DQPR system is a web-based system by which the mentor, local site operations staff, and the DQO are informed and communicate to resolve a data quality problem (e.g., instrument failure, data collection issue, etc.). A DQPR is typically initiated by the DQO or instrument mentor during data review. Data Quality Reports (DQR) are prepared by instrument mentors as needed to close out corresponding DQPRs. https://www.arm.gov/capabilities/instruments/gndrad
timeSeries Variables	SKYRA D	PIR	Downward surface long-wave radiation (W m ⁻²)	https://www.arm.gov/capabilities/instruments/skyrad	1 min	4.0 W m ⁻²	SIRS Instrument mentors review the Data Quality Office's (DQO) weekly Data Quality Assessment Reports (DQAR). If a problem is detected, a Data Quality Problem Report (DQPR) is issued. The DQPR system is a web-based system by which the mentor, local site operations staff, and the DQO are informed and communicate to resolve a data quality problem (e.g., instrument failure, data collection issue, etc.). A DQPR is typically initiated by the DQO or instrument mentor during data review. Data Quality Reports (DQR) are prepared by instrument mentors as needed to close out corresponding DQPRs. https://www.arm.gov/capabilities/instruments/skyrad

timeSeries Variables	Windmas ter Pro Anemom eter	Gill	Surfa ce turbul ent latent heat flux (eddy covari ance metho d) (W m ⁻²)	Standard arrangement is sonic sensor "North" mark pointing along the boom to the tower; the boom is usually pointing due south; u wind component is north- south with positive toward the north; v wind component is east- west with positive toward the west. NOTE: no correction is made to convert u and v component into meteorological "north" and "east" wind components when tower boom is not aligned to south; u wind component is "along boom", v wind component is "cross boom https://www.arm.gov/publications/tech_reports/doe-sc-arm-tr-223.pdf	1 min	<1.5 %	The QCECOR VAP currently contains two variables: surface latent heat flux (LH) and sensible heat flux (SH), together with their QC flags. When SEBS are collocated with ECOR, the wetness measurements from SEBS are used to flag the LH that may be incorrect due to hydrometeors such as precipitation, dew, or frost. An indeterminate flag is given to those that fail the wetness test. chrome-extension://efaidnbmnnnibpcajpcglclefindmkaj/https://www.arm.gov/publications/tech_reports/doe-sc-arm-tr-223.pdf
timeSeries Variables	Windmas ter Pro Anemom eter	Gill	Surfa ce turbul ent sensib le heat flux (eddy covari ance metho d) (W m ⁻²)	Standard arrangement is sonic sensor "North" mark pointing along the boom to the tower; the boom is usually pointing due south; u wind component is north- south with positive toward the north; v wind component is east- west with positive toward the west. NOTE: no correction is made to convert u and v component into meteorological "north" and "east" wind components when tower boom is not aligned to south; u wind component is "along boom", v wind component is "cross boom https://www.arm.gov/publications/tech_reports/doe-sc-arm-tr-223.pdf	1 min	<1.5 %	The QCECOR VAP currently contains two variables: surface latent heat flux (LH) and sensible heat flux (SH), together with their QC flags. When SEBS are collocated with ECOR, the wetness measurements from SEBS are used to flag the LH that may be incorrect due to hydrometeors such as precipitation, dew, or frost. An indeterminate flag is given to those that fail the wetness test. chrome-extension://efaidnbmnnnibpcajpcglclefindmkaj/https://www.arm.gov/publications/tech_reports/doe-sc-arm-tr-223.pdf

timeSeries Variables	HFT-3, SMP1, STP-1	Radiation and Energy Balance Systems, Inc.	Ground heat flux (W m^{-2})	Soil measurements are performed by three sets of soil heat flow (5 cm depth), soil temperature (0–5 cm average), and soil moisture (centered at 2.5 cm) probes. Soil heat flow is adjusted for the effect of soil moisture above the soil heat flow plate. The storage of energy in the soil above the soil heat flow plate is determined from the change in soil temperature with time.	1 min	10 mV	Instrument mentor routinely views graphic displays that include plots (day courses) of all calculated quantities and comparison plots (time series or scatter plots) of relevant parameters with data from collocated ECOR, SEBS, EBBR (SGP CF and EF39 only), and surface meteorological instrumentation (MET) (Cook et al. 2006). chrome-extension://efaidnbmnnnibpcajpcglclefindmkaj/https://www.arm.gov/publications/tech_reports/handbooks/sebs_handbook.pdf
timeSeries Profile Variables	WS425	Vaisala	Eastward wind component (m s^{-1})	The Barrow meteorology station (BMET) uses mainly conventional in situ sensors mounted at four different heights (2m, 10m, 20m and 40m) on a 40 m tower to obtain profiles of wind speed, wind direction, air temperature, dew point and humidity. It also obtains barometric pressure, visibility and precipitation data from sensors at the base of the tower. https://www.arm.gov/capabilities/instruments/twr	1 min	0.135 ms^{-1}	Beyond the standard Vaisala processing, observations were checked against other instrumentation on the tower and compared with the surface meteorological instruments and the energy balance bowen ratio. Data was also compared with the SONDE data that was launched some distance away from the tower: https://www.arm.gov/publications/tech_reports/handbooks/twr_handbook.pdf
timeSeries Profile Variables	WS425	Vaisala	Northward wind component (m s^{-1})	The Barrow meteorology station (BMET) uses mainly conventional in situ sensors mounted at four different heights (2m, 10m, 20m and 40m) on a 40 m tower to obtain profiles of wind speed, wind direction, air temperature, dew point and humidity. It also obtains barometric pressure, visibility and precipitation data from sensors at the base of the tower. https://www.arm.gov/capabilities/instruments/twr	1 min	0.135 ms^{-1}	Beyond the standard Vaisala processing, observations were checked against other instrumentation on the tower and compared with the surface meteorological instruments and the energy balance bowen ratio. Data was also compared with the SONDE data that was launched some distance away from the tower: https://www.arm.gov/publications/tech_reports/handbooks/twr_handbook.pdf

timeSeries Profile Variables	HMT337 (previously HMP35D /HMP45 D)	Vaisala	Air temperature (K)	The Barrow meteorology station (BMET) uses mainly conventional in situ sensors mounted at four different heights (2m, 10m, 20m and 40m) on a 40 m tower to obtain profiles of wind speed, wind direction, air temperature, dew point and humidity. It also obtains barometric pressure, visibility and precipitation data from sensors at the base of the tower. https://www.arm.gov/capabilities/instruments/twr	1 min	0.2 K	Beyond the standard Vaisala processing, observations were checked against other instrumentation on the tower and compared with the surface meteorological instruments and the energy balance bowen ratio. Data was also compared with the SONDE data that was launched some distance away from the tower: https://www.arm.gov/publications/tech_reports/handbooks/twr_handbook.pdf
timeSeries Profile Variables	HMT337 (previously HMP35D /HMP45 D)	Vaisala	Dew-point temperature (K)	The Barrow meteorology station (BMET) uses mainly conventional in situ sensors mounted at four different heights (2m, 10m, 20m and 40m) on a 40 m tower to obtain profiles of wind speed, wind direction, air temperature, dew point and humidity. It also obtains barometric pressure, visibility and precipitation data from sensors at the base of the tower. https://www.arm.gov/capabilities/instruments/twr	1 min	0.2 K	Beyond the standard Vaisala processing, observations were checked against other instrumentation on the tower and compared with the surface meteorological instruments and the energy balance bowen ratio. Data was also compared with the SONDE data that was launched some distance away from the tower: https://www.arm.gov/publications/tech_reports/handbooks/twr_handbook.pdf
timeSeries Profile Variables	HMT337 (previously HMP35D /HMP45 D)	Vaisala	Relative humidity (%)	The Barrow meteorology station (BMET) uses mainly conventional in situ sensors mounted at four different heights (2m, 10m, 20m and 40m) on a 40 m tower to obtain profiles of wind speed, wind direction, air temperature, dew point and humidity. It also obtains barometric pressure, visibility and precipitation data from sensors at the base of the tower. https://www.arm.gov/capabilities/instruments/twr	1 min	1.7 %	Beyond the standard Vaisala processing, observations were checked against other instrumentation on the tower and compared with the surface meteorological instruments and the energy balance bowen ratio. Data was also compared with the SONDE data that was launched some distance away from the tower: https://www.arm.gov/publications/tech_reports/handbooks/twr_handbook.pdf

pabilities/instruments/twr							
timeSeries Profile Variables	PT100	in-house	Soil temperature profile (K)	Instrument is located on broadband radiation albedo rack	1 min	n/a	Data is compared against meteorological and global radiation data to verify accuracy; pollution/technical events are flagged and/or removed from data set; data values not physically possible are removed
timeSeries Profile Variables	KAZR	KAZR	Snowfall flux per unit area	Installed on top of the ARM facility roof	1 min	n/a	https://doi.org/10.1525/elementa.2021.00101 chrome-extension://efaidnbmninnibpcjpcglclefindmkaj/https://www.arm.gov/publications/tech_reports/handbooks/kazr_handbook.pdf
timeSeries ProfileSonde Variables	SONDE	Radiosonde	Atmospheric pressure (Pa)	The SONDE system originally located at Barrow was an old CLASS-type that was originally operated by NOAA's Climate Measurements and Diagnostics Laboratory on TWP's Manus site.	30 min	1 hPa	The manufacturer defines the cumulative sensor uncertainty at the 2-sigma (95.5%) confidence level. Repeatability is estimated from the standard deviation of differences between two successive repeated calibrations (2-sigma). Reproducibility is estimated from the standard deviation of differences in twin soundings. Citation recommendation: Atmospheric Radiation Measurement (ARM) user facility. 2002. Balloon-Borne Sounding System (SONDEWNP). 2002-04-28 to 2022-11-17, North Slope Alaska (NSA) Central Facility, Barrow AK (C1). Compiled by K. Burk. ARM Data Center. Data set accessed 2022-11-18 at http://dx.doi.org/10.5439/1595321 .
timeSeries ProfileSonde Variables	SONDE	Radiosonde	Eastward wind component ($m s^{-1}$)	The SONDE system originally located at Barrow was an old CLASS-type that was originally operated by NOAA's Climate Measurements and Diagnostics Laboratory on TWP's Manus site.	30 min	n/a	The manufacturer defines the cumulative sensor uncertainty at the 2-sigma (95.5%) confidence level. Repeatability is estimated from the standard deviation of differences between two successive repeated calibrations (2-sigma). Reproducibility is estimated from the standard deviation of differences in twin soundings. Citation recommendation: Atmospheric Radiation Measurement (ARM) user facility. 2002. Balloon-Borne Sounding System (SONDEWNP). 2002-04-28 to 2022-11-17, North Slope Alaska (NSA) Central Facility, Barrow AK (C1). Compiled by K. Burk. ARM Data Center. Data set accessed 2022-11-18 at http://dx.doi.org/10.5439/1595321 .
timeSeries ProfileSonde Variables	SONDE	Radiosonde	Northward wind component ($m s^{-1}$)	The SONDE system originally located at Barrow was an old CLASS-type that was originally operated by NOAA's Climate Measurements and Diagnostics Laboratory on TWP's Manus site.	30 min	n/a	The manufacturer defines the cumulative sensor uncertainty at the 2-sigma (95.5%) confidence level. Repeatability is estimated from the standard deviation of differences between two successive repeated calibrations (2-sigma). Reproducibility is estimated from the standard deviation of differences in twin soundings. Citation recommendation: Atmospheric Radiation Measurement (ARM) user facility. 2002. Balloon-Borne Sounding System (SONDEWNP). 2002-04-28 to 2022-11-17, North Slope Alaska (NSA) Central Facility, Barrow AK (C1). Compiled by K. Burk. ARM Data Center. Data set accessed 2022-11-18 at http://dx.doi.org/10.5439/1595321 .

timeSeries ProfileSon de Variables	SONDE	Radios onde	Temp eratur e (K)	The SONDE system originally located at Barrow was an old CLASS-type that was originally operated by NOAA's Climate Measurements and Diagnostics Laboratory on TWP's Manus site.	30 min	0.5 K	The manufacturer defines the cumulative sensor uncertainty at the 2-sigma (95.5%) confidence level. Repeatability is estimated from the standard deviation of differences between two successive repeated calibrations (2-sigma). Reproducibility is estimated from the standard deviation of differences in twin soundings. Citation recommendation: Atmospheric Radiation Measurement (ARM) user facility. 2002. Balloon-Borne Sounding System (SONDEWNP). 2002-04-28 to 2022-11-17, North Slope Alaska (NSA) Central Facility, Barrow AK (C1). Compiled by K. Burk. ARM Data Center. Data set accessed 2022-11-18 at http://dx.doi.org/10.5439/1595321 .
timeSeries ProfileSon de Variables	SONDE	Radios onde	Dew- point tempe rature (K)	The SONDE system originally located at Barrow was an old CLASS-type that was originally operated by NOAA's Climate Measurements and Diagnostics Laboratory on TWP's Manus site.	30 min	0.5 K	The manufacturer defines the cumulative sensor uncertainty at the 2-sigma (95.5%) confidence level. Repeatability is estimated from the standard deviation of differences between two successive repeated calibrations (2-sigma). Reproducibility is estimated from the standard deviation of differences in twin soundings. Citation recommendation: Atmospheric Radiation Measurement (ARM) user facility. 2002. Balloon-Borne Sounding System (SONDEWNP). 2002-04-28 to 2022-11-17, North Slope Alaska (NSA) Central Facility, Barrow AK (C1). Compiled by K. Burk. ARM Data Center. Data set accessed 2022-11-18 at http://dx.doi.org/10.5439/1595321 .
timeSeries ProfileSon de Variables	SONDE	Radios onde	Relati ve humi dity (%)	The SONDE system originally located at Barrow was an old CLASS-type that was originally operated by NOAA's Climate Measurements and Diagnostics Laboratory on TWP's Manus site.	30 min	5%	The manufacturer defines the cumulative sensor uncertainty at the 2-sigma (95.5%) confidence level. Repeatability is estimated from the standard deviation of differences between two successive repeated calibrations (2-sigma). Reproducibility is estimated from the standard deviation of differences in twin soundings. Citation recommendation: Atmospheric Radiation Measurement (ARM) user facility. 2002. Balloon-Borne Sounding System (SONDEWNP). 2002-04-28 to 2022-11-17, North Slope Alaska (NSA) Central Facility, Barrow AK (C1). Compiled by K. Burk. ARM Data Center. Data set accessed 2022-11-18 at http://dx.doi.org/10.5439/1595321 .

872

873

874

Table 8. List of the instruments that contributed to the Tiksi MODF, including details about the instrument manufacturer, measured variables, configuration, temporal resolution, measurement uncertainty, and quality control applied.

<u>MODF featureType</u>	<u>Instrument</u>	<u>Manufacturer</u>	<u>Measured variable</u>	<u>Instrument Configuration</u>	<u>Temporal Resolution</u>	<u>Uncertainty (+/-)</u>	<u>Quality Control</u>
timeSeries Variables	PTB110	Vaisala	Surface pressure (Pa)	Located on the fluxtower at 5m height	1 min	0.3 hPa	Data are manually QC'ed to identify and eliminate instrument malfunction; outliers are filtered out if values are physically impossible; values are compared to other local variables if/when possible
timeSeries Variables	3001	RM Young	Near-surface (4m) eastward wind (m s^{-1})	Located on the fluxtower at 4m height	1 min	0.5 m s^{-1}	Data are manually QC'ed to identify and eliminate instrument malfunction; outliers are filtered out if values are physically impossible; values are compared to other local variables if/when possible
timeSeries Variables	3001	RM Young	Near-surface (4m) northward wind (m s^{-1})	Located on the fluxtower at 4m height	1 min	0.5 m s^{-1}	Data are manually QC'ed to identify and eliminate instrument malfunction; outliers are filtered out if values are physically impossible; values are compared to other local variables if/when possible
timeSeries Variables	HMT330	Vaisala	Near-surface (2m) air temperature (K)	Located on the fluxtower at 2m height	1 min	0.2 K	Data are manually QC'ed to identify and eliminate instrument malfunction; outliers are filtered out if values are physically impossible; values are compared to other local variables if/when possible
timeSeries Variables	HMT330	Vaisala	Near-surface (2m) relative humidity (%)	Located on the fluxtower at 2m height	1 min	$1.5 + 0.015 \times \text{reading}$	Data are manually QC'ed to identify and eliminate instrument malfunction; outliers are filtered out if values are physically impossible; values are compared to other local variables if/when possible
timeSeries Variables	SR50A	Campbell Scientific	Surface snow thickness (m)	Located on the albedo rack	1 min	1 cm	Data are manually QC'ed to identify and eliminate instrument malfunction; outliers are filtered out if values are physically impossible; values are compared to other local variables if/when possible
timeSeries Variables	SI-111	Apogee	Surface (skin) temperature (K)	Located on the fluxtower at 2m height	1 min	0.2 K	Data are manually QC'ed to identify and eliminate instrument malfunction; outliers are filtered out if values are physically impossible; values are compared to

								other local variables if/when possible
timeSeries Variables	PSP	Eppley	Upward surface short-wave radiation ($W m^{-2}$)	Located on the albedo rack	1 min	2.0 m^{-2}	W	Data are manually QC'ed to identify and eliminate instrument malfunction; outliers are filtered out if values are physically impossible; values are compared to other local variables if/when possible
timeSeries Variables	CM22	Kipp & Zonen	Downward surface short-wave radiation ($W m^{-2}$)	Located on the tracker at the MET station building	1 min	5.0 m^{-2}	W	Data are manually QC'ed to identify and eliminate instrument malfunction; outliers are filtered out if values are physically impossible; values are compared to other local variables if/when possible
timeSeries Variables	PIR	Eppley	Upward surface long-wave radiation ($W m^{-2}$)	Located on the albedo rack	1 min	2.0 m^{-2}	W	Data are manually QC'ed to identify and eliminate instrument malfunction; outliers are filtered out if values are physically impossible; values are compared to other local variables if/when possible
timeSeries Variables	PIR	Eppley	Downward surface long-wave radiation ($W m^{-2}$)	Located on the tracker at the MET station building	1 min	4.0 m^{-2}	W	Data are manually QC'ed to identify and eliminate instrument malfunction; outliers are filtered out if values are physically impossible; values are compared to other local variables if/when possible
timeSeries Variables	HPF01	Hukseflux	Ground heat flux ($W m^{-2}$)	Located at the base of the fluxtower at 5cm depth	1 min	3 %		Data are manually QC'ed to identify and eliminate instrument malfunction; outliers are filtered out if values are physically impossible; values are compared to other local variables if/when possible
timeSeries Variables	HPF01	Hukseflux	Ground heat flux ($W m^{-2}$)	Located at the base of the fluxtower at 5cm depth	1 min	3 %		Data are manually QC'ed to identify and eliminate instrument malfunction; outliers are filtered out if values are physically impossible; values are compared to other local variables if/when possible
timeSeriesProfile Variables	HMT330, HMP155	Vaisala	Air temperature (K)	Located on the fluxtower at 2m, 6m, 10m height	1 min	0.2 K		Data are manually QC'ed to identify and eliminate instrument malfunction; outliers are filtered out if values are physically impossible; values are compared to

other local variables if/when possible

timeSeriesProfile Variables	HMT330, HMP155	Vaisala	Relative humidity (%)	Located on the fluxtower at 2m, 6m, 10m height	1 min	1.5 + 0.015 × reading	Data are manually QC'ed to identify and eliminate instrument malfunction; outliers are filtered out if values are physically impossible; values are compared to other local variables if/when possible
timeSeriesProfile Variables	TP-101	MRC	Soil temperature profile (K)	Located at albedo rack at depths: 5cm, 10cm, 15cm, 20cm, 25cm, 30cm, 45cm, 70cm, 95cm, 120cm	1 min	n/a	Data are manually QC'ed to identify and eliminate instrument malfunction; outliers are filtered out if values are physically impossible; values are compared to other local variables if/when possible
timeSeriesProfileSonde Variables	SONDE	Radiosonde	Atmospheric pressure (Pa)	https://www.ncei.noaa.gov/pub/data/igra/data/data-por/	30 min	1 hPa	https://www.ncei.noaa.gov/pub/data/igra/data/data-por/
timeSeriesProfileSonde Variables	SONDE	Radiosonde	Eastward wind component (m s ⁻¹)	https://www.ncei.noaa.gov/pub/data/igra/data/data-por/	30 min	n/a	https://www.ncei.noaa.gov/pub/data/igra/data/data-por/
timeSeriesProfileSonde Variables	SONDE	Radiosonde	Northward wind component (m s ⁻¹)	https://www.ncei.noaa.gov/pub/data/igra/data/data-por/	30 min	n/a	https://www.ncei.noaa.gov/pub/data/igra/data/data-por/
timeSeriesProfileSonde Variables	SONDE	Radiosonde	Temperature (K)	https://www.ncei.noaa.gov/pub/data/igra/data/data-por/	30 min	0.5 K	https://www.ncei.noaa.gov/pub/data/igra/data/data-por/
timeSeriesProfileSonde Variables	SONDE	Radiosonde	Dew-point temperature (K)	https://www.ncei.noaa.gov/pub/data/igra/data/data-por/	30 min	0.5 K	https://www.ncei.noaa.gov/pub/data/igra/data/data-por/
timeSeriesProfileSonde Variables	SONDE	Radiosonde	Relative humidity (%)	https://www.ncei.noaa.gov/pub/data/igra/data/data-por/	30 min	5%	https://www.ncei.noaa.gov/pub/data/igra/data/data-por/

877

878

879

Table 9. List of the instruments that contributed to the Ny-Ålesund MODF, including details about the instrument manufacturer, measured variables, configuration, temporal resolution, measurement uncertainty, and quality control applied.

<u>MODF featureT ype</u>	<u>Instrument</u>		<u>Manuf acture r</u>	<u>Measured variables</u>	<u>Instrument Configuration</u>	<u>Tempo ral Resolut ion</u>	<u>Uncer tainty (+/-)</u>	<u>Quality Control</u>
timeSeries Variables	Digiquarz 16B	6000-	Parosci entic, Inc.	Pressure (Pa)	Installed within a naturally vented protective enclosure.	1 min	0.08 hPa	Observations were checked against site- based climatology ranges and the rate of change thresholds.
timeSeries Variables	Pluvio2		OTT	Total precipitation of water in all phases per unit area (kg m ⁻² s ⁻¹)	Single Alter shield	1 min	5%	Operated and analysed by the University of Cologne. No additional QC was applied; data is raw and should be treated with caution.
timeSeries Variables	Combined Transmitter 4.3324.32.073	Wind	Thies Clima	Eastward Wind (m s ⁻¹)	Opto-electronically scanned three-cup anemometer with low starting speed. The position of the wind vane is detected opto- electronically.	1 min	0.4 ms ⁻¹	Instrument is checked on a daily basis. Observations were checked against site- based climatology ranges, the rate of change thresholds, and redundant measurements in close proximity.
timeSeries Variables	Combined Transmitter 4.3324.32.073	Wind	Thies Clima	Northward Wind (m s ⁻¹)	Opto-electronically scanned three-cup anemometer with low starting speed. The position of the wind vane is detected opto- electronically.	1 min	0.4 ms ⁻¹	Instrument is checked on a daily basis. Observations were checked against site- based climatology ranges, the rate of change thresholds, and redundant measurements in close proximity.
timeSeries Variables	Ventilated temperature transmitter 2.1265.20.000	air	Thies Clima	Temperature (K)	The sensor is protected by a double thermal radiation shield. A built-in ventilator provides for the necessary air flow.	1 min	0.1 K	Instrument is checked on a daily basis. Observations were checked against site- based climatology ranges, the rate of change thresholds, and redundant measurements in close proximity.
timeSeries Variables	HMP155		Vaisala	Relative Humidity (1 or %)	The sensor with additional temperature sensor is installed in a vented radiation shelter.	1 min	0.80%	Instrument is checked on a daily basis. Observations were checked against site- based climatology ranges, the rate of change thresholds, and redundant measurements in close proximity.
timeSeries Variables	CMP22		Kipp and Zonen	Upward Short-wave Radiation (W m ⁻²)	Sensor installed in an Eigenbrodt ventilation system to prevent from icing.	1 min	5 Wm ⁻²	Instrument is checked on a daily basis. Data quality check is performed according to BSRN requirements.

timeSeries Variables	CMP22		Kipp and Zonen	Downward Short-wave Radiation ($W m^{-2}$)	Sensor installed in an Eigenbrodt ventilation system to prevent from icing.	1 min	5 Wm^{-2}	Instrument is checked on a daily basis. Data quality check is performed according to BSRN requirements.
timeSeries Variables	Precision Radiometer	Infrared	Eppley	Upward Long-wave Radiation ($W m^{-2}$)	Sensor installed in an Eigenbrodt ventilation system to prevent from icing.	1 min	5 Wm^{-2}	Instrument is checked on a daily basis. Data quality check is performed according to BSRN requirements.
timeSeries Variables	Precision Radiometer	Infrared	Eppley	Downward Long-wave Radiation ($W m^{-2}$)	Sensor is shaded and installed in an Eigenbrodt ventilation system to prevent from icing.	1 min	5 $W/m2$	Instrument is checked on a daily basis. Data quality check is performed according to BSRN requirements.
timeSeries Profile Variables	CL51		Vaisala	Cloud Base Height (m)	Proprietary algorithm determines the lowest cloud base height	1 min	~10 m	Operated with the standard Vaisala proprietary algorithm that retrieves cloud base height. Additional check for unphysical outliers.
timeSeries Profile Sonde Variables	RS41		Vaisala	Atmospheric pressure (Pa)	Standard radiosonde launch	6 hr	0.5 hPa	No additional QC beyond the standard Vaisala proprietary algorithm.
timeSeries Profile Sonde Variables	RS41		Vaisala	Eastward Wind ($m s^{-1}$)	Standard radiosonde launch	6 hr	0.15 ms^{-1}	No additional QC beyond the standard Vaisala proprietary algorithm.
timeSeries Profile Sonde Variables	RS41		Vaisala	Northward Wind ($m s^{-1}$)	Standard radiosonde launch	6 hr	0.15 ms^{-1}	No additional QC beyond the standard Vaisala proprietary algorithm.
timeSeries Profile Sonde Variables	RS41		Vaisala	Temperature (K)	Standard radiosonde launch	6 hr	0.3 K	No additional QC beyond the standard Vaisala proprietary algorithm.
timeSeries Profile Sonde Variables	RS41		Vaisala	Relative Humidity (1 or %)	Standard radiosonde launch	6 hr	4%	No additional QC beyond the standard Vaisala proprietary algorithm.

882

883

884

Table 10. List of the instruments that contributed to the Eureka MODF, including details about the instrument manufacturer, measured variables, configuration, temporal resolution, measurement uncertainty, and quality control applied.

<u>MODF featureType</u>	<u>Instrument</u>	<u>Manufacturer</u>	<u>Measured variables</u>	<u>Instrument Configuration</u>	<u>Temporal Resolution</u>	<u>Uncertainty (+/-)</u>	<u>Quality Control</u>
timeSeries Variables	PTB220	Vaisala	Surface pressure (Pa)	Located on Flux Tower at 2 m height	1 min	0.3 hPa	Data are manually QC'ed to identify and eliminate instrument malfunction; outliers are filtered out if values are physically impossible; values are compared to other local variables if/when possible
timeSeries Variables	VENTUS-UMB Ultrasonic	Lufft	Near-surface (6m) eastward wind (m s^{-1})	Located on Flux Tower at 6 m	1-10 s	0.1 ms^{-1}	Data are manually QC'ed to identify and eliminate instrument malfunction; outliers are filtered out if values are physically impossible; values are compared to other local variables if/when possible
timeSeries Variables	VENTUS-UMB Ultrasonic	Lufft	Near-surface (6m) northward wind (m s^{-1})	Located on Flux Tower at 6 m t	1-10 s	0.1 ms^{-1}	Data are manually QC'ed to identify and eliminate instrument malfunction; outliers are filtered out if values are physically impossible; values are compared to other local variables if/when possible
timeSeries Variables	HMT-337	Vaisala	Near-surface (2m) air temperature (K)	Located on Flux Tower at 2 m height	1 min	0.2 K	Data are manually QC'ed to identify and eliminate instrument malfunction; outliers are filtered out if values are physically impossible; values are compared to other local variables if/when possible
timeSeries Variables	HMT-337	Vaisala	Near-surface (2m) relative humidity (%)	Located on Flux Tower at 2 m height	1 min	1.5 + 0.015 \times reading	Data are manually QC'ed to identify and eliminate instrument malfunction; outliers are filtered out if values are physically impossible; values are compared to other local variables if/when possible
timeSeries Variables	SR50A	Campbell Scientific	Surface Snow Thickness	Located on Flux Tower at 2 m height	1 min	1 cm	Manually QC'ed to identify and eliminate instrument malfunction and remove non-physical values.
timeSeries Variables	IRTS-P	Apogee	Surface (skin) temperature (K)	Located on Flux Tower at 2 m height	1 min	0.2 K	Data are manually QC'ed to identify and eliminate instrument malfunction; outliers are filtered out if values are physically impossible; values are compared to other local variables if/when possible
timeSeries Variables	PSP	Eppley	Upward surface short-wave radiation (W m^{-2})	Located on Flux Tower at 11 m height	1 min	2.0 W m^{-2}	Processed through Long QCRad; Historical Quality Control Techniques: Long, C. N., & Shi, Y. (2008). An Automated Quality Assessment and Control Algorithm for Surface Radiation Measurements. OASJ, 2, 23-

								37. doi: 10.2174/1874282300802010023 Younkin, K., & Long, C. N. (2004). Improved Correction of IR Loss in Diffuse Shortwave Measurements: An ARM Value Added Product.
timeSeries Variables	CM22	Kipp and Zonen	Downward surface short-wave radiation (W m ⁻²)	Located on Tower at 11 m height	Flux	1 min	5.0 W m ⁻²	Processed through Long QCRad; Historical Quality Control Techniques: Long, C. N., & Shi, Y. (2008). An Automated Quality Assessment and Control Algorithm for Surface Radiation Measurements. OASJ, 2, 23-37. doi: 10.2174/1874282300802010023 Younkin, K., & Long, C. N. (2004). Improved Correction of IR Loss in Diffuse Shortwave Measurements: An ARM Value Added Product.
timeSeries Variables	CM22	Kipp and Zonen	Upward surface long-wave radiation (W m ⁻²)	Located on Tower at 11 m height	Flux	1 min	5.0 W m ⁻²	Processed through Long QCRad; Historical Quality Control Techniques: Long, C. N., & Shi, Y. (2008). An Automated Quality Assessment and Control Algorithm for Surface Radiation Measurements. OASJ, 2, 23-37. doi: 10.2174/1874282300802010023 Younkin, K., & Long, C. N. (2004). Improved Correction of IR Loss in Diffuse Shortwave Measurements: An ARM Value Added Product.
timeSeries Variables	PIR	Eppley	Downward surface long-wave radiation (W m ⁻²)	Located on Tower at 11 m height	Flux	1 min	4.0 W m ⁻²	Processed through Long QCRad; Historical Quality Control Techniques: Long, C. N., & Shi, Y. (2008). An Automated Quality Assessment and Control Algorithm for Surface Radiation Measurements. OASJ, 2, 23-37. doi: 10.2174/1874282300802010023 Younkin, K., & Long, C. N. (2004). Improved Correction of IR Loss in Diffuse Shortwave Measurements: An ARM Value Added Product.
timeSeries Variables	HPFO1	Hukseflux	Ground heat flux (W m ⁻²)	Depth 3 cm		1 min	3 %	Manually QC'ed to identify and eliminate instrument malfunction
timeSeriesPro file Variables	HMT-337	Vaisala	Air temperature (K)	Located on Tower at 2, 6, 10 m	Flux	1 min	0.2 K	Manually QC'ed to identify and eliminate instrument malfunction. The lowest level of temperature profile is also saved in the timeSeries file as surface temperature tas
timeSeriesPro file Variables	HMT-337	Vaisala	Relative humidity (%)	Located on Tower at 2, 6, 10 m	Flux	1 min	1.5 + 0.015 × reading	Manually QC'ed to identify and eliminate instrument malfunction. The lowest level of humidity profile is also saved in the timeSeries file as surface humidity hurs

timeSeriesPro file Variables	TP-101	MRC	Soil temperature profile (K)	Depth: 5cm [mV], 10cm [mV], 15cm [mV], 20cm [mV], 25cm [mV], 30cm [mV], 45cm [mV], 70cm [mV], 95cm [mV], 120cm [mV]	1 min	n/a	Manually QC'ed to identify and eliminate instrument malfunction.
timeSeriesPro file Variables	VENTUS -UMB Ultrasoni c	Lufft	Eastward wind component (m s ⁻¹)	Located on Flux Tower at 6 m and 11 m	1-10 s	0.1 ms ⁻¹	Manually QC'ed to identify and eliminate instrument malfunction. The lowest level of wind speed profile is also saved in the timeSeries file as surface wind speed uas
timeSeriesPro file Variables	VENTUS -UMB Ultrasoni c	Lufft	Northward wind component (m s ⁻¹)	Located on Flux Tower at 6 m and 11 m	1-10 s	0.1 ms ⁻¹	Manually QC'ed to identify and eliminate instrument malfunction. The lowest level of wind speed profile is also saved in the timeSeries file as surface wind speed vas

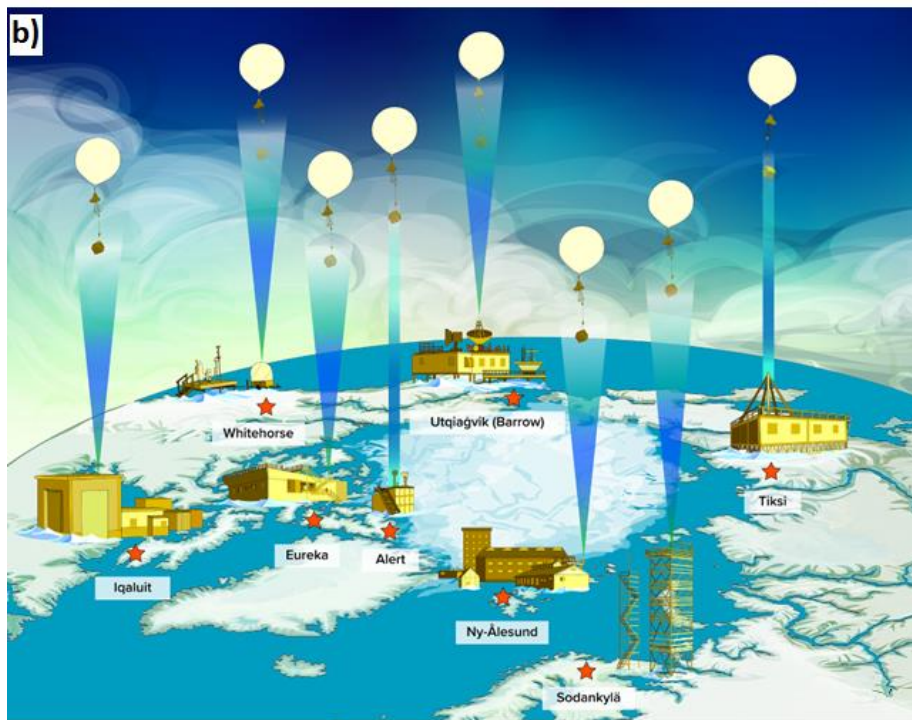
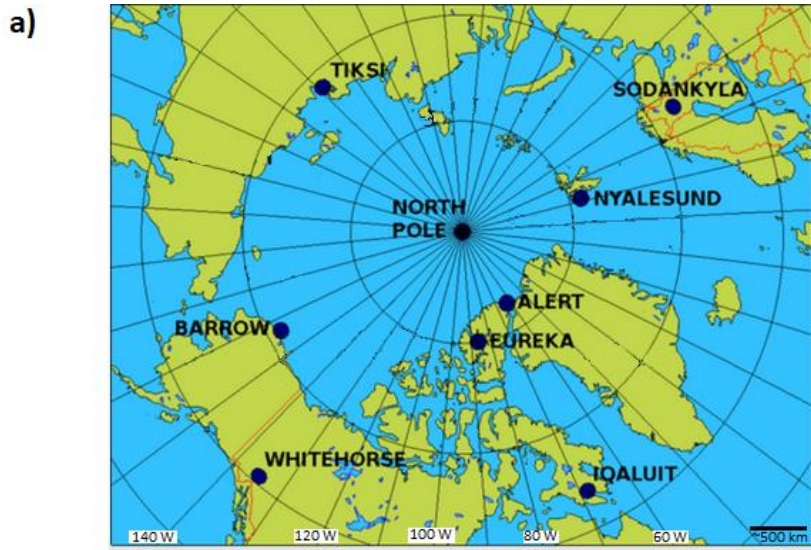
887

888

889

890

891

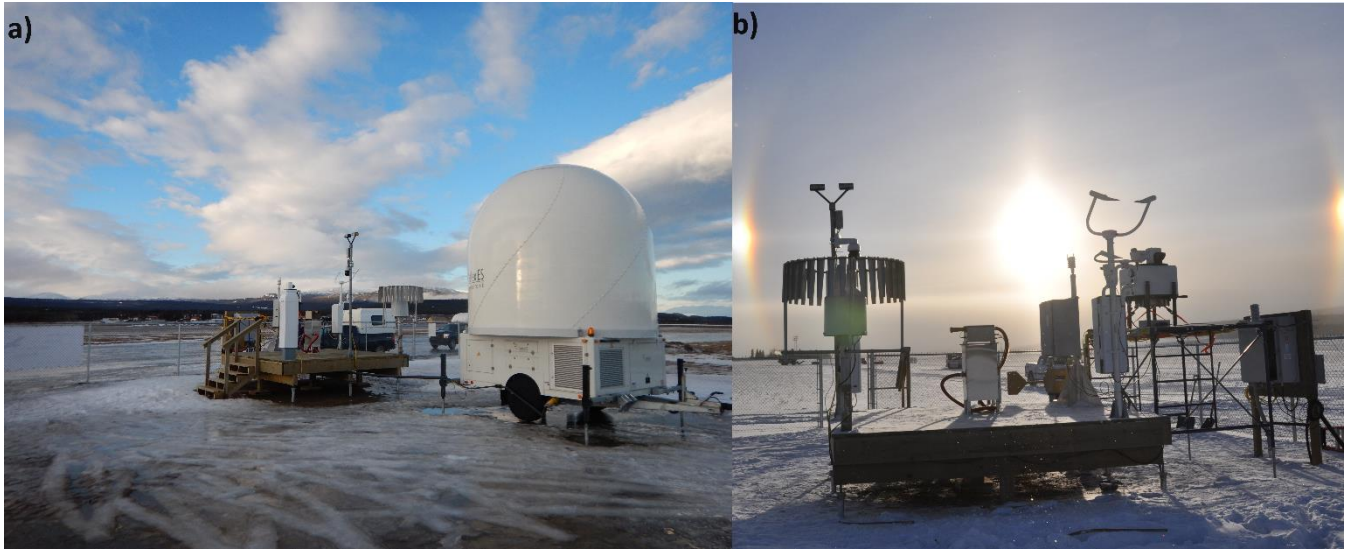


892

893 **Figure 1.** a) Locations of the MODF_{ysm} YOPP supersites (Antarctic sites not shown). (b) Infographic depicting iconic building(s) at each
 894 site. The infographic is roughly centred around the North Pole (centre). All locations shown have generated a MODF_{ysm}, with the exception
 895 of Alert (in progress).

896

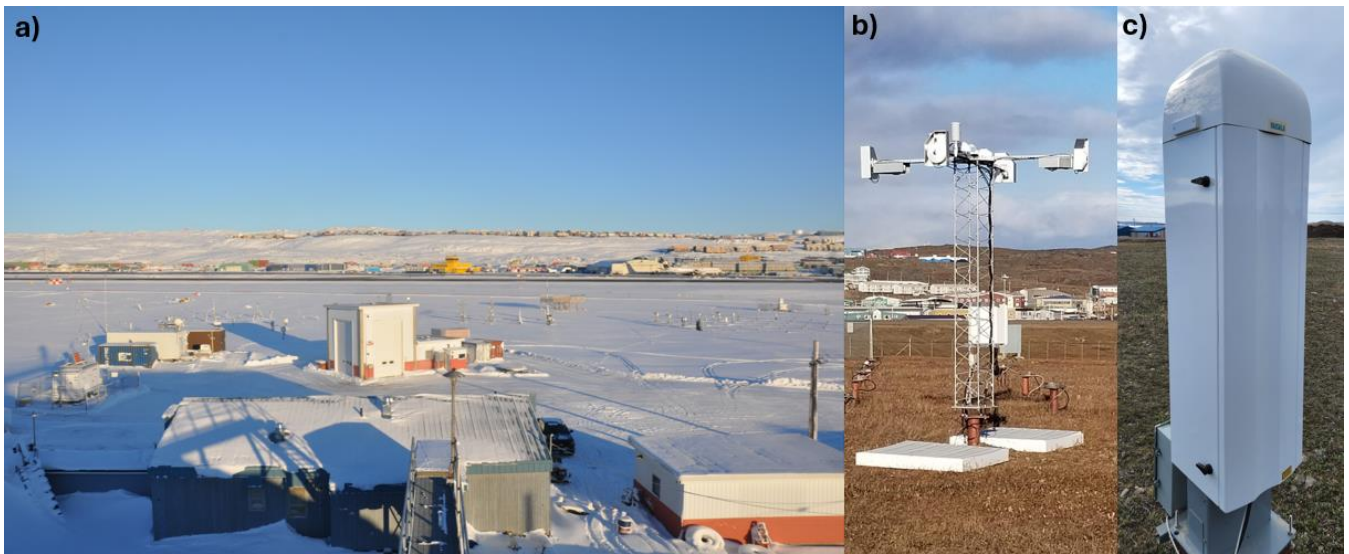
897



898

899 **Figure 2.** The Whitehorse site and the surrounding airfield in early spring 2018 with an X-band radar (white dome) in the foreground (a),
 900 and the main instrument platform, including a Pluvio2, Parsivel, FS11P, WXT520, and CL51 ceilometer (from left to right) with a sundog
 901 in the background (b). Photos adapted from Figure 5 in Mariani et al. (2022).

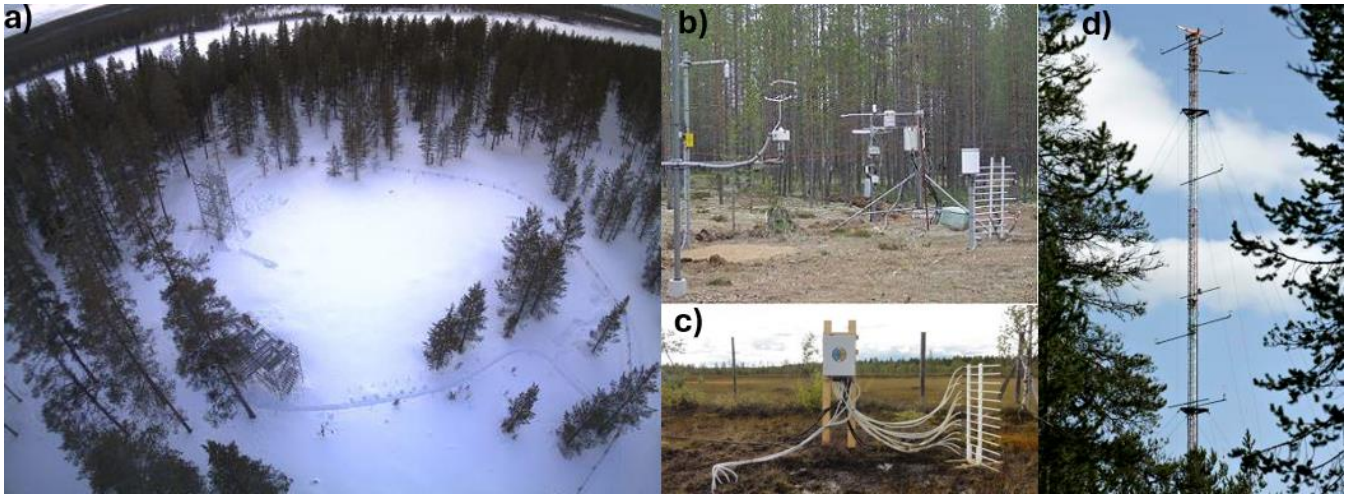
902



903

904 **Figure 3.** The Iqaluit site surroundings taken in winter 2018 with the Iqaluit airport in the background (a), the radiation flux sensor suite
 905 during the summer, consisting of several CMP10Ls, CGR4Ls, and SR50As (b), and the CL51 ceilometer during the summer (c). Photos
 906 adapted from Figure 2 (Mariani et al., 2022).

907



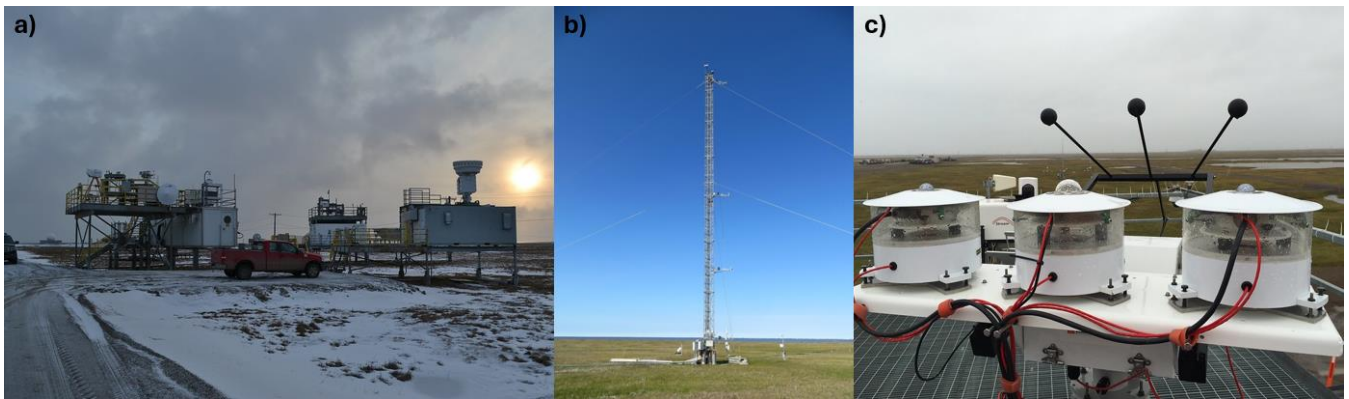
908

909

Figure 4. The Sodankylä site surroundings during the winter at the Intensive Observation Area, IOA, in the boreal forest (a), snow, soil and meteorological measurements in the MET measurement field (b), multi-level snow and soil measurements at the Peatland site, SUO, (c) and the meteorological tower with meteorological and radiation sensors (d). Photos: FMI (litdb.fmi.fi).

912

913

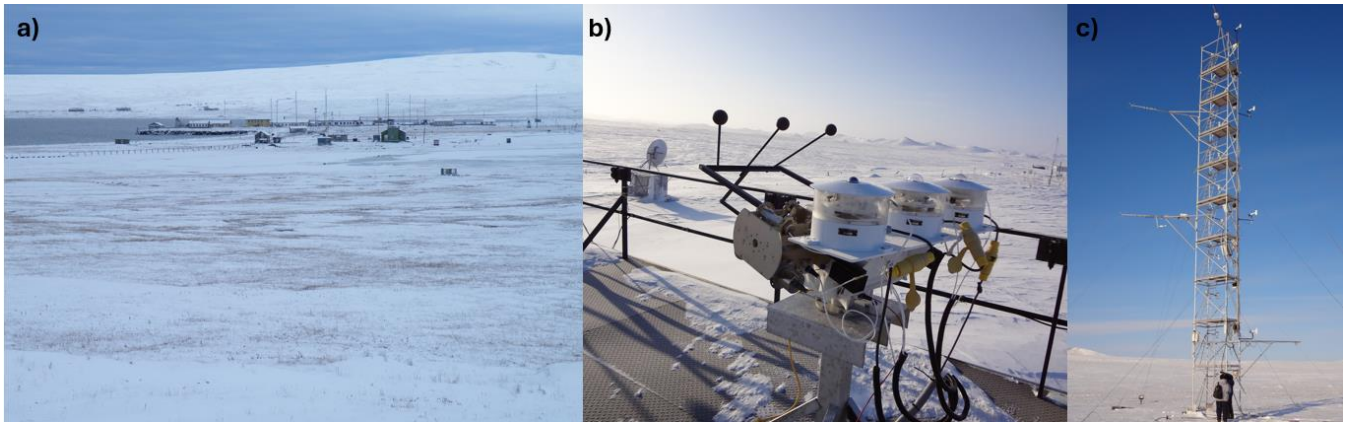


914

915

Figure 5. The Utqiagvik site surroundings during the winter, including the main observation stations and their rooftop instrument suites (a), the meteorological tower with radiation flux sensors deployed in the summer (b), and the SKYRAD downward longwave radiation sensor deployed on the roof in the spring (c). Photos: www.arm.gov.

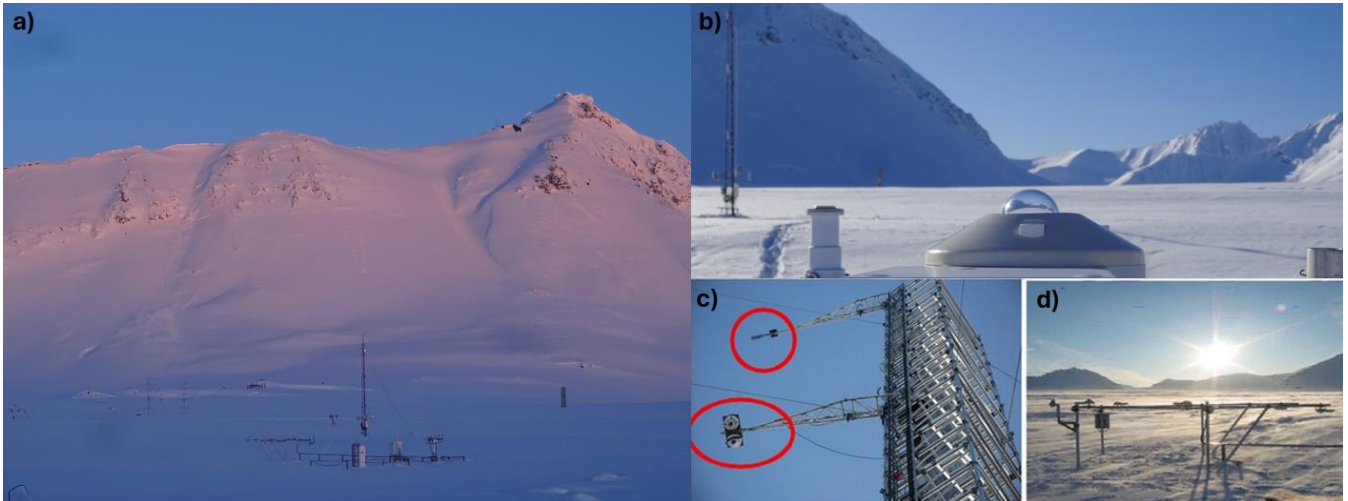
918



919

920 **Figure 6.** The Tiksi site surroundings, taken from afar in the winter (a), the SKYRAD downward longwave radiation sensor deployed on
 921 the roof of the Tiksi observation building (b), and the meteorological tower equipped with radiation flux sensors (c). Photos: Taneil Uttal
 922 (NOAA).

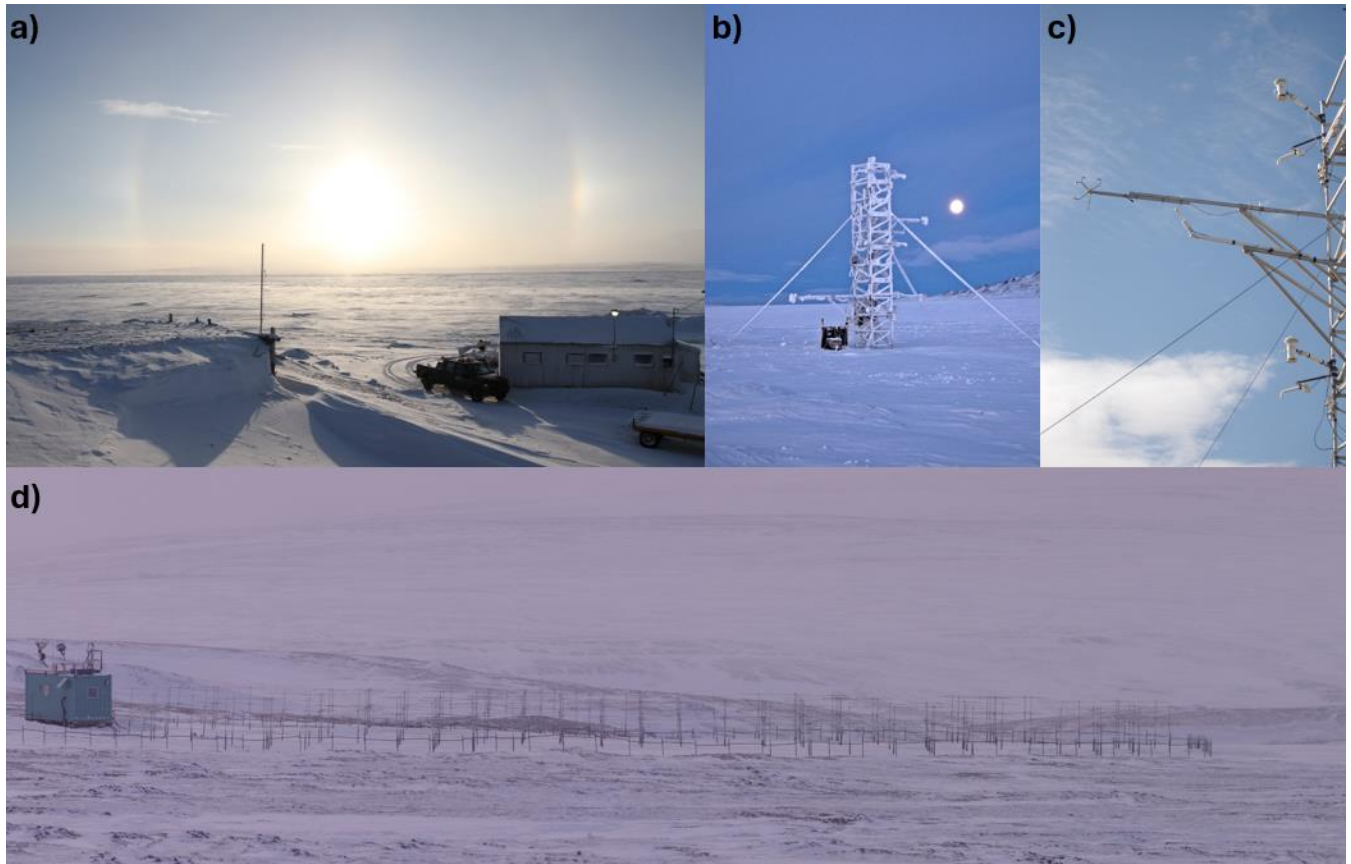
923



924

925 **Figure 7.** The Ny-Ålesund site surroundings taken in the winter with the meteorological sensors and radiation tower in the foreground (a),
 926 the CMP22 downward shortwave radiation sensor at the site (b), the meteorological tower with the radiation flux sensors circled (c), and
 927 several surface meteorological and albedo-measuring sensors at the BSRN station (d). Photos (c-d) are adapted from Figure 1 in Becherini
 928 et al., 2021.

929

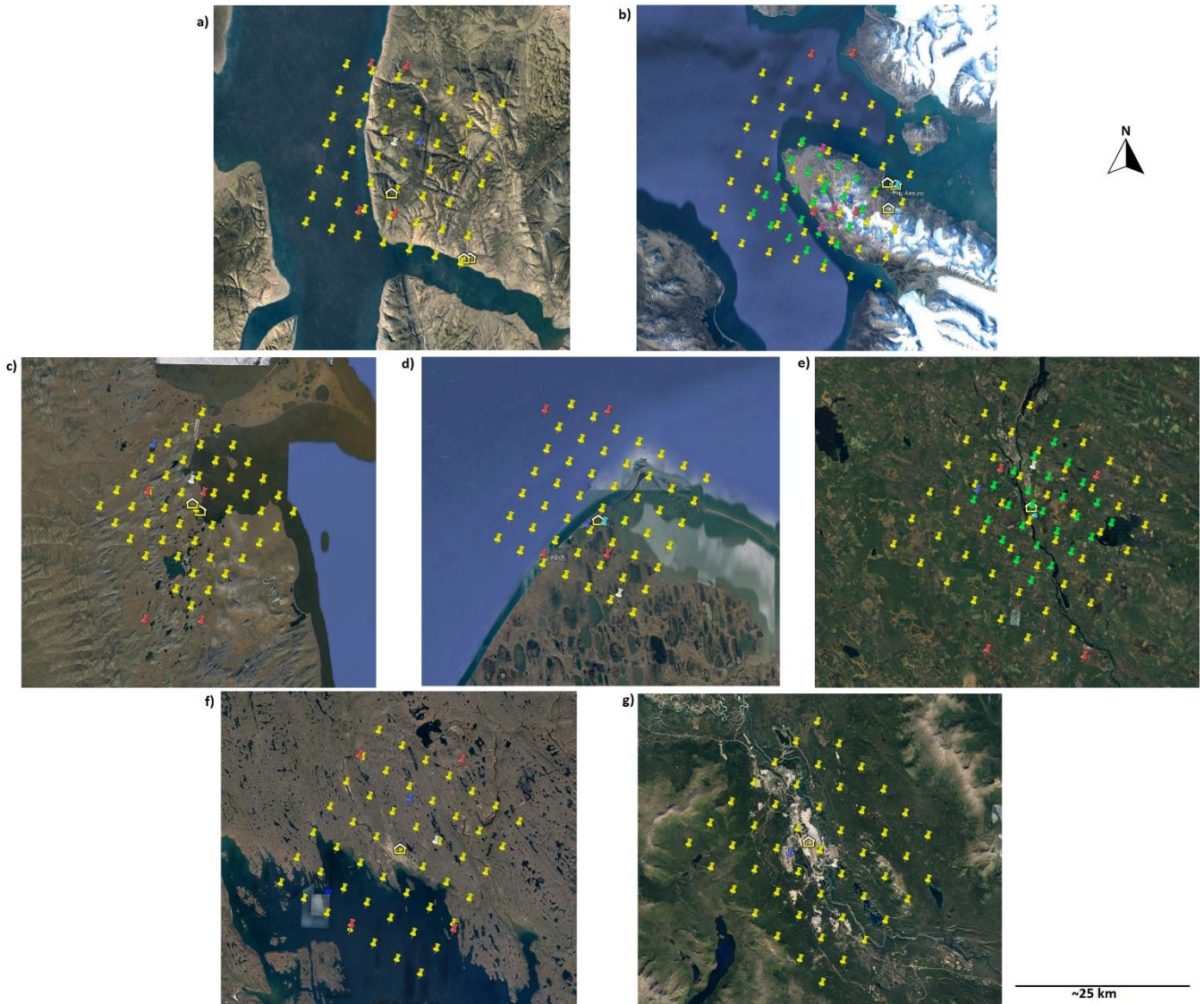


930

931 **Figure 8.** The Eureka site surroundings in the winter, facing south from the Eureka Weather Station (EWS) looking over the frozen fjord
932 with a sundog in the background (a), the meteorological tower at the Surface and Atmospheric Flux Irradiance Extension (SAFIRE)
933 (b) with radiation flux (e.g., PSP) and meteorological sensors deployed (c), and the SAFIRE site surroundings taken from afar (d).

934

935



936

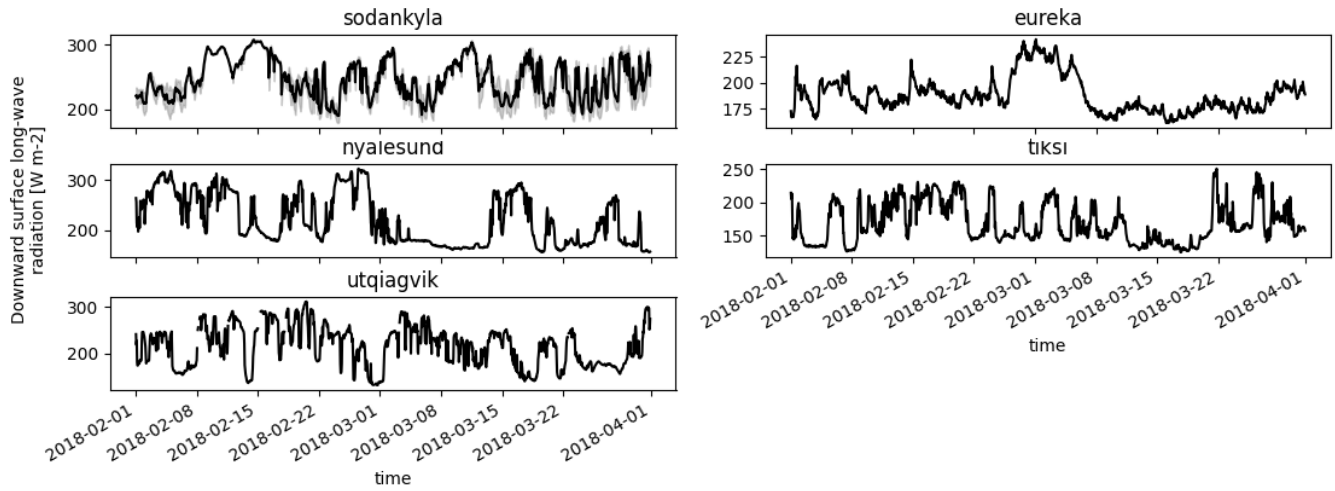
937 **Figure 9.** Model grid points at and around each site (a) Eureka, (b) Ny-Ålesund, (c) Tiksi, (d) Utqiagvik, (e) Sodankylä, (f) Iqaluit, and (g)
 938 Whitehorse, displayed through the Google Earth web-platform: *Image Landsat / Copernicus, Image ©2023 Maxar Technologies*. Sites are
 939 organized from highest latitude (Eureka) to lowest (Whitehorse). Yellow building icons represent the location of the facility on-site which
 940 contains all co-located instruments. Similarly, icons for the AROME-Arctic model grid are indicated by a green pin, ARPEGE pins are in
 941 white, DWD-ICON pins are light blue, ECCC-CAPS pins are yellow, ECMWF-IFS pins are dark blue, and SL-AV pins are in red. All
 942 images are north-aligned, nadir view.

943

944

945

946



948

949

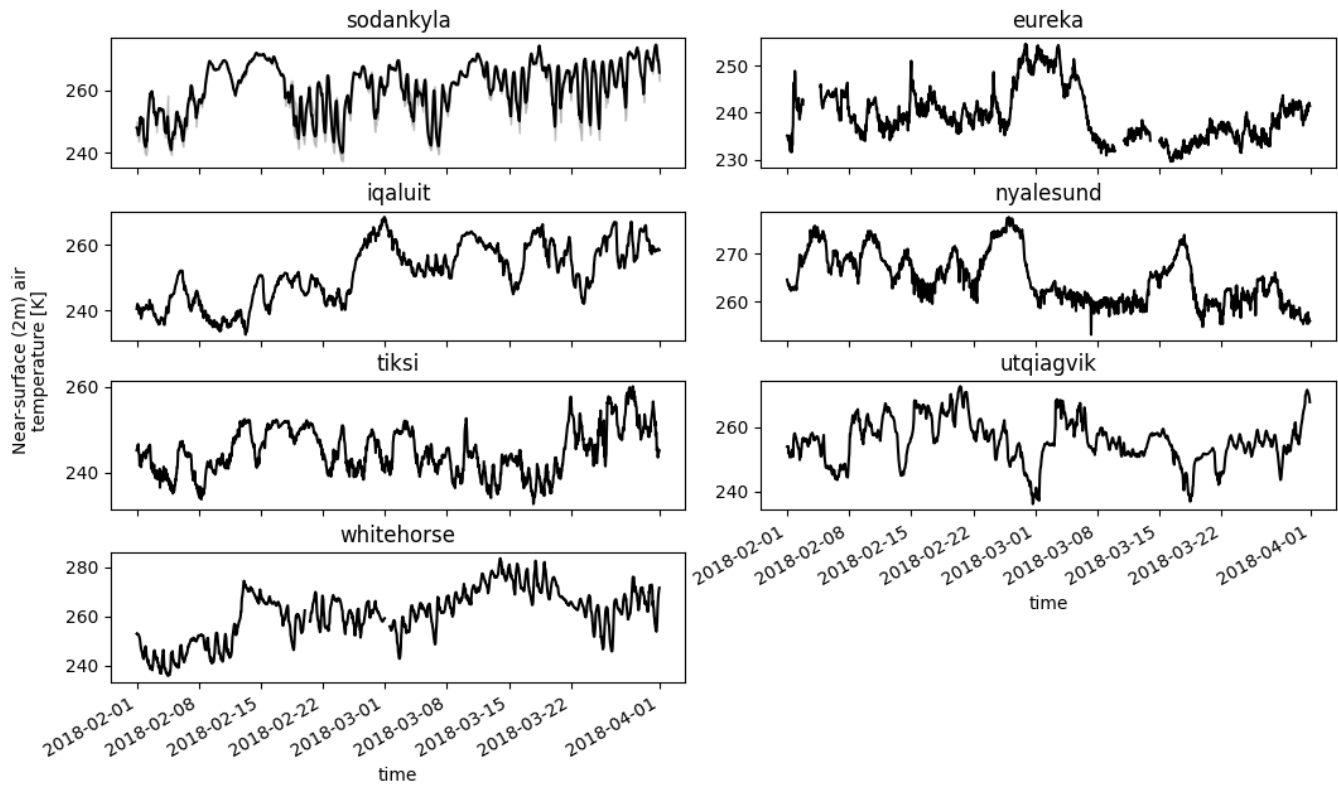
950

951

Figure 10. Observations (30-min) of downward surface long-wave radiation (“rlds”) conducted during SOP1 at each site. Observations from Whitehorse and Iqaluit were not available during SOP1. Sodankylä conducts multiple observations of rlds; the mean (black line) and min/max spread in observed rlds (grey shaded area) are shown.

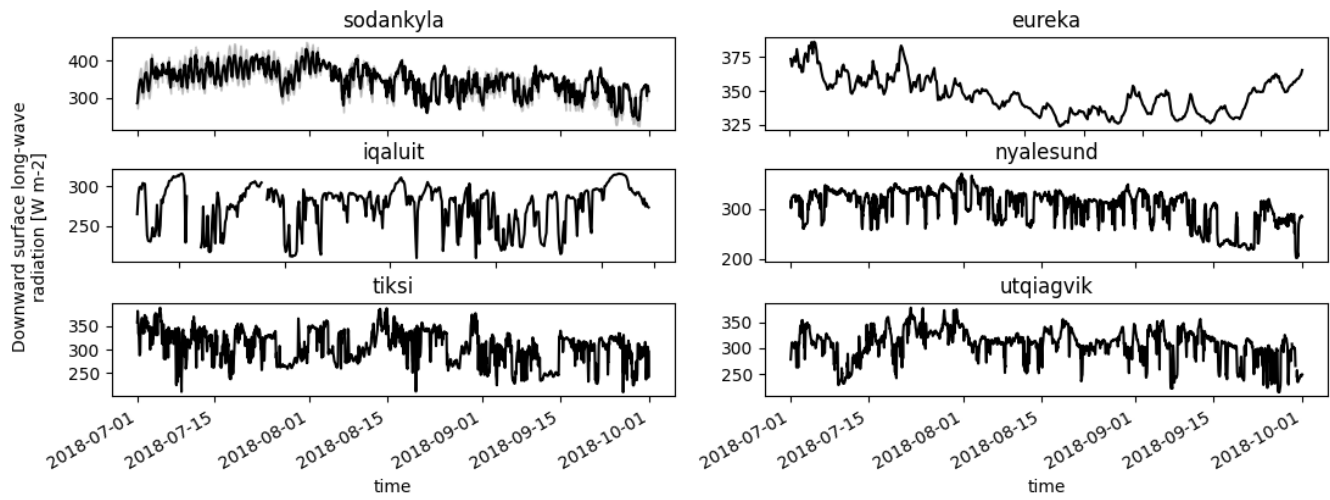
952

953



954
 955
 956

Figure 11. Similar to Figure 3, except for observations of near-surface (2 m) air temperature (“tas”) conducted at each site during SOP1.

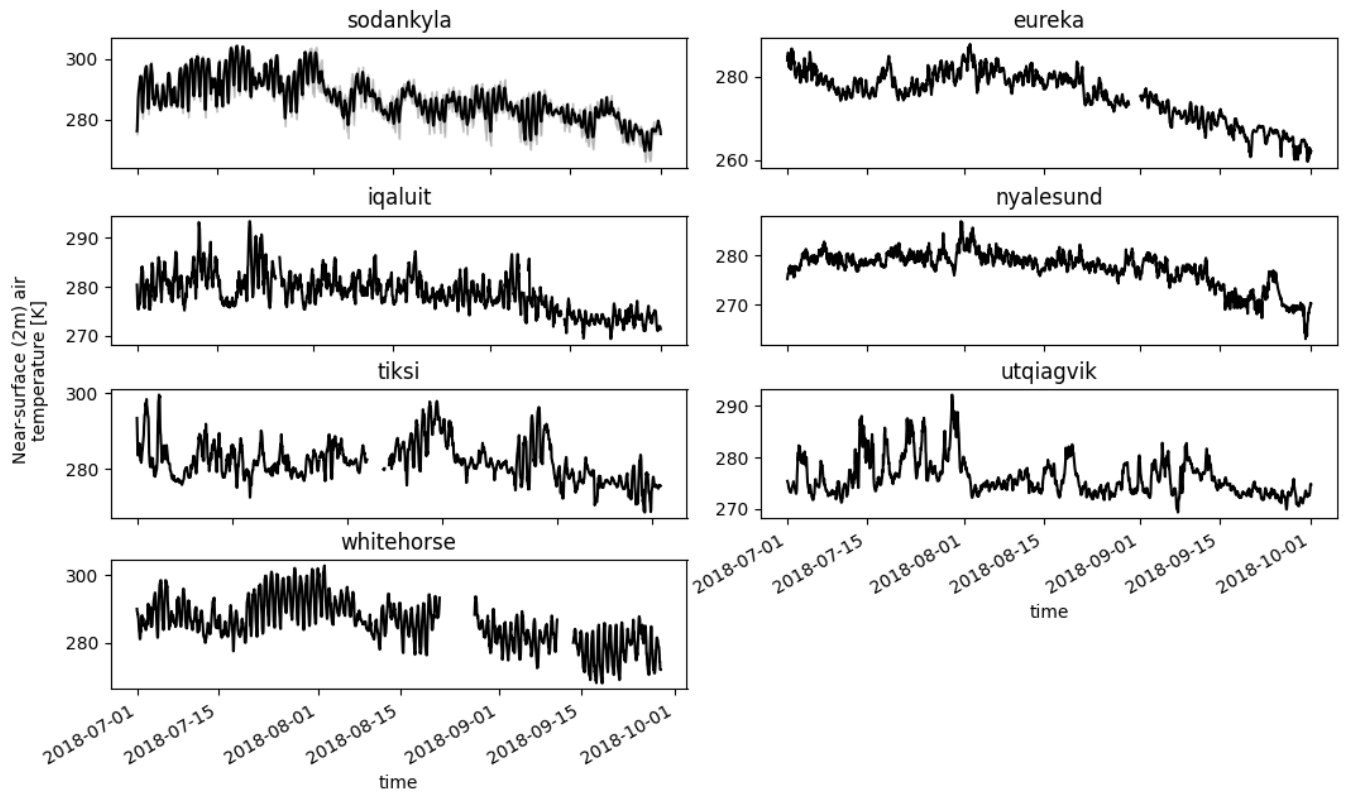


958

959 **Figure 12.** Similar to Figure 3, except for observations of downward surface long-wave radiation (“rlds”) conducted during SOP2 at each
 960 site. Observations from Whitehorse were not available during SOP2.

961

962



963

964

Figure 13. Similar to Figure 3, except for observations of near-surface (2 m) air temperature (“tas”) conducted at each site during SOP2.